Multiple resonance in foil-wound inductors

MULTIPLE RESONANCE IN FOIL WOUND INDUCTORS

by

NICHOLAS JAMES WALKER

A Master's Thesis

Submitted in partial fulfilment of the
requirements for the award of
Master of Science of the Loughborough University
of Technology.

October 1975

Supervisor: Dr.P.N.Murgatroyd
Department of Electronic and
Electrical Engineering.

LIST OF CONTENTS

ACKNOWLEDGEMENTS

My sincere thanks goes to my supervisor Dr.P.N. Murgatroyd for his inspiration and encouragement; to Prof. D.S.Campbell for his interest; to N.Phipps and S.Harris for their assistance. my thanks also goes to the staff of the Electronic and Electrical Engineering Department and the Computer Centre.

The work was supported by the Plessey Company Ltd.

Section 1 Introduction

Foil wound inductors (FWI) consist of a thin metal foil and an insulating film wound together in a spiral configuration. In some coils the insulation is a varnish coating on the metal foil, but in the coils used in this study the insulation is a separate polythene or polypropylene film. FWI differ from ordinary wire wound inductors (WWI) in one important respect; illustrated by Fig.1-1. A turn in a WWI is adjacent to eight other turns, whereas a turn in a FWI is adjacent to two other turns.

In a previous study (1), the coils were wound on a central core of perspex rod. This type of core was unsuited to this study for a number of reasons detailed in Section 2. Therefore the cores were changed to ones wound from the plastic insulation. Both types of coil are shown in Fig.1-2.

The FWI manufactured have turn numbers in the range ten to one thousand. The metal foil was in all cases aluminium. The thickness of both the metal and plastic foils was of the order of ten micro-metres. All the FWI were wound on a converted capacitor winding machine, described in (1).

Self-resonance in WWI is well known, yet is poorly understood in detail. Welsby (2) describes how the impedance of a WWI may be represented by the circuit in Fig.1-3. Consisting of an inductance, a d.c. resistance and an a.c. resistance in series, parallel by an effective capacitance. The inductance resonates with the capacitance at a frequency given by,

$$f_o = \frac{1}{2\pi}\left(\frac{1}{LC}\right)^{1/2}\left(1 - \frac{1}{Q^2}\right)^{1/2} \qquad 1\text{-}1\text{-}1$$

Where Q is given by

$$Q = \frac{1}{R}\left(\frac{L}{C}\right)^{1/2} \qquad 1\text{-}1\text{-}2$$

FIGURE 1-1

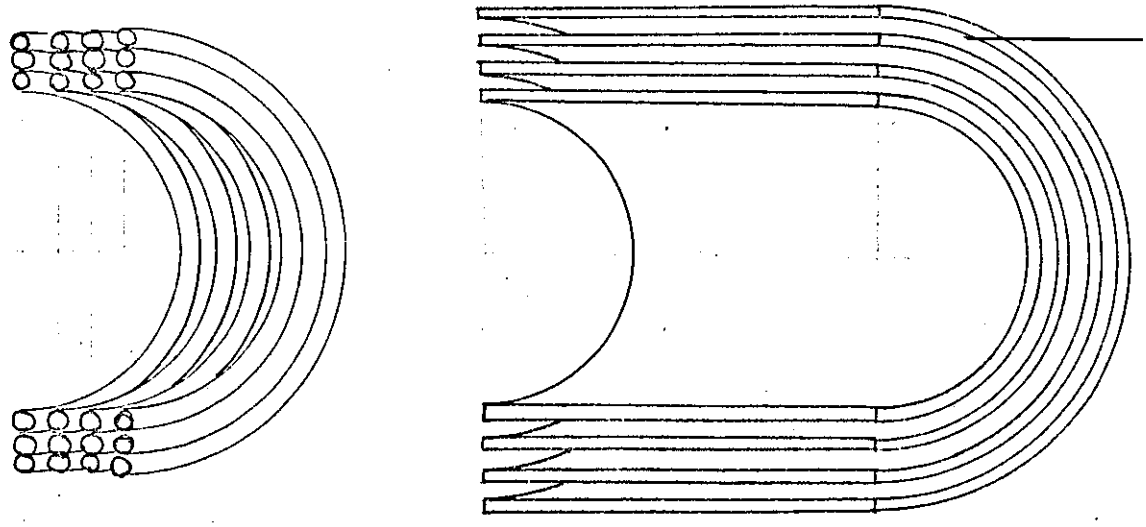

Wire wound coil

Foil wound coil

Figure 1-2

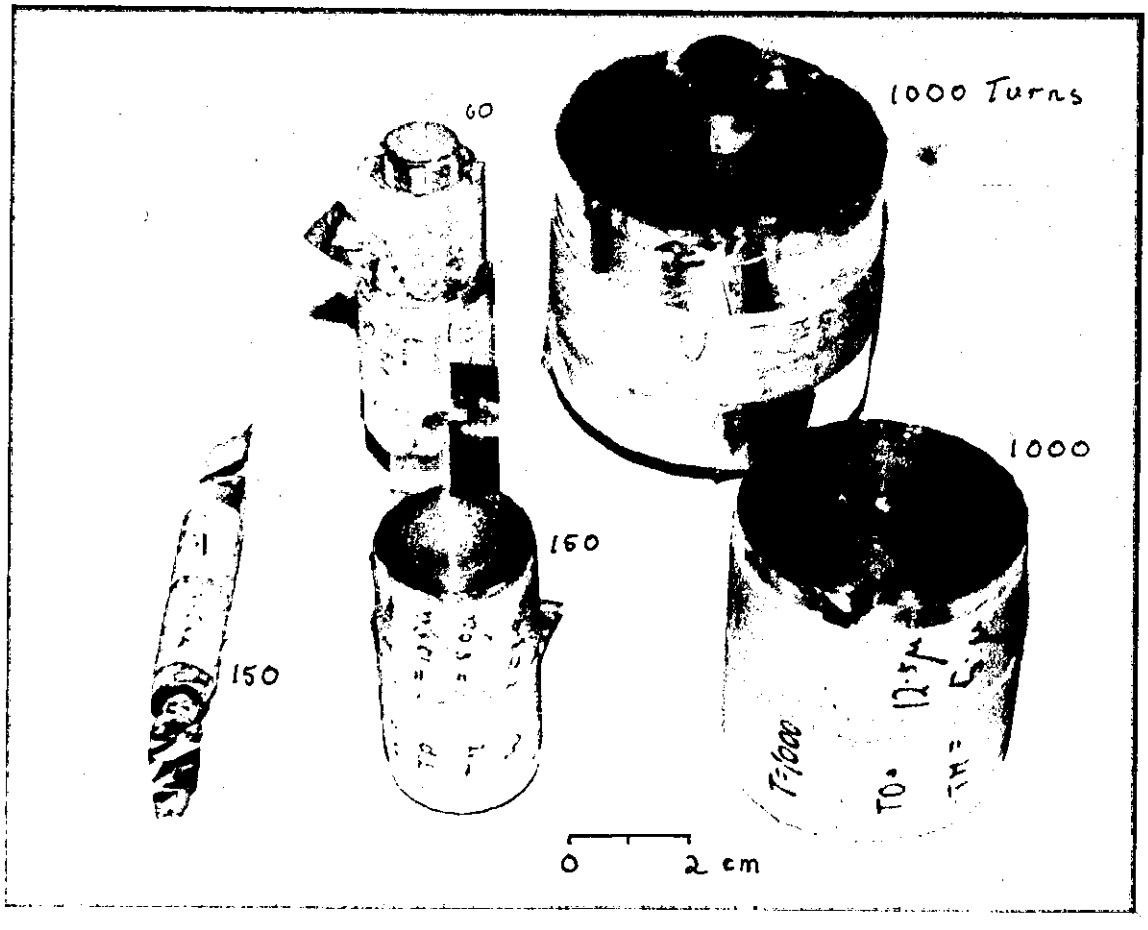

The photograph shows both types of coil, the older with a solid perspex core and more recent with a wound core.

When Q is large, f_o is to a good approximation, given by,

$$f_o = \frac{1}{2\pi}\left(\frac{1}{LC}\right)^{1/2} \qquad 1\text{-}1\text{-}3$$

At frequencies below the resonance the circuit is inductive and at frequencies above; capacitive. As the resonance is approached the impedance rises, until at resonance it has a maximum value of

$$Z = Q^2 R \qquad 1\text{-}1\text{-}4$$

At this point the impedance is wholly real.

When the impedance has fallen to $\frac{1}{\sqrt{2}}$ of its maximum value, the frequency has changed by a factor,

$$\frac{\delta f}{f_o} = \pm \frac{1}{2Q} \qquad 1\text{-}1\text{-}5$$

At the same time the power absorbed by the circuit has risen by a factor of 2.

At d.c. the a.c. resistance is zero and rises as the first or second power of the frequency depending on the geometrical construction of the coil.

Although in general this equivalent circuit is in general adequate, certain types of loosely coupled, single layer WWI resonate more than once with their self-capacitance, at frequencies higher than the normal resonance. This is said to occur (2) because the coil can behave as a transmission line. This phenomenon appears to be poorly understood as no references to a quantitative theory have been found.

Work performed at Loughborough (1), has shown that similar multiple resonant behaviour exists in FWI. This behaviour would not be expected from a transmission line point of view as a FWI is relatively tightly coupled.

The contacts to the FWI are made using thick Aluminium foil wound round the thinner winding foil; the contact is held in place by pressure and projects out beyond the plastic foil.

FIGURE 1-3

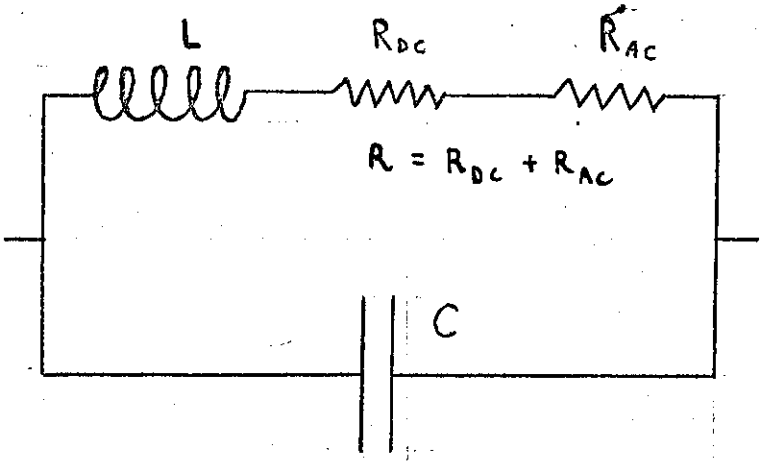

Equivalent circuit of a wire wound inductor

1. An experimental analysis of multiple resonance in FWI with turn numbers varying from 65 to 1000 turns was performed in (1). However there are a number of criticisms of the procedure used, therefore the experiments are repeated.

The coils used in (1) were wound on perspex cores. This on the winding machine used; resulted in poor packing of the coil windings. On average this meant that the turn to turn spacing was three times the plastic thickness. Clearly this would result in a large experimental error and a poorly defined turn to turn capacitance. Therefore it was decided to wind the core of the coil from the plastic insulation. This resulted in much improved packing, although it did not entirely remove the problem, which will be mentioned again in section 4.

The apparatus used to obtain the impedance/frequency spectrum is shown in Fig.2-1. The noise generator produces a noise signal with a spectrum flat to within $\pm$ 1.0dB from 20.Hz to 10.0 MHz and to $\pm$ 1.5dB from 10 MHz to 20 MHz. As the noise is white the spectrum seen at the spectrum analyser corresponds to the impedance spectrum of the coil.

Fig.2-2 shows the impedances of the situation. The output impedance of the noise generator and the input impedance of the spectrum analyser are both 50Ω. The cables are 50Ω, therefore they can be ignored as they are terminated correctly. The situation can be expressed as Equation2-1.1.

$$V_{SA} = \frac{50\ V_{NG}}{50+50+Z} \qquad 2\text{-}1\text{-}1$$

Where V_{NG} is the output from the noise generator and V_{SA} is the input to the spectrum analyser. To simplify the situation the zero level on the spectrum analyser is taken as that when the coil is shorted out. This corresponds to

$$V^{o}_{SA} = \frac{50\ V_{NG}}{50+50} \qquad 2\text{-}1\text{-}2$$

Figure 2-1

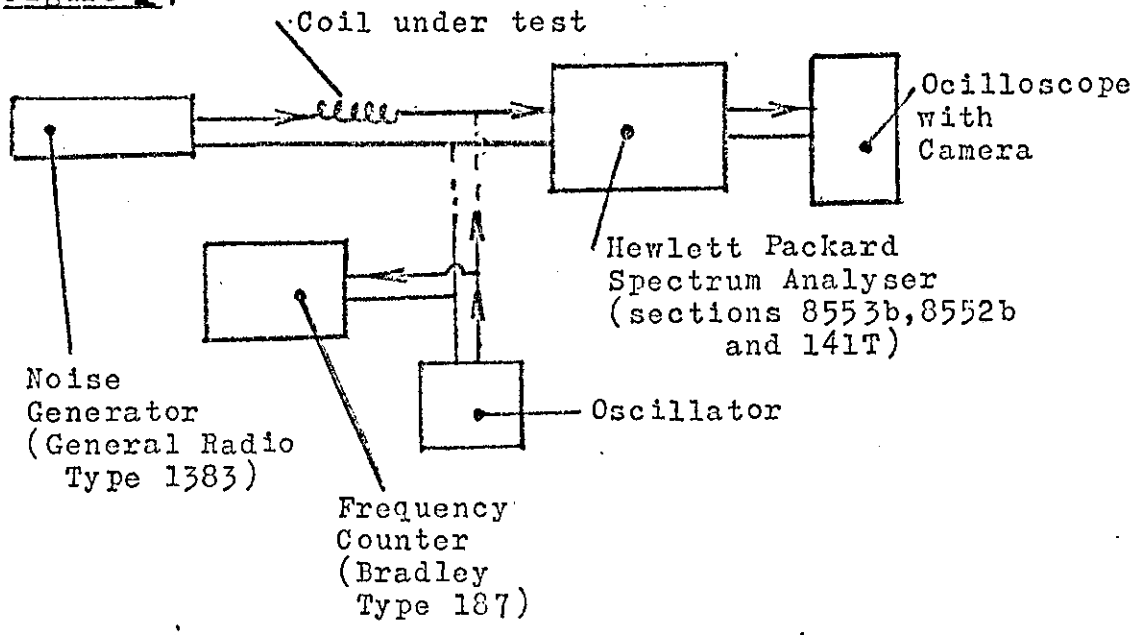

Appratus used to measure the impedance/frequency spectrum

Figure 2-2

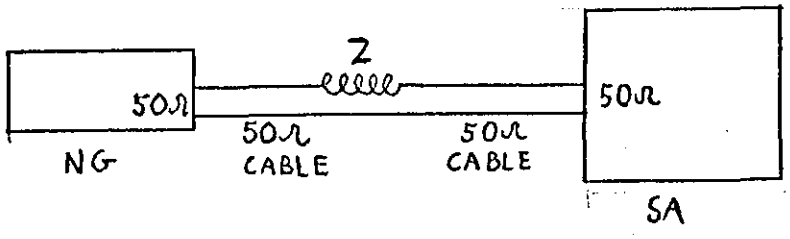

Thus on the 10dB power per division scale of the spectrum analyser

$$dBM = 20 \log\left(\frac{V_{SA}^{\circ}}{V_{SA}}\right) = 20 \log\left[\frac{(100+Z)}{100}\right] \qquad 2\text{-}1\text{-}3$$

Where dBM is the measured scale difference between the levels with and without the coil. This method, as can be seen from equation 2.1.3 is independent of V_{NG}, the voltage output from the noise generator.

Rearranging equation 1.3 gives Z as

$$Z = \text{alog}\left(2 + \frac{dBM}{20}\right) - 100 \quad \Omega \qquad 2\text{-}1\text{-}4$$

The accuracy of the frequency scale on the spectrum analyser was poor, therefore an oscillator and frequency counter were used for accurate frequency measurement. This was done by placing the oscillator peak at the desired point of the spectrum. With this method the accuracy was limited by the width of the resonance.

The spectrum of a 1000 turn coil is shown in Fig.2.3. The flat trace at the top is the spectrum of the noise generator with the coil shorted out. The jagged trace below is the spectrum of the noise generator measured with the coil in circuit. The frequency scale goes from 0 to 7.5 MHz. A minimum on the trace corresponds to a maximum of the impedance, as the analyser output shows dB loss w.r.t. the zero level.

Coils with turn numbers varying from 10 to 1000 were tested using the method described. These coils had aluminium foil of 3.9 cm width, 5.0μ m thickness, plastic film of 12.5μ m thickness made from polypropylene, and a core radius of 0.71 cm. Fig.2.4 shows the frequencies of the first five orders of maximum impedance resonances. The abcissal scale is from 10 to 1000 turns, logarithmically. The ordinate scale is 0.1 MHz to 20 MHz, logarithmically.

The lines join resonances of equal order. The curve at the bottom (order 1) represents the variation of the frequency of the fundamental resonance with the number of turns. For low N the gradient of this curve is approximately -0.53 and steepens to approximately -0.99 for large N.

Figure 2-3

Impedance/frequency spectrum of a 1000 turn coil.

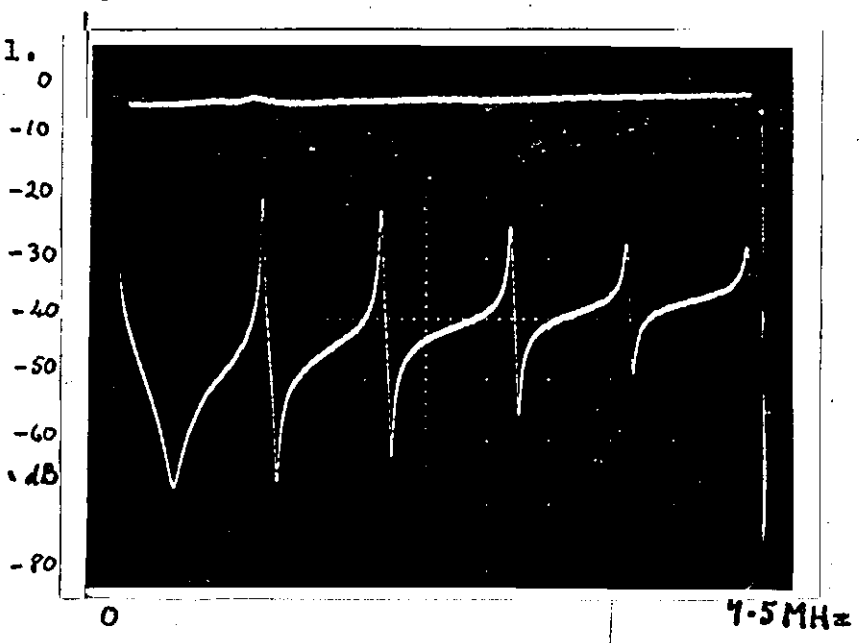

Figure 2-4

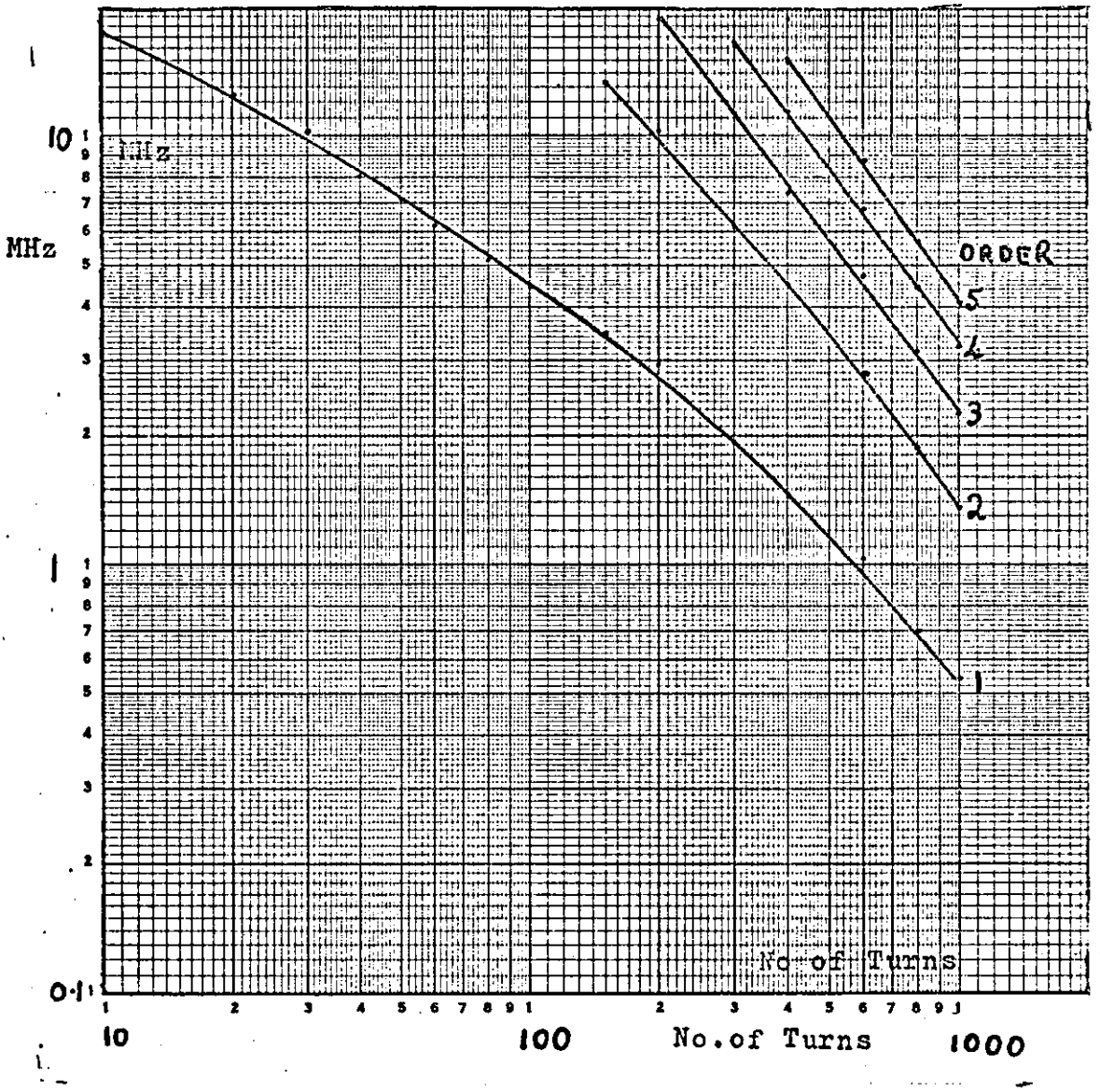

Frequency of resonance versus number of turns for the first five orders of maximum impedance resonance.

Therefore for small N

$$f_o \propto \frac{1}{N^{0.53}} \qquad 2\text{-}1\text{-}5$$

and for large N

$$f_o \propto \frac{1}{N^{0.99}} \qquad 2\text{-}1\text{-}6$$

The frequencies of the various orders of resonance do not form an harmonic series, although when N is large this situation is approached.

2. Although the experimental error in the measurement of frequency in the previous experiment is small, no bound could be put on the reproducibility of the results. Individual coils although wound to the same dimensions using the same materials will show variations in the resonant frequency, due to fluctuations of the winding tension and side to side shifting of the metal foil.

To estimate a bound to this error, 5 coils each of 150 turns were wound from the same metal and plastic reels. The coils differed from the 150 turn coil of the previous experiment, in that they had a core radius of 0.7 cm, instead of 0.71 cm. The 150 turn coil was chosen to conserve materials, it was the smallest coil to exhibit multiple resonance below 20 MHz.

The results are shown in Fig.2-6. The fundamental resonance has an average frequency of 3.26 MHz; with a total spread in frequency of 0.17 MHz. An estimate of the error is therefore, $\pm$ 2.6%. The secondary maximum impedance resonance has an average frequency of 13.09 MHz, with a total spread in frequency of 0.27, giving an error of $\pm$ 1.0%.

3. The fundamental problem with this method is that although the output from the noise generator is high; 1 Volt rms, the voltage per unit bandwidth is not, the voltage being spread from 0 to 20 MHz. The maximum signal to noise ratio at the spectrum analyser, with no coil in the circuit,

Figure 2-5

Coil No.	Freq of first resonance Error ±0.01 MHz	Freq of second max resonance Error ±0.01 MHz	Freq of first min resonance Error ±0.02 MHz
1	3.33	13.19	12.98
2	3.16	13.02	12.83
3	3.21	13.22	13.00
4	3.33	12.93	12.74
5	3.27	13.08	12.85
average	3·26	13·09	12·88

Figure 2-6

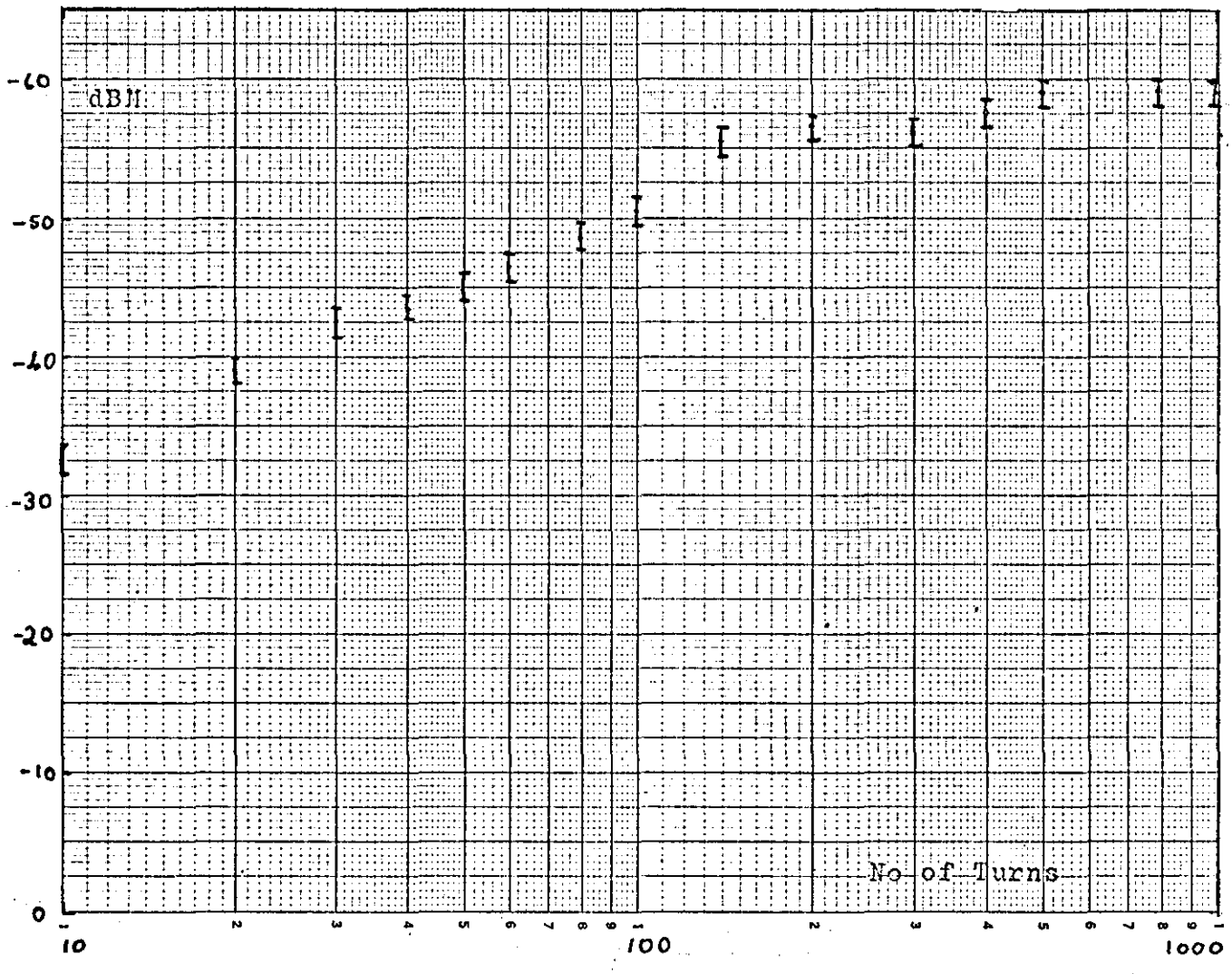

The dBM scale represents the dB power loss w.r.t. the reference level (coil shorted out).

is approximately 60dB. This means that for large coils, the signal from the noise generator, at the maximum impedance resonances, will be of the same order of magnitude as the noise of the spectrum analyser. Differences of greater than 60 dB will be conpressed to a maximum difference of 60 dB.

This is illustrated by Fig.2-6. This shows the impedance at the fundamental resonance versus the number of turns, for coils with turn numbers varying from 10 to 1000 turns. A maximum value of 59dB is reached. Hence the Q of a coil with greater than 100 turns cannot be measured accurately.

There is an instrument which can overcome this problem - The Hewlett Packard Tracking Generator-Counter 8443A. This is designed for use with the spectrum analyser. The tracking generator produces a signal which can be swept from 20 Hz to 110 MHz. The tracking generator also centres the swept filter of the spectrum analyser on the signal, to an accuracy of $\pm$ 5 Hz. The signal to noise ratio of this method is 190dB. The tracking-generator contains features which make accurate frequency measurement possible. Hence the Q can easily be measured.

The tracking generator replaces the noise generator in Fig.2-1. The output impedance is 50 Ω.

(The Electrical Engineering Department does not possess one of these instruments. The one used in the following experiment was on loan from Hewlett Packard for a short period.)

The Q of the fundamental resonance were measured for the set of coils (in the expt. in section 2-/. The accuracy to which the 3dB points could be found was limited by reading errors on the scales of the spectrum analyser and the frequency counter of the tracking generator. The accuracy was better than 1 KHz at 20 MHz and 0.5 KHz at 0.5 MHz.

The results are shown in Fig.2-7. The average Q is about 150 with a peak value of 214 at 60 turns. The large errors for large N are due to the decreasing half-height width of the resonance.

Figure 2-7

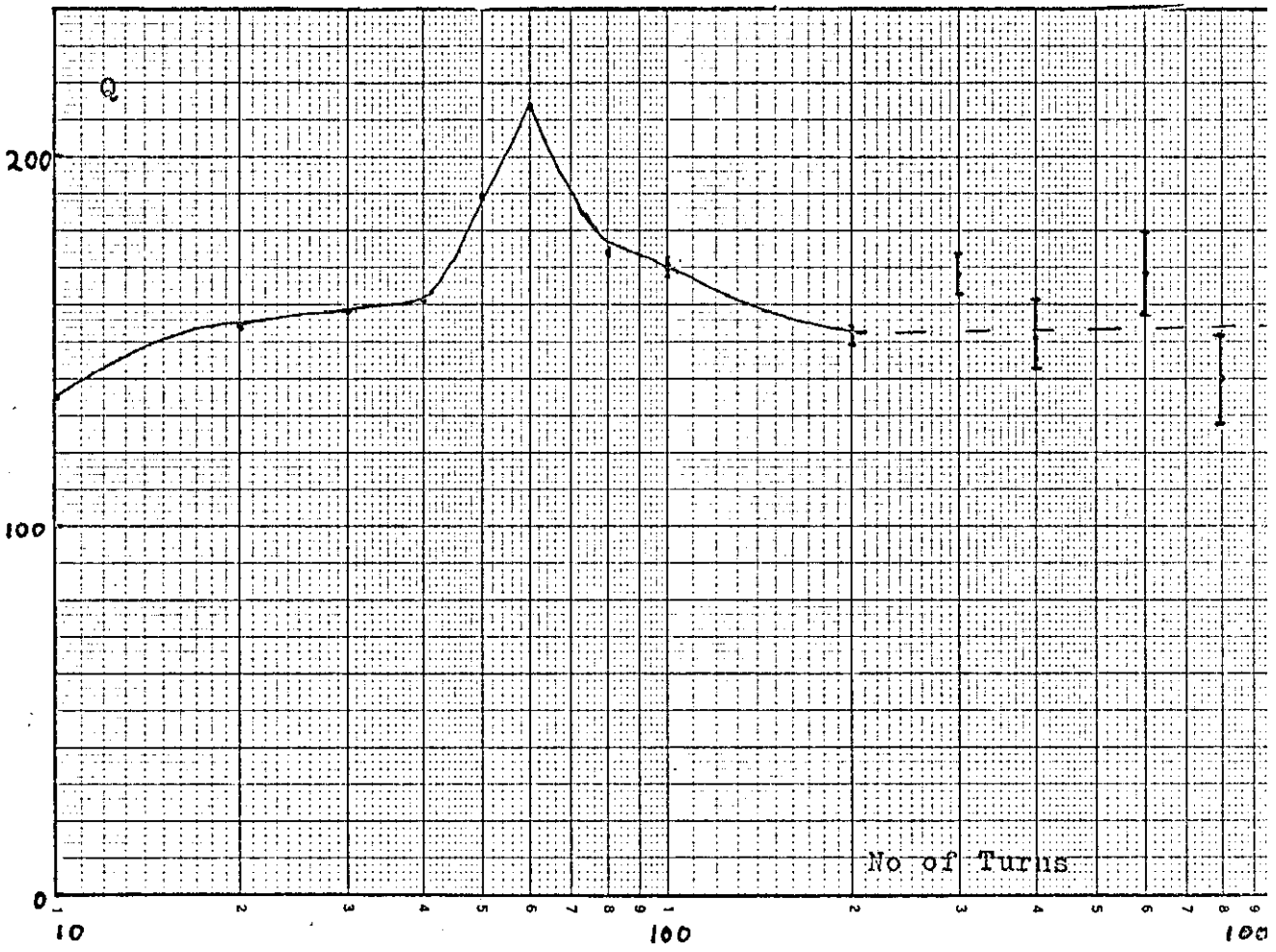

This graph shows the variation of the Q of the fundamental resonance with the number of turns.

FIGURE 2-8

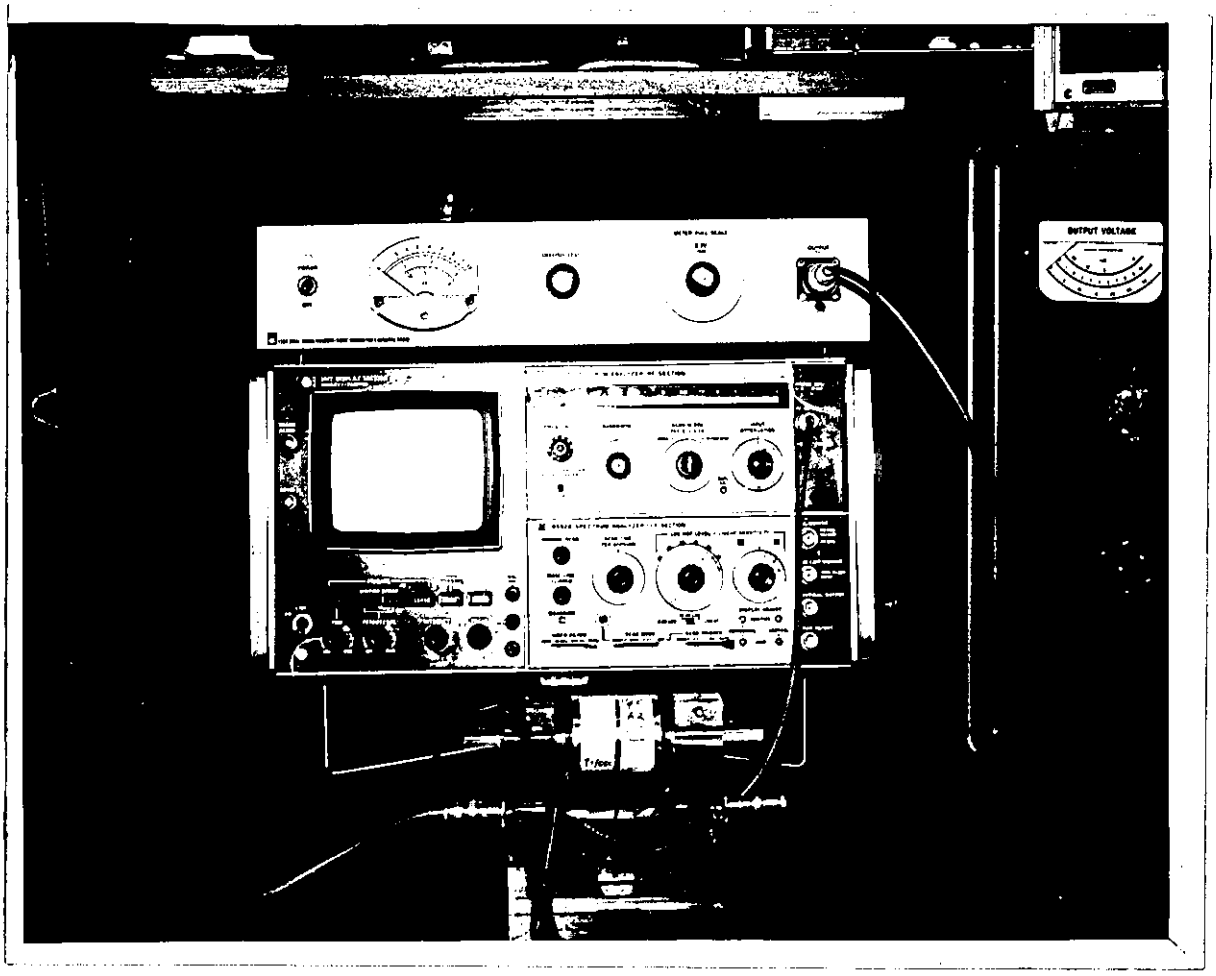

The photograph shows the appratus used to determine the impedance spectra of the foil wound inductors. A 1000 turn fWI is shown held in a perspex clamp. The spectrum analyser is in the centre of the photograph with the noise generator sitting on top. Visible on the right are the signal generator and the frequency counter

Section 3 Equivalent Circuit

1. An exact theory of multiple resonance in FWI would undoubtedly require an analytic field theory solution. However, the possibility of such a solution would seem remote; the configuration of the coil is a spiral, which is a difficult coordinate system to work in. A computational field theory solution may seem more practical, either in differential form via finite-difference methods or in integral form through equation3-1-1.

$$\underline{J} = -\sigma \left(\frac{\partial \underline{A}}{\partial t} - \underline{\nabla} V \right) \qquad 3\text{-}1\text{-}1$$

Where $\underline{J}$ is the current, $\underline{A}$ the vector magnetic potential, V the scalar potential and σ the conductivity.

But finite-difference methods incur the same penalty as the analytic method would, a spiral coordinate system is a difficult one to work in. Also a very large matrix would be required to attain any degree of accuracy. The same size limitation applies to the integral method. The coil would have to be split into a large number of small sections, $\underline{J}$ and $\underline{A}$ would have to be evaluated at each section. $\underline{A}$ would have contributions from the currents in all the other sections. Therefore the number of interactions to be calculated per cycle of the iteration is proportional to the square of the number of sections.

Clearly the computer time involved in either of these methods is too long for either of them to be considered practical. However, if we neglect the extreme field theory situation, at frequencies where the wavelength is of the same order of magnitude as the width of the foil, it is possible that the current is uniform across the width of the foil and that it has only a slow variation across the width of the coil. This

granted, the current would have only a small variation of magnitude and phase round any one turn, therefore an inductance per turn and a turn to turn capacitance could be defined, [Murgatroyd |4|.].

This leads to the postulated circuit in Fig. 3a. L/2 is the inductance of one half-turn and C is the turn to turn capacitance. The L's and C's will increase steadily from the centre of the coil outwards. When the L's and C's are untangled the circuit is that of Fig. 3b. Part-turns at the ends of the coil have been neglected, and a mutual-inductance M has been included to account for the magnetic coupling from turn to turn. The M's are positive, all the turns are wound in the same sense. The elements L_u and C_u are counted from the curcumference of the coil inwards starting from L_1 and C_1.

FIGURE 3-1

a/

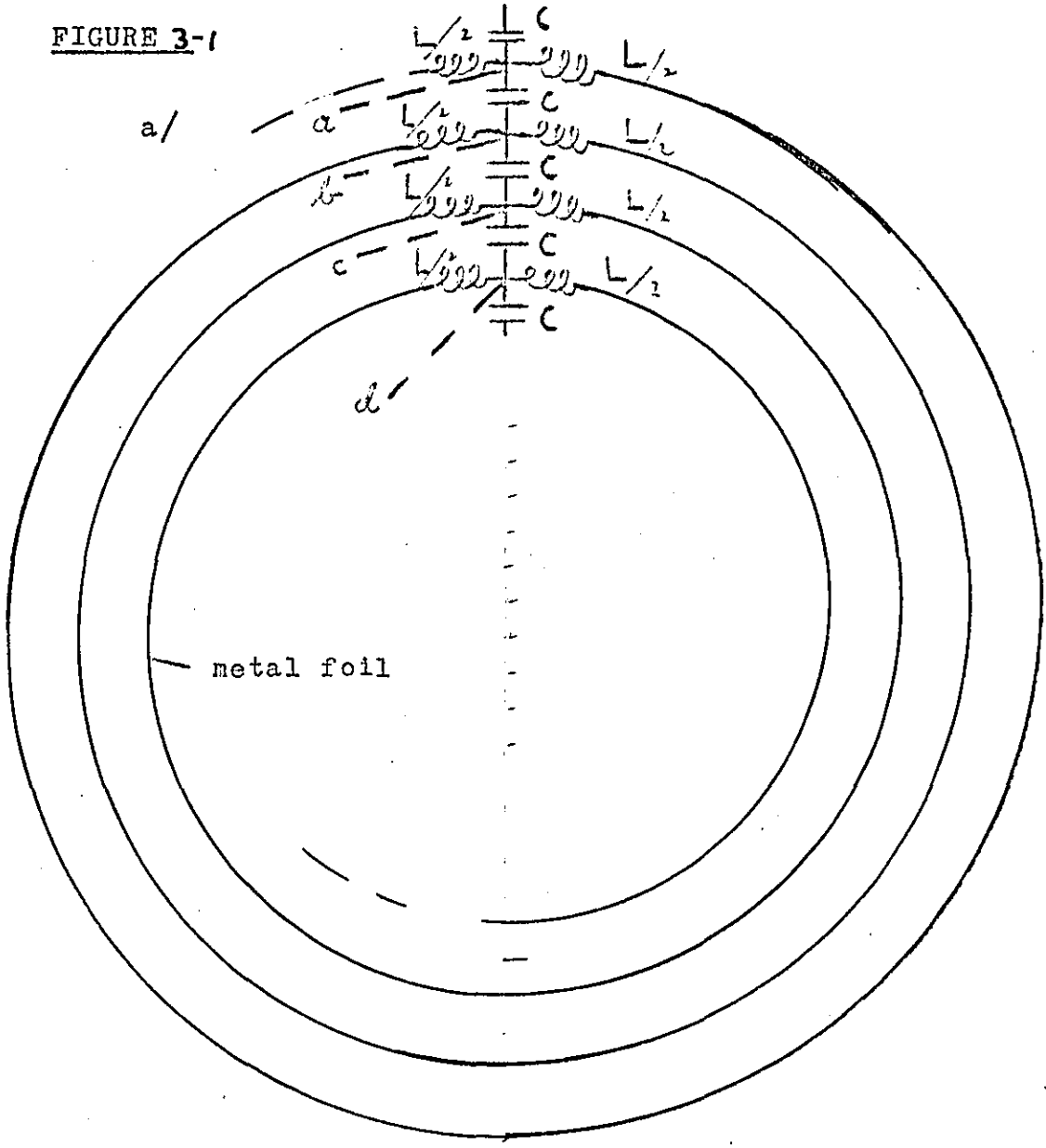

L is the turn inductance
C is the turn to turn capacitance

b/

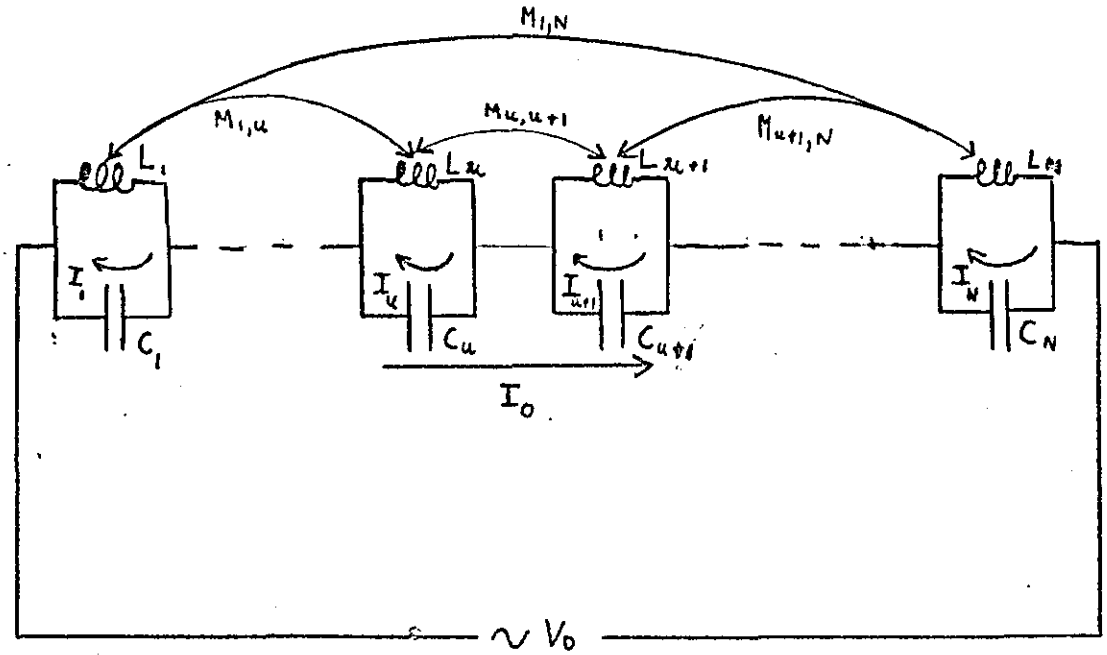

There are N + 1 mesh equations for this circuit. N of these have the form;

$$j\omega M_{u,1} I_1 + - - - + j\omega M_{u,u-1} I_{u-1} + \left(j\omega L_u + \frac{1}{j\omega C_u}\right) I_u + \quad 3\text{-}1\text{-}2$$

$$- - - - + j\omega M_{u,N} I_N = I_o / j\omega C_u \qquad 1 \leq u \leq N$$

The N + 1th equation has the form

$$V_o = (I_o - I_1)/j\omega C_1 + - - - + (I_o - I_u)/j\omega C_u$$

$$+ - - - + (I_o - I_N)/j\omega C_N \qquad 3\text{-}1\text{-}3$$

By dividing equations3-1-2 and3-1-3 by I, and putting $q_u = I_u / I_o$

$$j\omega M_{u,1} q_1 + - - - + \left(j\omega L_u + \frac{1}{j\omega C_u}\right) q_u +$$

$$- - - - + j\omega M_{u,N} q_N = 1/j\omega C_u \qquad 3\text{-}1\text{-}4$$

$$1 \leq u \leq N$$

$$V_o / I_o = Z_o = (1 - q_1)/j\omega C_1 + - - - + (1 - q_u)/j\omega C_u$$

$$- - - + (1 - q_N)/j\omega C_N \qquad 3\text{-}1\text{-}5$$

Equation 3-1-4 represents N equations with N unknowns; which are in terms of the q's. These equations can be solved for the q's, which can then be inserted in equation 3-1-5 to obtain the impedance of the coil.

2. Some elementary approximations can be made to equation3-1-4 to test its validity. When N is small the turn inductances L can be considered to be all the same, the mutual inductances M can all be considered to be equal to the turn inductance L, and the turn to turn capacitances can be considered to be all the same. With these approximations equation3-1-4 becomes;

$$(q_1 + q_2 + - - - - + q_N) j\omega L + q_u / j\omega C = 1/j\omega C \qquad 3\text{-}2\text{-}1$$

All N equations are the same, therefore the currents are identical.

$$q_u \left(j\omega NL + \frac{1}{j\omega C} \right) = \frac{1}{j\omega C} \qquad 3\text{-}2\text{-}2$$

Inserting this expression for qu in equation3-1-5 gives

$$Z_0 = \frac{N}{j\omega C} \left\{ 1 - \frac{1}{(\omega^2 NLC - 1)} \right\} \qquad 3\text{-}2\text{-}3$$

Equation3-2-3 is infinite at one frequency only, given by

$$\omega_0 = \frac{1}{\sqrt{NLC}} \qquad 3\text{-}2\text{-}4$$

The circuit has only one resonance, and the impedance is infinite as there is no resistive element. ω_0 is proportional to $N^{-0.5}$, which agrees with the findings of the experiment in Section 2-1, where the graph of the frequency of the fundamental resonance against N has a slope of -0.53 when N is small.

3. When a resistive element is included the equivalent circuit becomes that of Fig.3-1. With this addition equation3-1-4 becomes;

$$j\omega M_{u,1} q_1 + \cdots + \left(j\omega L_u + R_u + \frac{1}{j\omega C_u} \right) q_u + \cdots + j\omega M_{u,N} q_N = \frac{1}{j\omega C_u} \qquad 3\text{-}3\text{-}1$$

Making the same simple approximation for R as for L, M and C equation3-2-3 becomes

$$Z_0 = \frac{N}{j\omega C} \left\{ 1 - \frac{1}{(j\omega CR - \omega^2 L(N+1))} \right\} \qquad 3\text{-}3\text{-}2$$

Figure 3-2

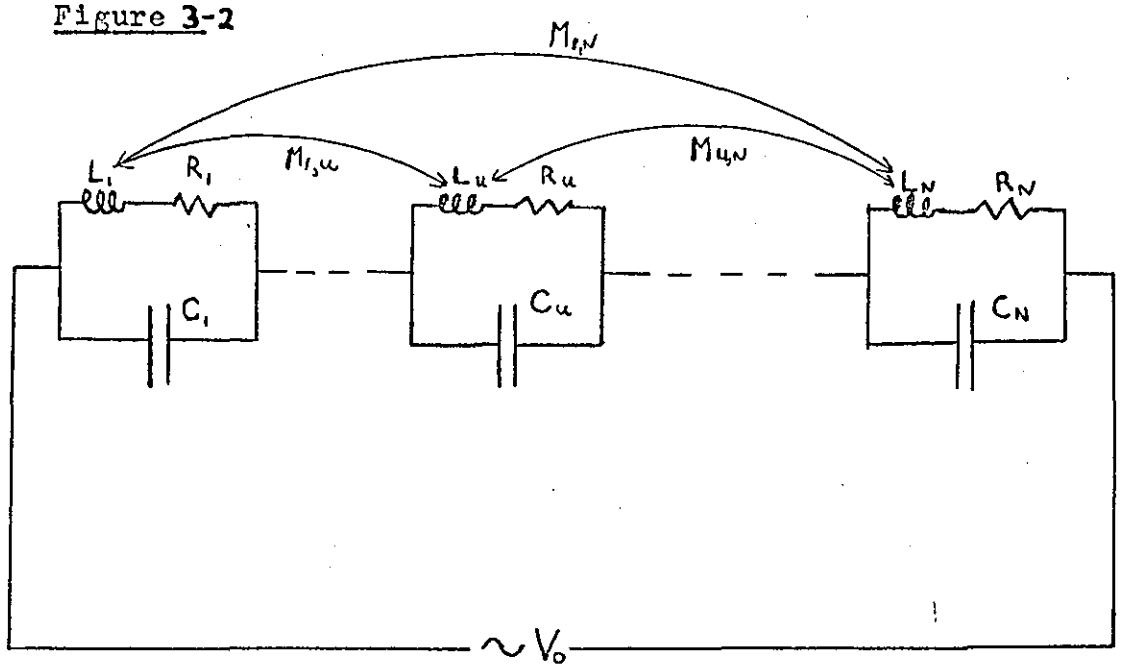

Equivalent circuit including the turn resistance.

Figure 3-3

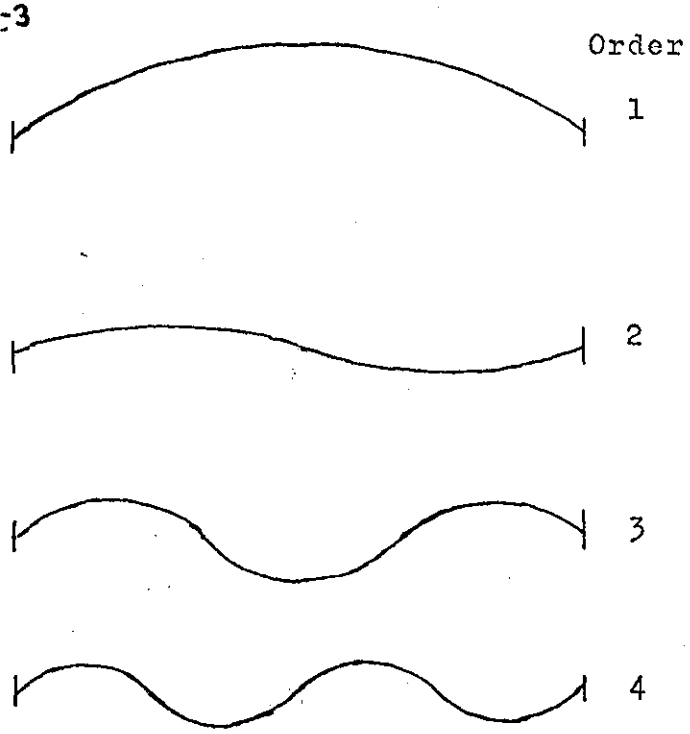

Modes of resonance of a set of coupled pendulums, modes of resonance of order greater than one, show phase changes of 180 degrees in the displacement.

This is equivalent to the single parallel resonant circuit of Fig. 1-3, which has only one resonance.

4. Fig. 3-2 represents what is in essence a set of N, damped, coupled oscillators. In general a set of N such coupled oscillators has N different modes of resonance; which are excited at different frequencies. A simply connected homogeneous oscillator chain has a particularly simple mode structure. Fig. 3-3 shows the amplitude distributions of such an oscillator chain for the first four modes of resonance, |5|. The displacement undergoes phase changes of 180°, or reversals of direction, for modes of resonance of order greater than one.

Fig. 3-2 represents an oscillatory system which is far from being a simply coupled homogeneous oscillator chain. However, it is possible that a type of standing wave behaviour could occur, similar to that shown in Fig. 3-3.

5. Equations 3-2-3 and 3-3-2 do not tend to the correct d.c. limit. When ω equals zero the right hand side of equation 3-1-3 is infinite. To obtain the correct d.c. limit the path of I_0 in Fig. 3-16 would have to be taken down the inductive side of the circuit rather than the capacitive side.

Section 4

Inductance, Resistance and Capacitance per Turn

1. Inductance

The self-inductance of a single turn of foil and the mutual inductance between two co-axial turns of foil are required. The situation for the single turn of foil is shown in Fig.4-1, the total current I is spread over the width of the foil. This makes the problem look similar to that of calculating the inductance of a single layer solenoid, which involves the magnetic field of a current sheet. The similarity is superficial as the current in a solenoid must have the magnitude throughout the coil, whereas the current density in a foil may not be uniform across the width.

This can be shown by assuming, for the moment, that the current is uniform across the width of the foil. The magnetic field $\underline{H}$ of this current sheet will vary along the Z axis, points near the end of the coil are further away from most of the current than are points near the centre. If we cut the width W of the foil into strips, each of width dz, each strip has inductance given by

$$L(z) = \frac{\underline{\Phi}(z)}{J(z)\,dz} \qquad 4\text{-}1\text{-}1$$

Where $\underline{\Phi}(z)$ is the total flux, $\underline{\beta}$ through the area the strip encloses, $J(z)$ is the current per unit width and $L(z)$ is the self-inductance of the strip. As $\underline{\Phi}(z)$ is dependent on z, $L(z)$ will be dependent on z. If $L(z)$ is dependent on z, $J(z)$ will be dependent on z, providing that there is a constant voltage V on the foil.

Neglecting the resistance of the foil, the admittance of the strip of foil is given by

$$\underline{Y}\,dz = \frac{J(z)\,dz}{j\omega\,\underline{\Phi}(z)} \qquad 4\text{-}1\text{-}2$$

Where $\underline{Y}$ is the admittance per unit width. The total admittance is given by

$$Y_T = \int_{-W/2}^{W/2} Y(z)\, dz = \int_{-W/2}^{W/2} \frac{J(z)\, dz}{j\omega \underline{E}(z)} \qquad 4\text{-}1\text{-}3$$

It would require a full field theory solution to establish the relationship between $J(z)$, $\underline{E}(z)$ and $Y(z)$. Such a solution has been attempted (6), but met with severe difficulties. Therefore the simpler method has been adopted of making $J(z)$ and $\underline{E}(z)$ independent of Z. The obvious approximation for $J(z)$ is to make the current density uniform across the width of the foil. The value of $\underline{H}$ at the centre of the foil or the value at the end of the foil could have been used, but the former method would give a high value for L while the latter would give a low value. So the average value of $\underline{H}$ was taken over the width of the foil.

$$\bar{H}_z = \frac{1}{W} \int_{-W/2}^{W/2} H_z\, dz \qquad 4\text{-}1\text{-}4$$

This was used to calculate an average value of $\underline{E}(z)$

$$\bar{\underline{E}} = \iint \bar{H}_z\, dx\, dy \qquad 4\text{-}1\text{-}5$$

where $\bar{H}_z$ and $\bar{\underline{E}}$ are the averaged values.

When these approximations are inserted in equation 4-1-3

$$Y = \int_{-W/2}^{W/2} \frac{J\, dz}{j\omega \bar{\underline{E}}} \qquad 4\text{-}1\text{-}6$$

giving an inductance of

$$L = \frac{\bar{\underline{E}}}{I} \qquad 4\text{-}1\text{-}7$$

where I is the total current flowing in the foil.

2. The magnetic field $\underline{H}$ is given by

$$\underline{H} = \frac{1}{4\pi} \iiint \frac{J\, \underline{n} \times \underline{r}_0\, d\tau}{r_0^3} \qquad 4\text{-}2\text{-}1$$

where J is a current element with direction $\underline{n}$, $d\tau$ is the volume element, and r_0 is the length vector between the point where H is being

evaluated and the current element J . This is shown in Fig.4-2. $\underline{H}$ is evaluated at the point (x, y, z) and J at the point (x_1, y_1, z_1)

Therefore

$$\underline{r}_0 = \underline{r}(x, y, z) - \underline{r}_1(x_1, y_1, z_1) \qquad 4\text{-}2\text{-}2$$

$\underline{n}$ lies on the circle $x_1^2 + y_1^2 = r_1^2$, z constant, in the direction of J . Therefore,

$$\underline{n} = \left(-y_1/r_1 , x_1/r_1 , 0\right) \qquad 4\text{-}2\text{-}3$$

As only the z component of $\underline{H}$ is of interest in evaluating $\bar{\Phi}$ we neglect the x and y components. Equation 4-2-1 when combined with 2-2 and 2-3 gives

$$H_z = \frac{1}{4\pi} \iiint J \left\{ -\frac{y_1}{r_1}(y - y_1) - \frac{x_1}{r_1}(x - x_1) \right\} \frac{d\tau}{r_0^3} \qquad 4\text{-}2\text{-}4$$

Equation 4-2-4 when transformed to cylindrical polar coordinates becomes

$$H_z = \frac{1}{4\pi} \iiint J \left\{ -\sin\theta_1 (r \sin\theta - r_1 \sin\theta_1) - \cos\theta_1 (r\cos\theta - r_1 \cos\theta_1) \right\} \frac{r_1 dr_1 d\theta_1 dz_1}{r_0^3} \qquad 4\text{-}2\text{-}5$$

where the $\theta = 0$ axis coincides with the x axis. The problem can be simplified if we evaluate the H_z component in the $\theta = 0$ plane, The situation has cylindrical symmetry, therefore all points lying on any circle r will have the same magnetic field. When $\theta = 0$ equation 4-2-5 becomes,

$$H_z = \frac{1}{4\pi} \iiint J \left(r_1 \sin^2\theta_1 - r\cos\theta_1 + r_1 \cos^2\theta_1 \right) \frac{r_1 dr_1 d\theta_1 dz_1}{r_0^3} \qquad 4\text{-}2\text{-}6$$

The limits on z_1 are $+W/2$ and $-W/2$. The limits on θ_1 are 0 and 2π . If the foil is taken to be infinitely thin, J goes from being a current per unit area to a current per unit length and the volume integral over three dimensions becomes one over two; θ_1 and z_1 . As the current is assumed to be uniform over the width

Figure 4-1

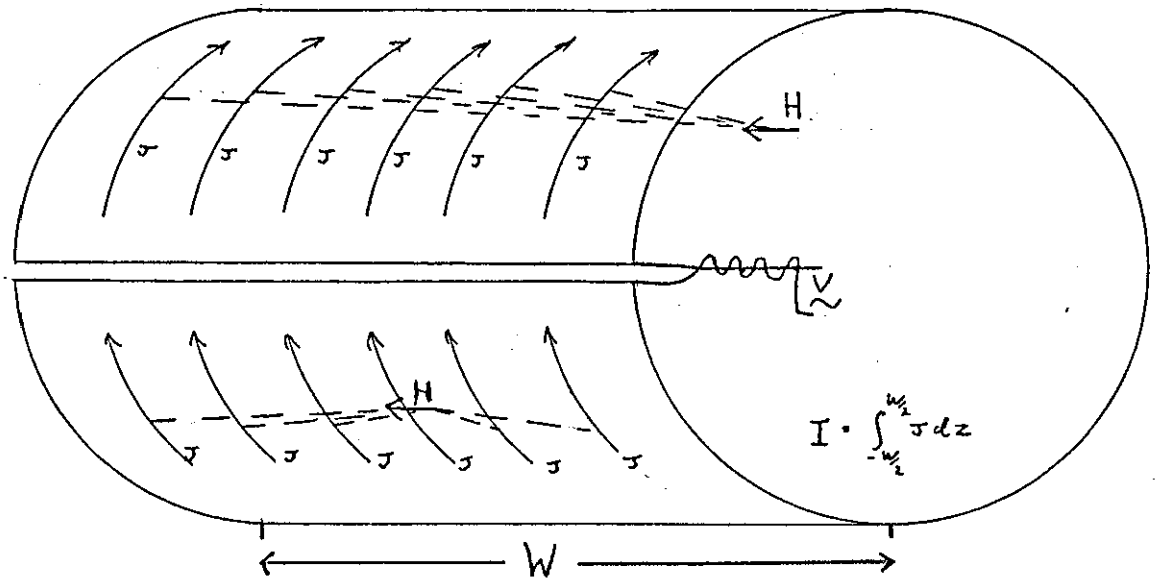

Figure 4-2

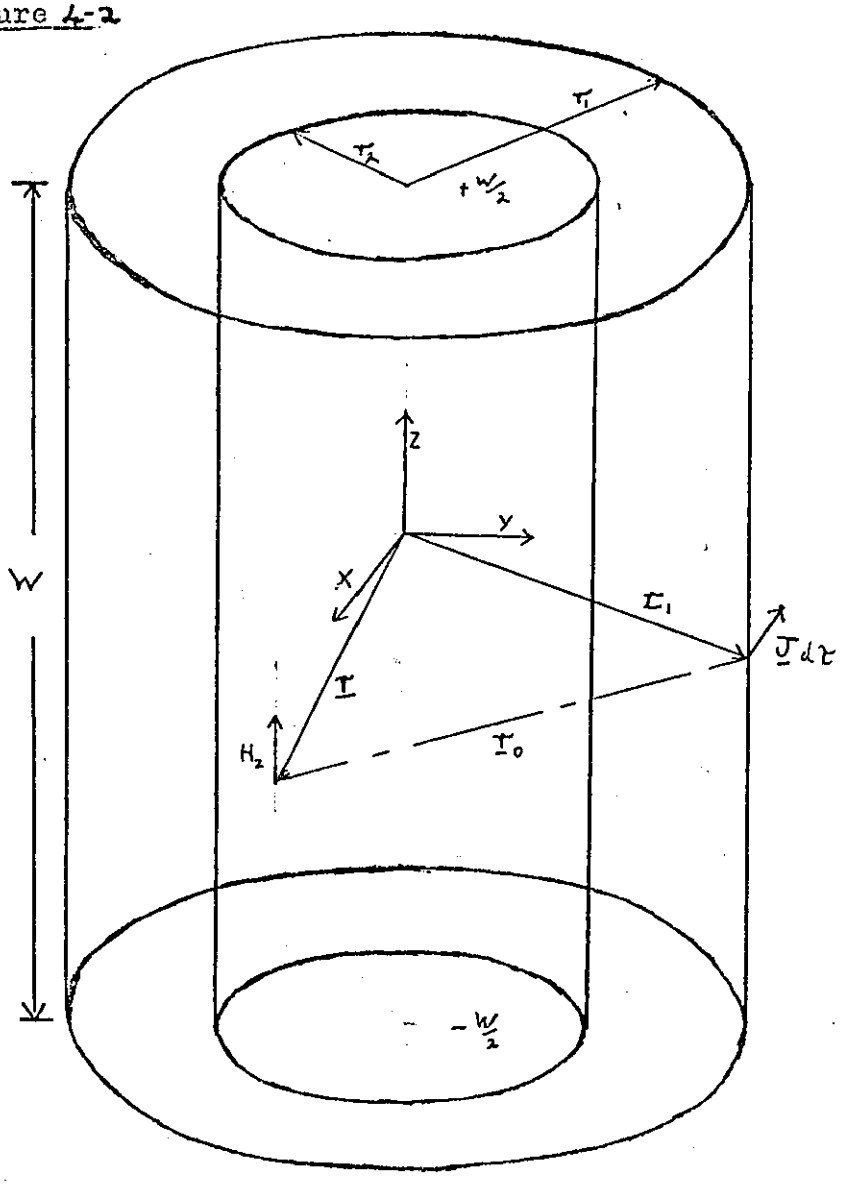

$$J = \frac{I}{W} \qquad 4\text{-}2\text{-}7$$

Now

$$r_0 = \left| \underline{r}(x, y, z) - \underline{r}_1(x_1, y_1, z_1) \right| \qquad 4\text{-}2\text{-}8$$

Expressing $\underline{r}$ and $\underline{r}_1$ in cylindrical polar form and remembering that $\theta = 0$, r_0 becomes

$$r_0 = \left| (r - r_1 \cos\theta_1 \; , - r_1 \sin\theta_1 \; , z - z_1) \right| \qquad 4\text{-}2\text{-}9$$

Taking the magnitude r_0 becomes

$$r_0 = \left\{ r_1^2 + r^2 - 2 r r_1 \cos\theta_1 + (z - z_1)^2 \right\}^{1/2} \qquad 4\text{-}2\text{-}10$$

Combining this expression for r_0 with equations 4-2-6 and 4-2-7, H_z becomes

$$H_z = \frac{I}{4\pi W} \int_0^{2\pi} \int_{-W/2}^{W/2} \frac{(r_1 - r\cos\theta_1)\, r_1 \, d\theta_1 \, dz_1}{\left\{ r_1^2 - r^2 - 2 r r_1 \cos\theta_1 + (z - z_1)^2 \right\}^{3/2}} \qquad 4\text{-}2\text{-}11$$

The integral over z_1 is of the form, (7)

$$\int \frac{dx}{(ax^2 + bx + c)^{3/2}} = \left[\frac{2(2ax + b)}{(4ac - b)(ax^2 + bx + c)^{1/2}} \right] \qquad 4\text{-}2\text{-}12$$

Performing this integration over z_1 in equation 4-2-11 gives

$$H_z = \frac{I}{4\pi W} \int_0^{2\pi} \left[\frac{r_1 (r_1 - r\cos\theta_1)(z_1 - z)\, d\theta_1}{(r_1^2 + r^2 - 2 r_1 r \cos\theta_1)\left[r_1^2 + r^2 - 2 r_1 r \cos\theta_1 + (z - z_1)^2 \right]^{1/2}} \right]_{-\frac{W}{2}}^{\frac{W}{2}} \qquad 4\text{-}2\text{-}13$$

When the limits are inserted

$$H_z = \frac{I}{4\pi W} \int_0^{2\pi} \frac{r_1 (r_1 - r\cos\theta_1)\, d\theta_1}{(r_1^2 + r^2 - 2 r_1 r \cos\theta_1)} \left\{ \frac{(W/2 - z)}{\left[r_1^2 + r^2 - 2 r_1 r \cos\theta_1 + (z - W/2)^2 \right]^{1/2}} \right.$$

$$\left. - \frac{(W/2 + z)}{\left[r_1^2 + r - 2 r_1 r \cos\theta_1 + (z + W/2)^2 \right]^{1/2}} \right\} \qquad 4\text{-}2\text{-}14$$

At this point we eliminate the variation of H_z w.r.t. z by

averaging over H_z

$$\bar{H}_z = \frac{1}{W}\int_{-W/2}^{W/2} H_z \, dz \qquad 4\text{-}2\text{-}15$$

This integral is of the form, (7)

$$\int \frac{x\,dx}{(ax^2+b)^{1/2}} = \left[\frac{(ax^2+b)^{1/2}}{a}\right] \qquad 4\text{-}2\text{-}16$$

if the substitutions $x = W/2 - z$ and $x = W/2 + z$ are made.

Performing the operations of equation 4-2-15 and 4-2-16 on the expression for H_z, equation 4-2-14, gives

$$\bar{H}_z = \frac{I}{2\pi W^2}\int_0^{2\pi} \frac{r_1(r_1 - r\cos\theta_1)\,d\theta_1}{(r_1^2 + r^2 - 2r_1 r\cos\theta_1)} \left\{ (r_1^2 + r^2 - 2r_1 r\cos\theta_1 + W^2)^{1/2} - (r_1^2 + r^2 - 2r_1 r\cos\theta_1)^{1/2} \right\} \qquad 4\text{-}2\text{-}17$$

The self-inductance on the foil of radius r_1 is obtained from the total flux $\bar{\Phi}_1$, which is given by

$$\bar{\Phi}_1 = \int_0^{r_1} 2\pi r \mu_0 \bar{H}_z \, dr \qquad 4\text{-}2\text{-}18$$

The mutual inductance of two foils, as shown in Fig. 4-2, is obtained from

$$\bar{\Phi}_{12} = \int_0^{r_2} 2\pi r \mu_0 \bar{H}_z \, dr \qquad 4\text{-}2\text{-}19$$

Combining equations 4-2-17 and 4-2-18 gives

$$\bar{\Phi}_1 = \frac{I\mu_0}{W^2}\int_0^{r_1}\int_0^{2\pi} \frac{d\theta_1\,dr\,r\,r_1(r_1 + r\cos\theta_1)}{(r_1^2 + r^2 - 2r_1 r\cos\theta_1)} \left\{ (r_1^2 + r^2 - 2r_1 r\cos\theta_1 + W^2)^{1/2} - (r_1^2 + r^2 - 2r_1 r\cos\theta_1)^{1/2} \right\} \qquad 4\text{-}2\text{-}20$$

Equation 4-2-20 could be evaluated in terms of Elliptic integrals. These are infinite series which have to be evaluated numerically. Rather than do this equation 4-2-16 would be better evaluated using a numerical double integration. However an approximation will be used which is derived by assuming that $\bar{H}_z$ is uniform over r and equal to the

field at $r = 0$. This gives,

$$\Phi_1 = \frac{I \mu_0}{W^2} \int_0^{r_1} \int_0^{2\pi} d\theta_1 \, dr_1 \, r \left\{ (W^2 + r_1^2)^{1/2} - r_1 \right\} \qquad 4\text{-}2\text{-}21$$

When the integrations are performed

$$\Phi_1 = \frac{\pi r_1^2 I \mu_0}{W^2} \left\{ (W^2 + r_1^2)^{1/2} - r_1 \right\} \qquad 4\text{-}2\text{-}22$$

The self-inductance is given by

$$L_1 = \frac{\Phi_1}{I} \qquad 4\text{-}2\text{-}23$$

Combining equations 4-2-23 and 4-2-22 gives L_1 as

$$L_1 = \frac{\pi r_1^2 \mu_0}{W^2} \left\{ (W^2 + r_1^2)^{1/2} - r_1 \right\} \qquad 4\text{-}2\text{-}24$$

The mutual-inductance from the foil radius r_1 to the foil radius r_2 is given by

$$M_{12} = \frac{\Phi_{12}}{I} \qquad 4\text{-}2\text{-}25$$

where I is the current flowing in the foil radius r_1 .

Therefore

$$M_{12} = \frac{\pi r_2^2 \mu_0}{W^2} \left\{ (W^2 + r_1^2)^{1/2} - r_1 \right\} \qquad 4\text{-}2\text{-}26$$

By the mutual-inductance reciprocity theorem, [see appendix 1,]

$$M_{12} = M_{21} \qquad 4\text{-}2\text{-}27$$

When $W \ll r_1$, equation 4-2-24 reduces to

$$L_1 = \frac{\pi r_1^2 \mu_0}{W^2} \left\{ r_1 \left(1 + \frac{W^2}{r_1^2} \right)^{1/2} - r_1 \right\} \qquad 4\text{-}2\text{-}28$$

$$\underset{W \to 0}{=} \pi r_1^2 \mu_0 \left\{ \frac{1}{W^2} \cdot \frac{W^2}{2 r_1} \right\} \qquad 4\text{-}2\text{-}29$$

$$= \frac{\pi r_1^2 \mu_0}{2} \qquad 4\text{-}2\text{-}30$$

crude
This is the usual approximation for the inductance of a single turn of wire.

One point to note is that in an actual foil wound coil a large volume of the outer turns will contain the aluminium of the inner turns, However the relative permeability of aluminium is close to 1, and therefore can reasonably be neglected.

3. At low frequency the circuit of Fig. 3-16 Section 3 reduces to a pure inductance. The impedance of the capacitances will be large. Since the current must then be the same through all the inductances, L_1 to L_N, the total inductance will be given by

$$L = \sum_{u=1}^{N} \left(L_u + \sum_{v=1, v \neq u}^{N} M_{u,v} \right) \qquad 4\text{-}3\text{-}1$$

By inserting the expressions in equations 4-2-20 and 4-2-21 for the self and mutual inductances and evaluating equations 4-3-1 for an actual coil, a measure of the accuracy of the approximations may be found. For convenience the coil chosen was the 150 turn coil used in Section 2-2. Numerical evaluation on the computer gave a value for L of:

$$L = 113.4\ \mu H \qquad 4\text{-}3\text{-}2$$

The experimental values for the inductance were, for the five coils:-

Self Inductance	error
109.0 μH	$\pm$ 0.5 μH
104.5 "	"
108.5 "	"
108.5 "	"
104.0 "	"

values were measured on a Wayne Kerr Universal R.F. Bridge (Sections B602 and SR268) at 100 kHz. The frequency is far enough away from the first resonance at 3.26 MHz.

The average self-inductance for the 5 coils is 108.1 μH with a

spread of $\pm 1.0\,\mu H$, giving an error of ±1%. The calculated value is $113.4\,\mu H$ giving an error of +4.9%. From this short example in the relevant range of parameters we conclude that the approximations used to calculate the individual inductances are in fact reasonable and can give reasonable answers without further elaboration at this stage.

4. Resistance

The d.c. resistance per turn is given by

$$R_u = 2\pi r_u \rho / W m \qquad 4\text{-}4\text{-}1$$

Where r_u is the radius of the turn, W the width and m the thickness of the metal. ρ is the resistivity of the metal.

The a.c. resistance, which will be significant in the MHz frequency range, is difficult to calculate, and therefore it will be attempted later in Section 7, At this stage only the d.c. resistance will be used. Although this will probably result in large errors in predicted Q values, it should be possible to tell if the proposed equivalent circuit has any general validity.

5. Capacitance

Neglecting end effects and the curve of the foil, the turn to turn capacitance will be given by the parallel plate formula

$$C_u = \frac{\varepsilon \varepsilon_0 \text{ Area of the Plates}}{\text{Separation of the Plates}} \qquad 4\text{-}5\text{-}1$$

For two turns of mean radius r_u width W and a dielectric of thickness d, equation 4-5-1 becomes

$$C_u = \frac{2\pi r_u W \varepsilon \varepsilon_0}{d} \qquad 4\text{-}5\text{-}2$$

where ε is the dielectric constant of the plastic.

The problem with equation 4-5-2 is not that it is fundamentally wrong, but the winding tension and the side slip of the metal foil, when the coils

are wound , make the parameters W and d inaccurate. A standard method of tackling this in wound plastic and foil capacitors is to heat them to 100°C for 1 hour. This shrinks the plastic, decreasing the foil separation. To test this a 30 turn capacitor with polypropylene dielectric of 12·5 μm thickness, metal foil of 5·0 μm thickness and 3·9 cm width was use The core radius was 1·0 cm. The total capacitance is given by

$$C = \sum_{u=1}^{2N-1} \frac{2\pi r_u \varepsilon \varepsilon_0 W}{d} \qquad 4\text{-}5\cdot3$$

Where N is the number of turns

As the core is large, the increase in radius is neglected and a mean radius r used.

Inserting the dimensions in equation 6-3 yields a value for C of

$$C = 0\cdot2254\ \mu F$$

The experimental value measured on a Hewlett Packard Universal Bridge (Type 4265A), at a frequency of 1 KHz, is

$$C = 0\cdot2115\ \mu F \pm 0\cdot002\ \mu F$$

This value before the capacitor was heat treated is low by 6%. After the capacitor was heated to 100°C for 1 hour the capacitance increased to

$$C = 0\cdot2304\ \mu F \pm 0\cdot002\ \mu F$$

This value is high, compared with the theory, by 2.2%. The heat treatment has over-compensated and the experimental value has gone from being low to being high. However the error, after the heat treatment, has been reduced to ±2.2%; therefore heat treated FWI should have a better characterised turn-to-turn capacitance.

6. Heat treatment

It would appear that to obtain a calculable turn to turn capacitance

Figure 4-3

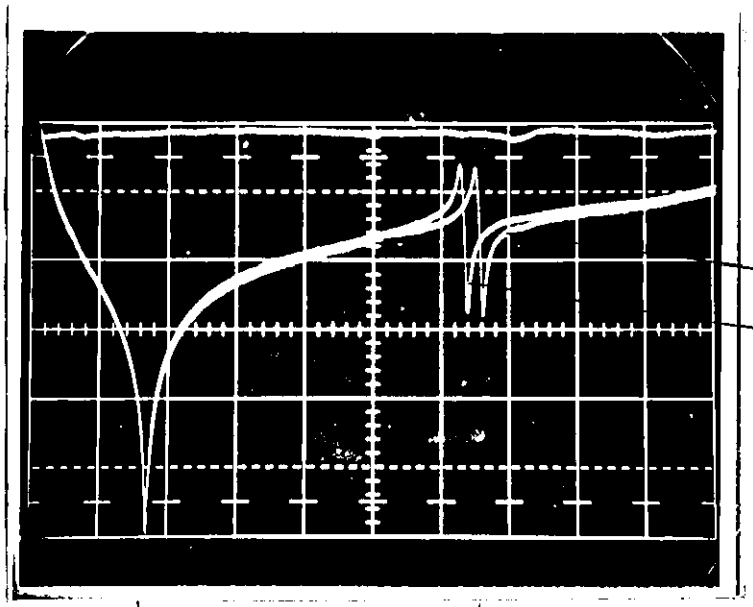

Effect of heating to 100c for 1 hour on a 150 turn coil.

Figure 4-4

Coil No.	Freq.of first resonance,MHz Error ±0.01 Before	After	Freq.of second max.resonance, MHz.Error±0.01 Before	After
2	3.16	3.12	13.02	12.85
3	3.21	3.12	13.22	13.00
4	3.33	3.31	12.93	12.77
5	3.27	3.25	13.08	12.94
Average	3.26	3.24	13.09	12.87
Total spread	0.17	0.12	0.27	0.23

the coils require to be heat treated. To test the effect of this, four of the 150 turn FWI made for the reproducability test of section 2-2 were heated to 100°C for 1 hour. Fig.4-3 shows the result for one of the coils, the fundamental resonance has hardly moved, but the secondary resonance has moved 0.4 MHz. Fig.4-4 shows the results for all four coils. The frequency of the fundamental resonance has moved -0.02 MHz, which is much less than the spread of the results. The frequency of the second maximum impedance resonance has moved -0.22 MHz which is more significant, although it is not much larger than the spread.

The conclusion is that when comparing the theory with experiment the coils should be heat treated first.

7. One point to note is that if the FWI has foil of width much greater than the radii of the turns of the coil, equation 4-2-24

$$L_1 = \frac{\pi r_1^2 \mu_0}{W^2} \left[(W^2 + r_1^2)^{1/2} - r_1 \right] \qquad 4\text{-}2\text{-}24$$

can be approximated as

$$L_1 = \frac{\pi r_1^2 \mu_0}{W} \qquad 4\text{-}2\text{-}30$$

When equation 4-7-1 is combined with the capacitance formula equation 4-5-2

$$C_1 = \frac{2\pi r_1 W \epsilon \epsilon_0}{d} \qquad 4\text{-}5\text{-}2$$

the resonant frequency of one turn is given by

$$\omega_1 = \left(\frac{1}{L_1 C_1} \right)^{1/2} = \frac{1}{\pi} \left(\frac{d}{2 \mu_0 \epsilon \epsilon_0 r} \right)^{1/2} \qquad 4\text{-}7\text{-}1$$

For coils with an outside radius much less than the width the resonant frequency of the coils should be independent of their width.

Section 5 Numerical Solution of the Equivalent Circuit

1. The equivalent circuit is described by N equations of the type 3-3-1, where the q's are the unknowns.

$$\cdots + j\omega M_{u,1} q_1 + \cdots + \left(j\omega L_u + R_u + \frac{1}{j\omega C_u}\right) q_u + \cdots + j\omega M_{u,N} q_N = \frac{1}{j\omega C_u} \qquad 1 \le u \le N \qquad 3\text{-}3\text{-}1$$

These N equations can be expressed as a matrix equation of the form

$$\left\{[A_R] + j\,[A_I]\right\}\left\{\underset{\sim}{x} + j\,\underset{\sim}{y}\right\} = j\,\underset{\sim}{\beta} \qquad 5\text{-}1\text{-}1$$

Where $[A_R]$ and $[A_I]$ are N x N matrices, $[A_R]$ being the real coefficients and $[A_I]$ the imaginary coefficient of the L.H.S. of equation 3-3-1. $\underset{\sim}{x}$, $\underset{\sim}{y}$ and $\underset{\sim}{B}$ are N vectors, $\underset{\sim}{x}$ and $\underset{\sim}{y}$ being the real and imaginary parts of the q's respectively, $\underset{\sim}{B}$ being the R.H.S. of equation 3-3-1.

Equation 1-1 could possible be solved by several different numerical methods; elimination, iteration or matrix inversion. However each of these methods is suited to a different type of matrix. The matrix $[A_R]$ has the form;

$$\begin{bmatrix} R_1 & \cdot & \cdot & \cdot \\ \cdot & R_2 & \cdot & \cdot \\ \cdot & \cdot & \ddots & \cdot \\ \cdot & \cdot & R_u & \cdot \\ \cdot & \cdot & \cdot & \ddots \\ \cdot & \cdot & \cdot & R_N \end{bmatrix} \qquad 5\text{-}1\text{-}2$$

All the off diagonal elements are zero.

The matrix $[A_I]$ has the form

$$\begin{bmatrix} \omega L_1 - \frac{1}{\omega C_1} & - & - & \omega M_{1,u} & - & \omega M_{1N} \\ - & \omega L_2 - \frac{1}{\omega C_2} & - & - & - & - \\ \omega M_{u,1} & - & \omega L_u - \frac{1}{\omega C_u} & & \omega M_{u,N} & \\ \omega M_{N,1} & - & - & \omega M_{N,u} & \omega L_N - \frac{1}{\omega C_N} & \end{bmatrix} \qquad 5\text{-}1\text{-}3$$

The matrix $[A_I]$ is symmetrical; $M_{u,v} = M_{v,u}$. At low frequency the matrix is diagonally dominant, $\frac{1}{\omega C} >> \omega L$. When the frequency is raised the matrix becomes less diagonal, until the diagonal elements go through zero in turn starting at (1,1), which lies on the circumference of the coil and has a larger L and C, at a frequency given by

$$\omega_o^u = \left(\frac{1}{L_u C_u}\right)^{1/2} \qquad 5\text{-}1\text{-}4$$

If all the ω_o^u are grouped close together in frequency, the matrix will not be diagonally dominant. In this frequency range the matrix equation will not be amenable to a straight-forward iterative solution [8]. Although an iterative scheme could be found an elimination or matrix inversion method would seem more suitable, as these are usable over the whole frequency range.

To solve equation 5-1-1 by an elimination method it is expanded into a wholly real form.

$$\left.\begin{aligned} [A_R]\underset{\sim}{x} - [A_I]\underset{\sim}{y} &= \underset{\sim}{0} \\ [A_I]\underset{\sim}{x} + [A_R]\underset{\sim}{y} &= \underset{\sim}{\beta} \end{aligned}\right\} \qquad 5\text{-}1\text{-}5$$

This is equivalent to the 2N x 2N matrix equation

$$\begin{bmatrix} [A_R], & -[A_I] \\ [A_I], & [A_R] \end{bmatrix} \begin{bmatrix} \underset{\sim}{x} \\ \underset{\sim}{y} \end{bmatrix} = \begin{bmatrix} \underset{\sim}{0} \\ \underset{\sim}{\beta} \end{bmatrix} \qquad 5\text{-}1\text{-}6$$

To solve equation 5-1-1 by a matrix inversion method, equations 5-1-5 are eliminated to find $\underset{\sim}{x}$ and $\underset{\sim}{y}$

$$\begin{aligned} \left([A_I]^{-1}[A_R] + [A_R]^{-1}[A_I]\right)\underset{\sim}{x} &= [A_R]^{-1}\underset{\sim}{\beta} \\ \left([A_I]^{-1}[A_R] + [A_R]^{-1}[A_I]\right)\underset{\sim}{y} &= [A_I]^{-1}\underset{\sim}{\beta} \end{aligned} \qquad 5\text{-}1\text{-}7$$

Since the coefficients of the L.H.sides of both equations 5-1-7 are the same, the equations can be solved at the same time by having two R.H.sides to the final inversion or elimination.

The elimination of equation 5-1-6 requires approximately $8\frac{N^3}{3}$ computations whereas the matrix inversion, equation 1-7 requires approximately $7\frac{N^3}{3}$ computations, [9].

However, before either method can be implemented one problem still remains. As it stands, the equivalent circuit is too large for practical purposes, The matrices $[A_R]$ and $[A_I]$ for a 1000 turn coil would be 1000 x 1000 in size. To solve a matrix equation of this size the large number of times required to form the impedance/frequency spectrum would require an inordinately large amount of computer time. Therefore the equivalent circuit has to be reduced in size without destroying its validity.

2. The reducting can be carried out by using a number of approximations. The first is an extension of the approximation used to derive the equivalent circuit. It is assumed that the coil can be divided into S sections, each composed of T consecutive turns, and that the magnitude and phase of the current does not vary within any section. The second approximation is that in any section the inductance and resistance per turn and the turn to turn capacitance can be represented by an average value. It follows that the turns within one section are perfectly coupled and that the mutual inductance from a turn in one section to a turn in another is the same for all turns in both sections.

The situation is now that shown in Fig. 5-1. The inductances, self and mutual, can be added to give a total inductance of $T^2L_{u'}$ the resistances add to give a total resistance of $TR_{u'}$ and the capacitances add to give a total capacitances of Cu/T. The mutual inductance from one section to another becomes $T^2M_{u,v}$.

Figure 5-1

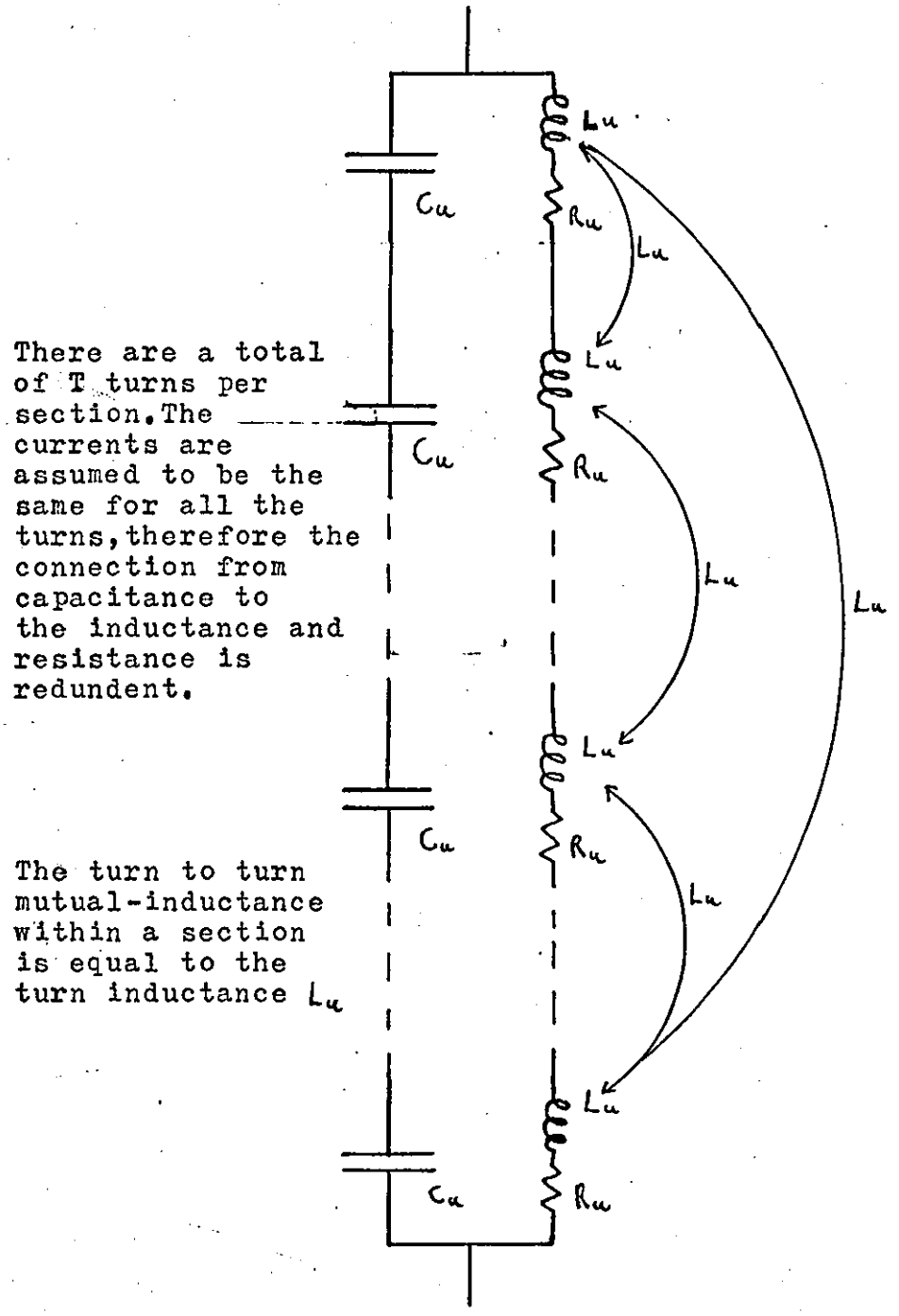
There are a total of T turns per section. The currents are assumed to be the same for all the turns, therefore the connection from capacitance to the inductance and resistance is redundent.
The turn to turn mutual-inductance within a section is equal to the turn inductance L_u
L_u
C_u
R_u
L_u
L_u
C_u
R_u
L_u
L_u
L_u
C_u
R_u
L_u
L_u
C_u
R_u

As the total number of sections is S, the circuit equations 3-3-1 and 3-1-5 become,

$$j\omega T^2 M_{u,1} q_1 + \cdots + (j\omega T^2 L_u + \frac{T}{j\omega C_u} + TR_u) q_u + \cdots + j\omega T^2 M_{u,s} q_s = \frac{T}{j\omega C_u} \qquad 1 \le u \le S \qquad 5\text{-}2\text{-}1$$

and

$$\frac{V_0}{T_0} = Z_0 = (1-q_1)\frac{T}{j\omega C_1} + \cdots + (1-q_u)\frac{T}{j\omega C_u} + \cdots \qquad 5\text{-}2\text{-}2$$

The average Lu, Cu and Ru are calculated using the mean radius of the particular section. The mutual inductance Mu, ν is calculable using the mean radii of the particular sections in question.

3. The Gaussian elimination was finally chosen, although it takes longer—it is easier to implement, and many books deal with it specifically, e.g. [10]

The Gaussian method of solving simultaneous equations is in essence simple. If we have a set of equations as shown below

$$a_{11}x_1 + a_{12}x_2 + a_{13}x_3 = b_1 \qquad 5\text{-}3\text{-}1$$

$$a_{21}x_1 + a_{22}x_2 + a_{23}x_3 = b_2 \qquad 5\text{-}3\text{-}2$$

$$a_{31}x_1 + a_{32}x_2 + a_{33}x_3 = b_3 \qquad 5\text{-}3\text{-}3$$

Then to eliminate a_{21} we multiply 5-3-1 by m_2 and subtract from 5-3-2, where $m_2 = a_{21}/a_{11}$.

This gives; $(a_{21} - m_2 a_{11})x_1 + (a_{22} m_2 a_{12})x_2 + (a_{23} - m_2 a_{13})x_3$

$$= b_2 - m_2 b_1 \qquad 5\text{-}3\text{-}4$$

Putting,

$$\left.\begin{aligned} a'_{22} &= a_{22} - m_2 a_{12} \\ a'_{23} &= a_{23} - m_2 a_{13} \\ b_2' &= b_2 - m_2 b_1 \end{aligned}\right\} \qquad 5\text{-}3\text{-}5$$

gives, when inserted in §3-4:

$$a'_{22}\, x_2 + a'_{23}\, x_3 = b'_2 \qquad 5\text{-}3\text{-}6$$

Letting $m_3 = {}^{a}31/a_{11}$ and repeating the above procedure gives for §3-3;

$$a'_{32}\, x_2 + a'_{33}\, x_3 = b'_3 \qquad 5\text{-}3\text{-}7$$

Therefore,

$$a_{11} x_1 + a_{12} x_2 + a_{13} x_3 = b_1 \qquad 5\text{-}3\text{-}1$$

$$a'_{22}\, x_2 + a'_{23} x_3 = b'_2 \qquad 5\text{-}3\text{-}6$$

$$a'_{23}\, x_2 + a'_{33} x_3 = b'_3 \qquad 5\text{-}3\text{-}7$$

Multiplying §3-6 by m'_3 and subtracting from §3-7, where $m'_3 = {}^{a'}32/a_{22}$, gives,

$$a''_{33}\, x_3 = b_3'' \qquad 5\text{-}3\text{-}8$$

Back substituting into §3-6 and §3-1 gives,

$$\left.\begin{aligned} x_3 &= b_3''/a''_{33} \\ x_2 &= (b'_2 - a'_{23} x_3)/a'_{22} \\ x_3 &= (b_1 - a_{12} x_2 - a_{13} x_3)/a_{11} \end{aligned}\right\} \qquad 5\text{-}3\text{-}9$$

The equations §3-9 give the solution. However if the element a_{11} or a'_{22} is small, then the corresponding multiplier m_2, m_3 or m'_3 will be large Clearly this would give rise to large errors or totally meaningless answers.

Therefore the technique of Partial Pivoting is used. This involves hunting the column to be eliminated for the largest element and using the row containing this element as the eliminating row..

The flow diagrams for eliminating a matrix of size H and form

$$[a]\underset{\sim}{x} = \underset{\sim}{b} \qquad 5\text{-}3\text{-}10$$

are shown in Figs5-2,5-3 and5-4.

After the matrix equation is solved for the currents, the q's, they are then inserted in equation 3-1-5, to find Z_o the impedance of the coil.

The actual program used, written in 1900 Fortran, is shown in Appendix 3.

The program for calculating the values of the mutual-inductance, self-inductance, capacitance and resistance per section is shown in Appendix 2.

Figure 5-2 The Flow Diagram of the Gaussian Elimination

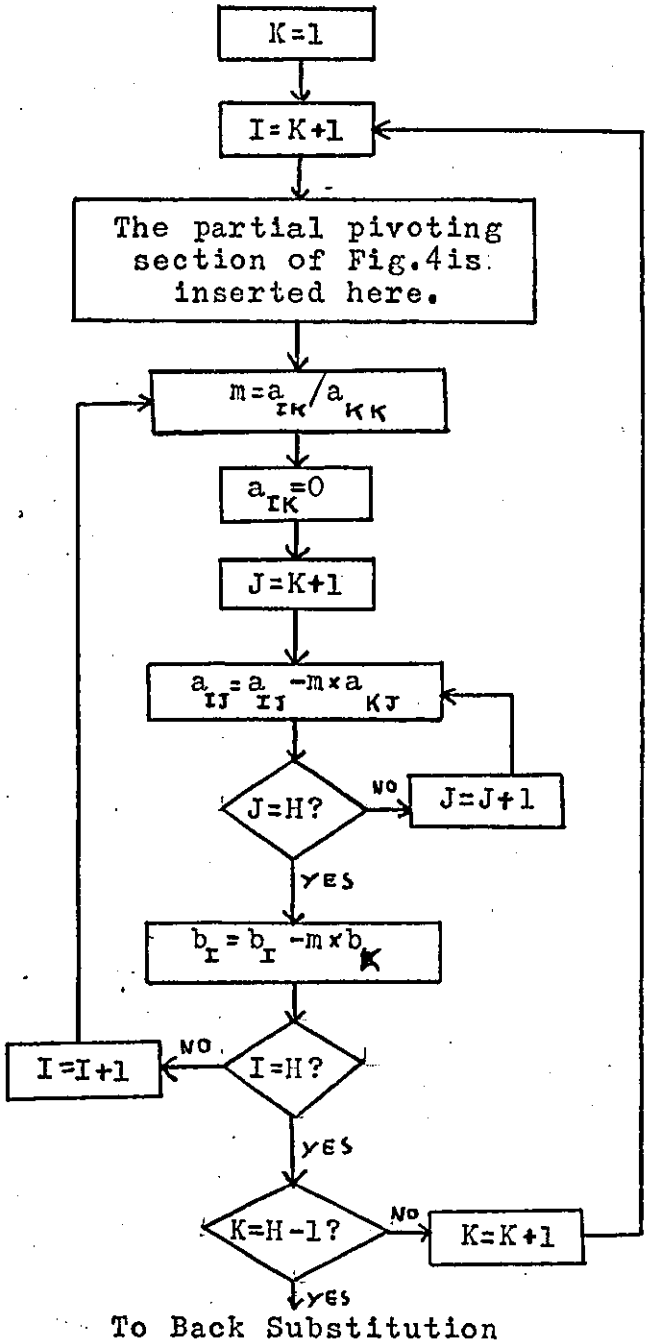

Figure 5-3 The Flow Diagram of the Back Substitution

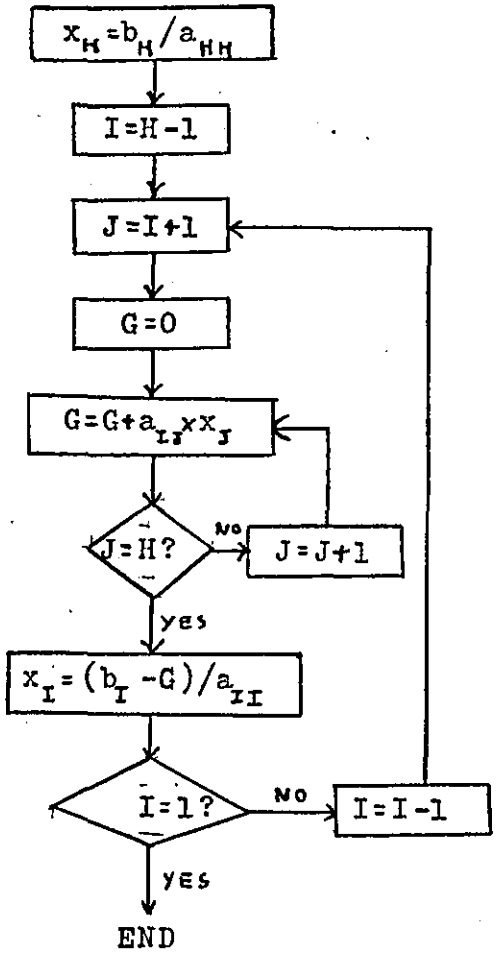

Figure 5-4 The flow Diagram of the Partial Pivoting Section of the Program

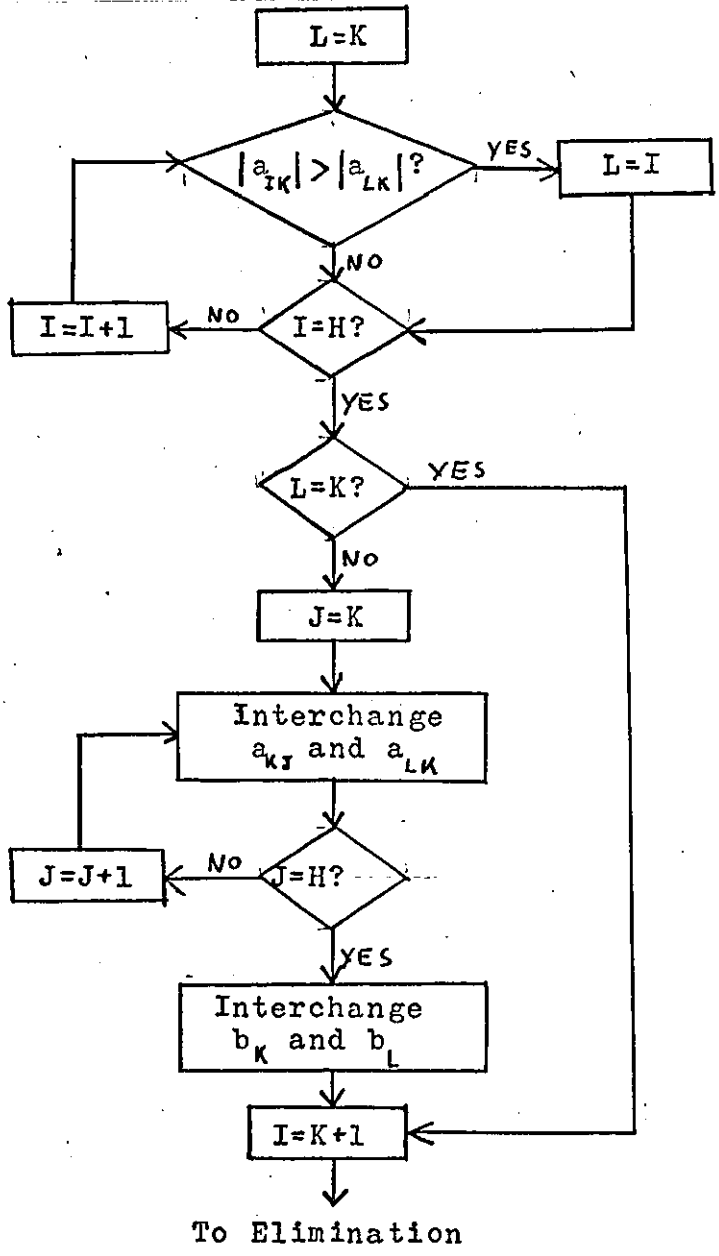

Section 6 Theoretical Impedance - Frequency Spectra.

1. The first coil chosen for study was a 150 turn coil, with the dimensions shown in Fig.6-1, this coil has only a fundamental resonance and one secondary resonance below 20 MHz. The equivalent circuit was split into 10 sections, each of 15 turns. The average L_u, M_u,r, C_u and R_u were calculated from equations 4-2-24, 4-2-26, 4-5-2 and 4-4-1 respectively.

$$L_u = \frac{\pi r_u^2}{W^2} \mu_o \left[(W^2 + r_u^2)^{\frac{1}{2}} - r_u \right] \qquad 4\text{-}2\text{-}24$$

$$M_{u'v} = \frac{\pi r_v^2}{W^2} \mu_o \left[(W^2 + r_u^2)^{\frac{1}{2}} - r_u \right] \qquad 4\text{-}2\text{-}26$$

$$C_u = \frac{2\pi r_u W \varepsilon \varepsilon_o}{d} \qquad 4\text{-}5\text{-}2$$

$$R_u = \frac{2\pi r_u \rho}{W m} \qquad 4\text{-}4\text{-}1$$

where r_u is the radius of the average turn of the section.

One point to note is that, in the approximation adopted, the mutual inductance has to be calculated from the larger turn to the smaller.

The values of L, M, C and R were calculated using the program in Appendix 2, then inserted as data in the Gaussian Elimination program. The output of the Elimination program at each frequency is in terms of the relative current in each section, the impedance per section and the total impedance of the coil. The Matrix was solved at a sufficient number of points between 0 and 20 MHz to form the impedance spectrum. Figs.6-2a and6-2b show the results, Fig.6-2a being the magnitude of the impedance and Fig.6-2b the phase. Fig.6-2a is plotted on an inverted log scale going from 0 to 10^7 ohms, the scale is inverted to correspond with the output from the spectrum analyser. The spectrum shows a fundamental resonance at 3.201 MHz and what is clearly a secondary resonance with a maximum at 12.47 MHz. The experiment with the four

Figure 6-1

Number of Turns	150
Thickness of Metal Foil	5.0 μm
Width " " "	3.9 cm
Permittivity of Plastic Foil	2.2
Thickness " " "	12.5 μm
Radius of Core	0.7 cm

Figure 6-1

Theoretical Plot of Impedance versus Frequency for a 150 Turn Coil.

a/

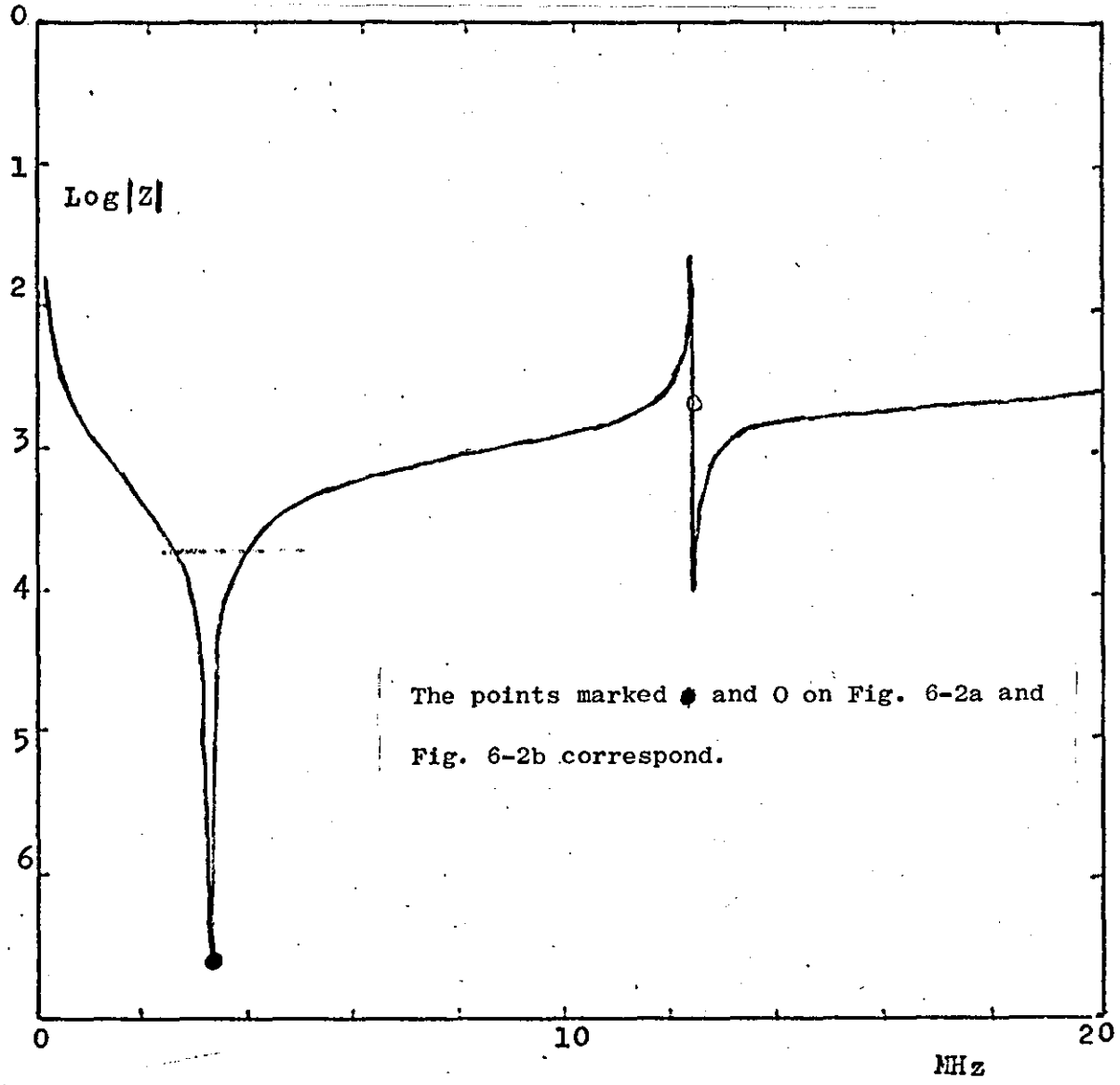

The points marked ● and O on Fig. 6-2a and Fig. 6-2b correspond.

Theory for a 150 turn coil, the resonance maxima occur at 3.201 MHz and 12.47 MHz.

b/

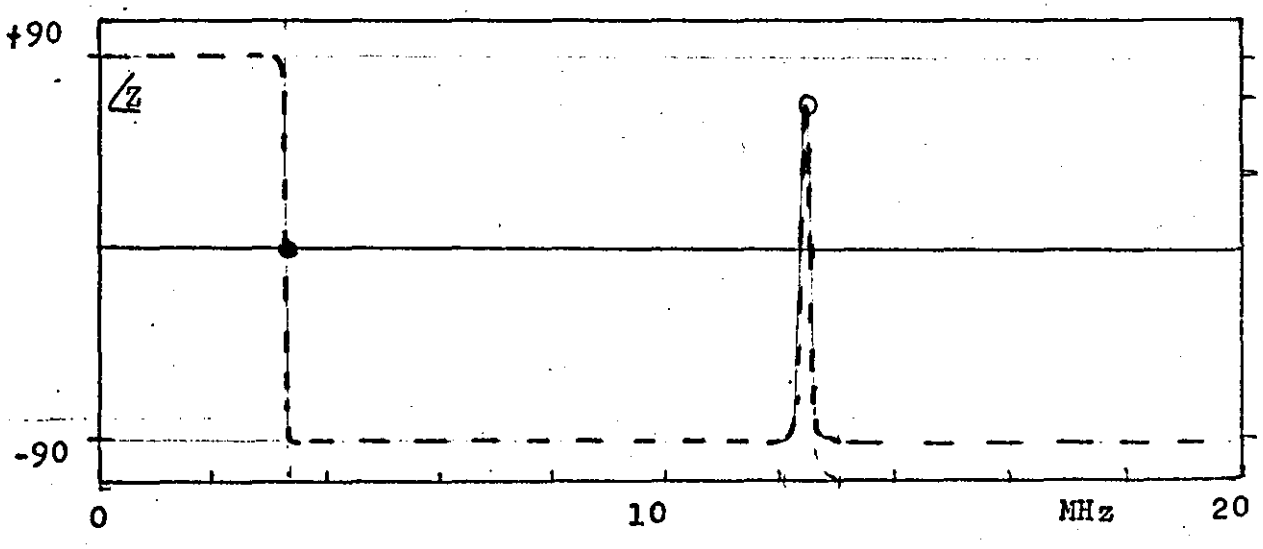

heat treated coils, with the same dimensions, in Section 4-6 showed that the fundamental resonance is at 3.24 MHz and the secondary maximum resonance is at 12.87 MHz.

	Expt.	Expt.Error	Theory	% Difference
Fundamental Resonance	3.24	±1.8%	3.201	+1.2%
Secondary Max. Impedance Resonance	12.87	±0.9%	12.47	+3.3%

The theory and the experiment agree to within the experimental error on the fundamental resonance, the error on the secondary resonance is larger than the experimental error. The accuracy is not poor considering that the approximations used for the inductances and capacitances are accurate to+5% and-2% respectively. These results show that the equivalent circuit will produce reasonably accurate multiple resonance, albeit in a relatively simple case.

As is expected Fig.6-2b shows that the equivalent circuit is inductive below the fundamental resonance and capacitive above it. However, during the secondary resonance the circuit becomes inductive again, being at its most "inductive" midway between the minima and the maxima of the resonance.

2. The possibility was mentioned in section 3 that a current standing wave could occur at the secondary resonances. This would mean that the current would vary in magnitude and phase across the radius of the coil. In the model used the coil is split into ten sections across the radius, so any standing wave would be evident as a variation of the magnitude and phase of the current from section to section.

Figs.6-3a to 6-3h show the magnitude and phase of the current in each section relative to the current to the coil, for the frequency shown. Fig.6-3a was obtained at a frequency just below the first resonance, the phase does not vary signficantly, but the magnitude of the current already shows a

Figure 4-3

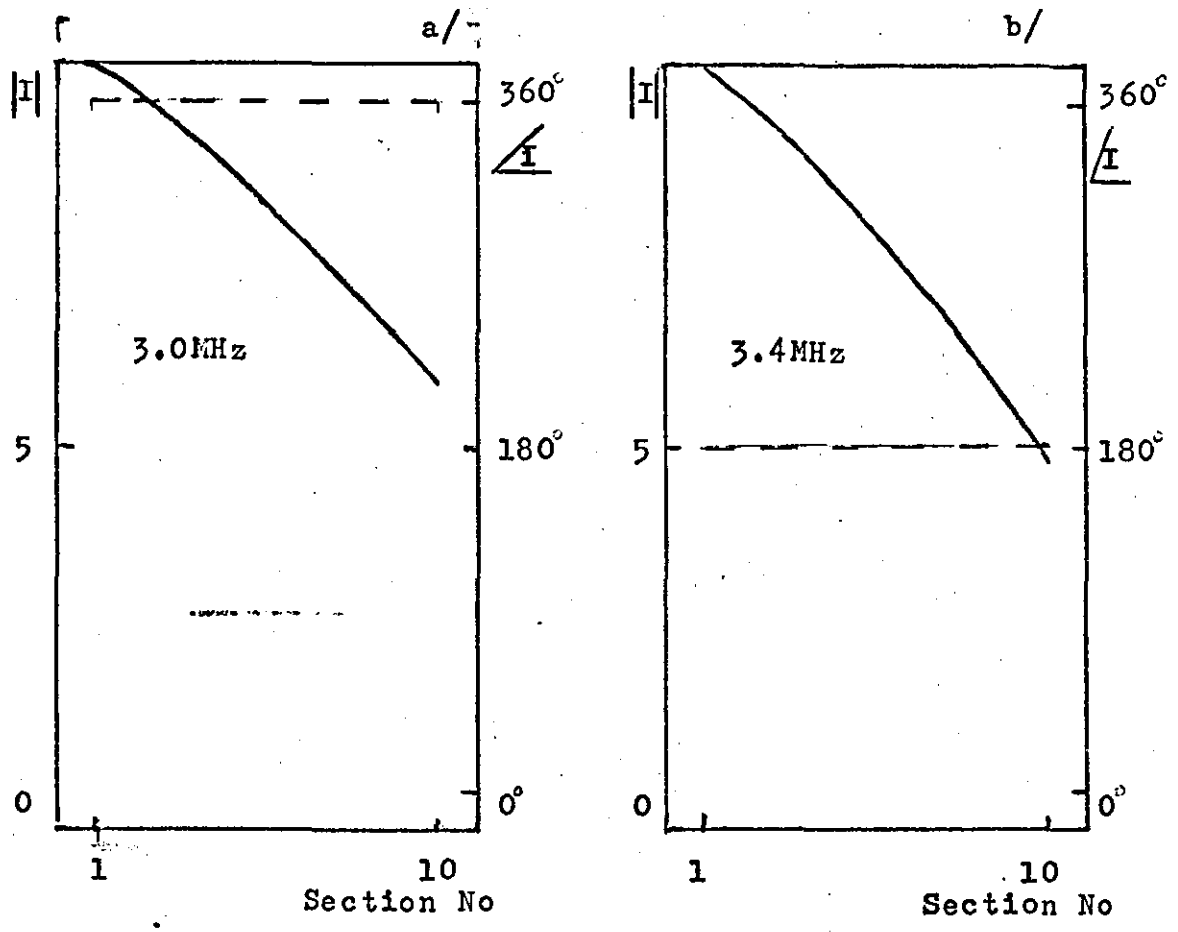

These graphs show the magnitude and phase of the current in each section for the frequency shown.
——— Magnitude — — — Phase

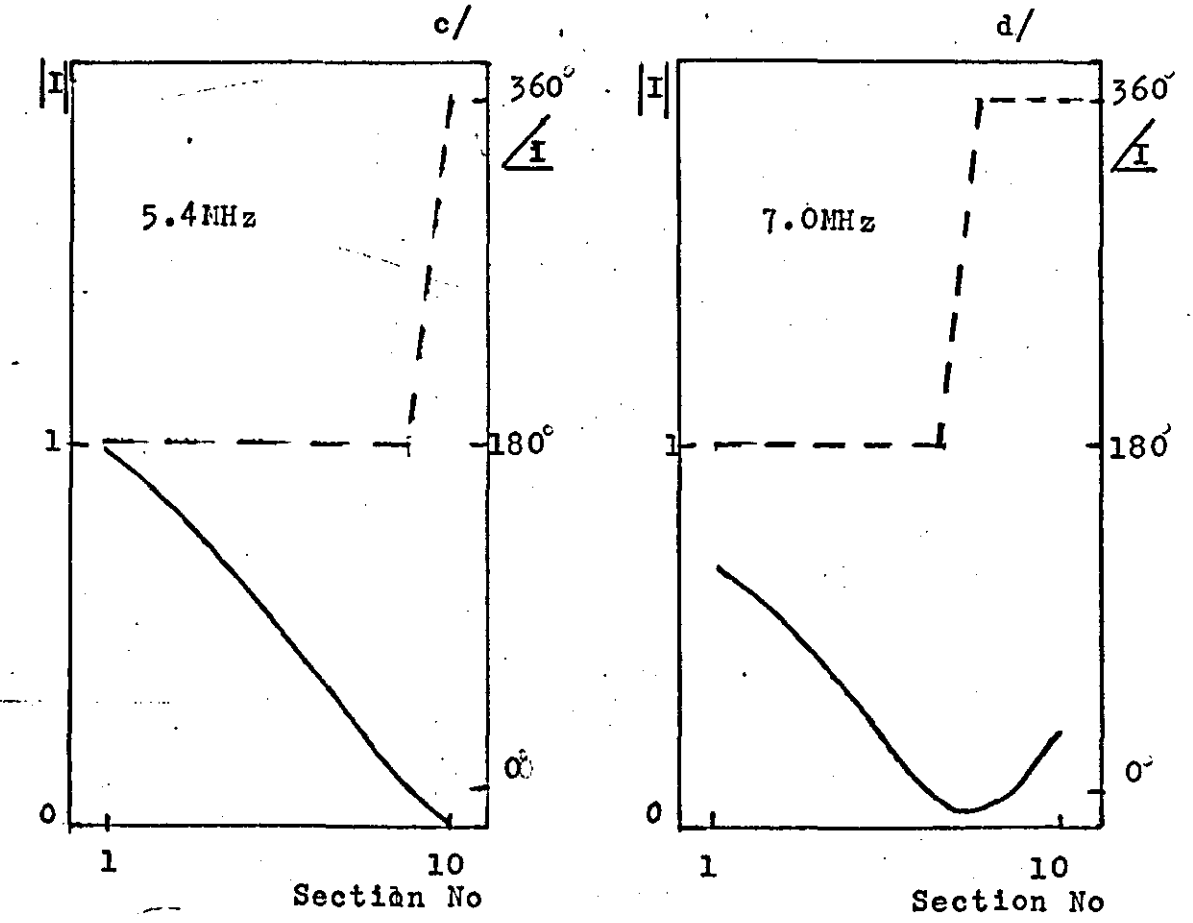

Figure 6-3

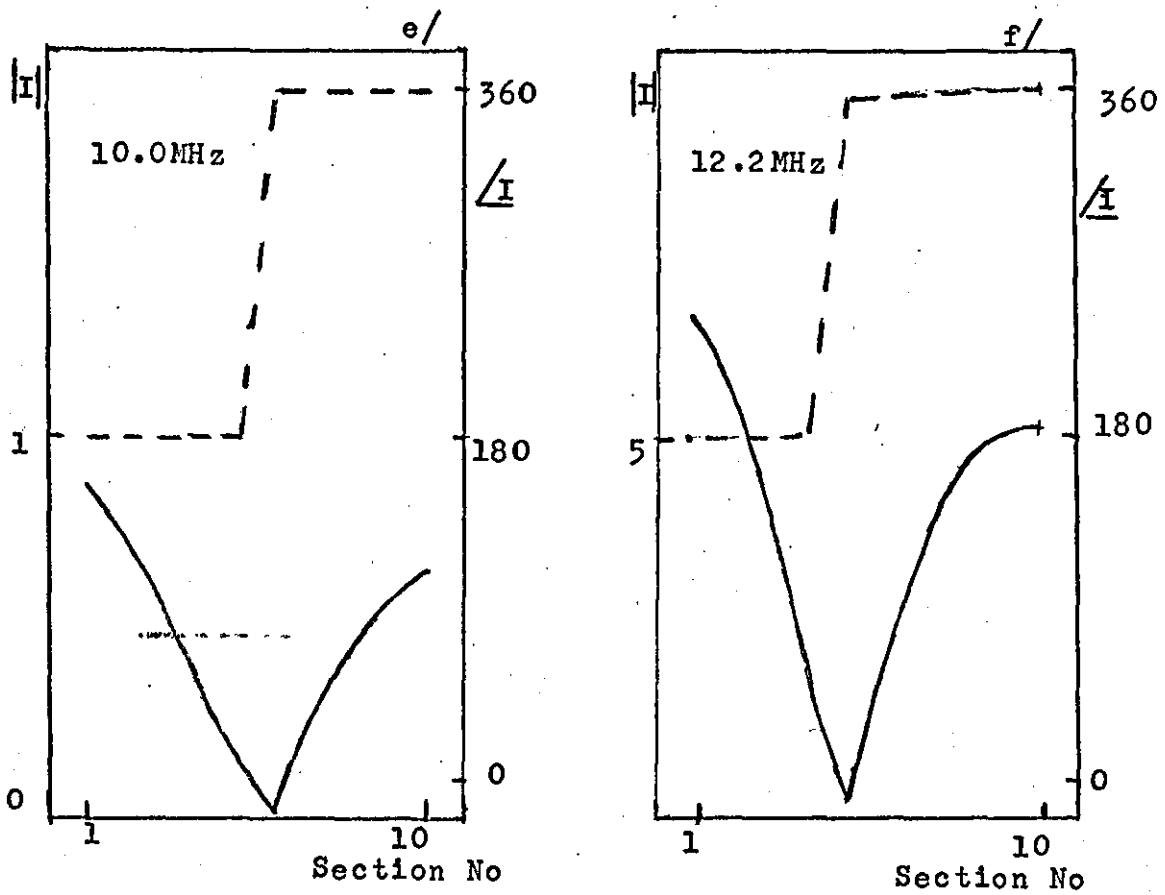

These graphs show the magnitude and phase of the current in each section for the frequency shown.
——— Magnitude — — - Phase

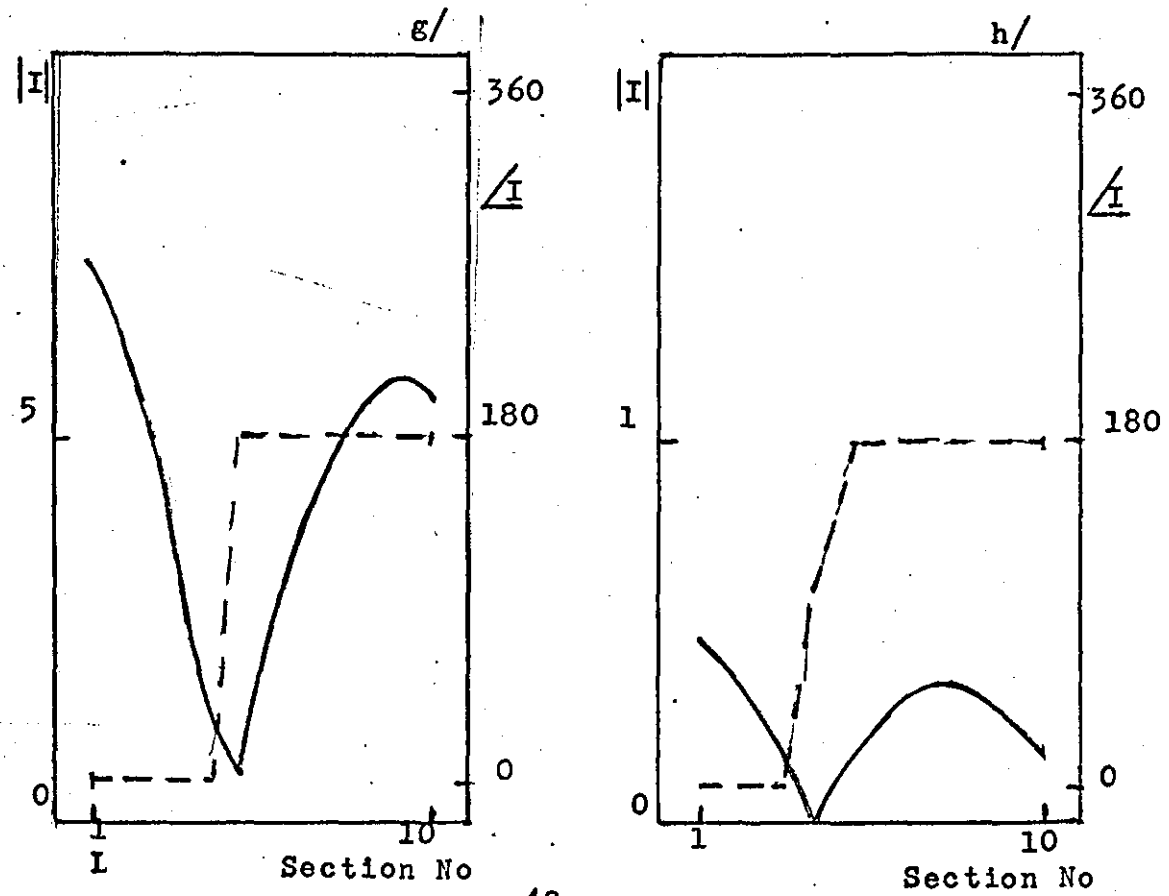

variation. Fig. 6-3b was obtained at a frequency just above the fundamental resonance; the phase of the whole distribution has changed by 180° as is expected. However in Fig. 6-3c the current in section 10, at the centre of the coil, is 180° out of phase with the current in the other sections. The current in section 10 is flowing in the opposite direction to the currents in the other sections. It might seem odd that the current changes in this manner, but the calculation is only giving the resistive-inductive part and when the capacitive current is counted there is constant sum.

Fig.6-3d, e and f show that the phase difference moves out from section 10 as the secondary resonance is approached. After the secondary resonance, (Fig.s 6-3g and h,) the whole distribution has shifted 180° in phase without changing its relative shape.

This type of behaviour is that of a current standing wave. In the light of this it would be expected that for higher orders of resonance the current distribution will change phase more than once. However, as the number of sections into which the equivalent circuit is split is limited, the order of resonance to which the model will be able to follow the changes in the current distribution is limited. For this reason the next coil chosen for study had 1000 turns and shows a large number of resonances below 20.0 MHz, (Fig. 2-3.)

3. The 1000 turn coil is that studied experimentally in section 2. The equivalent circuit was again split into 10 sections. Fig.6-4a and 6-4b show the impedance frequency spectra , the frequency scale is to 7.5 MHz. The only significant difference, apart from the number of resonances, from the 180 turn coil is that at the secondary resonances the model is inductive over a wider frequency span.

The table in Fig.6-5 compares the experimental results for the 1000 turn coil, after it had been heat treated, with the theoretical results, up to the 8th order of resonance. The accuracy of the first 3 orders

Figure 6-4 Theoretical Plot of Impedance versus Frequency for a 1000 Turn Coil

a/

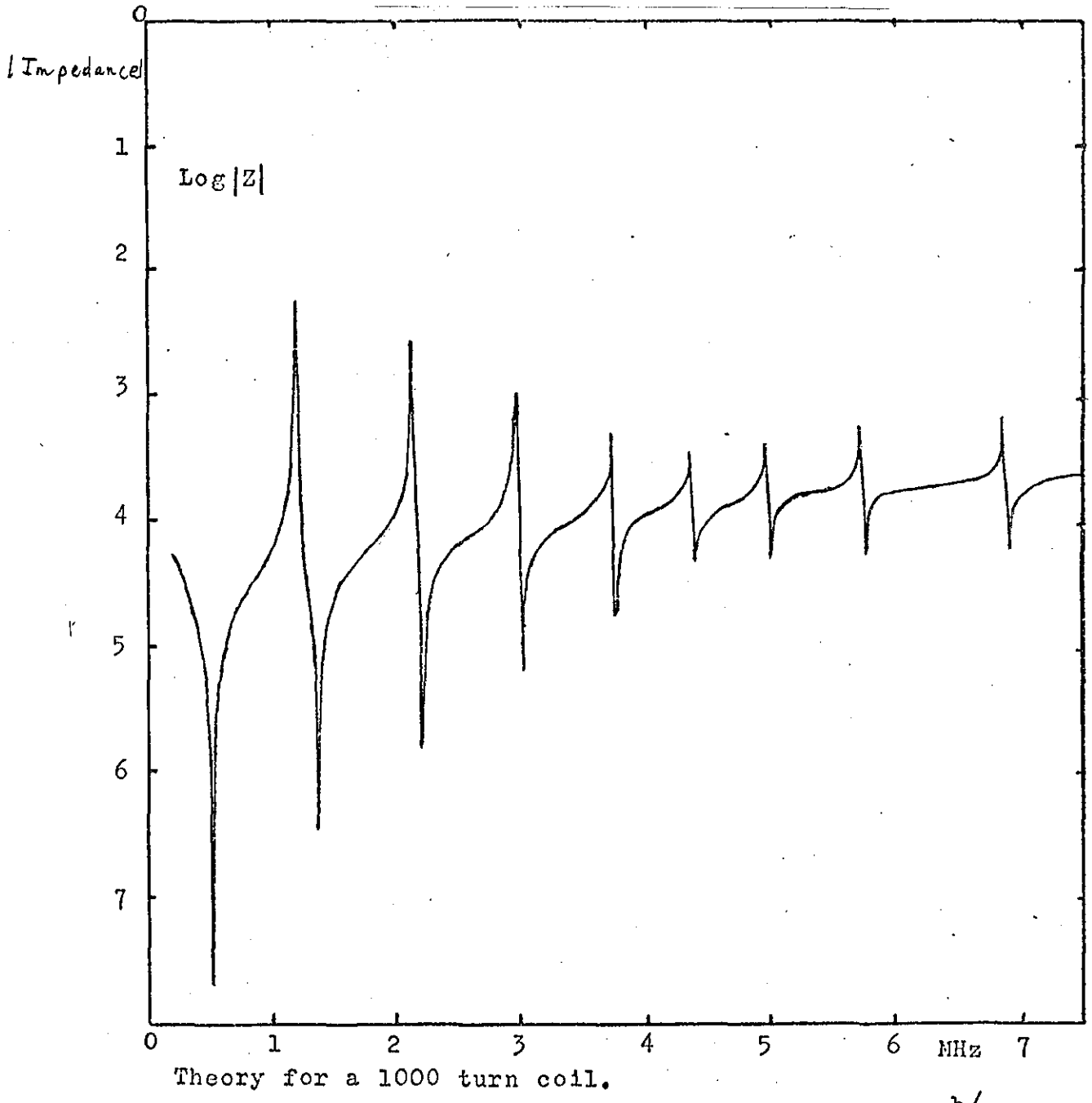

Theory for a 1000 turn coil.

b/

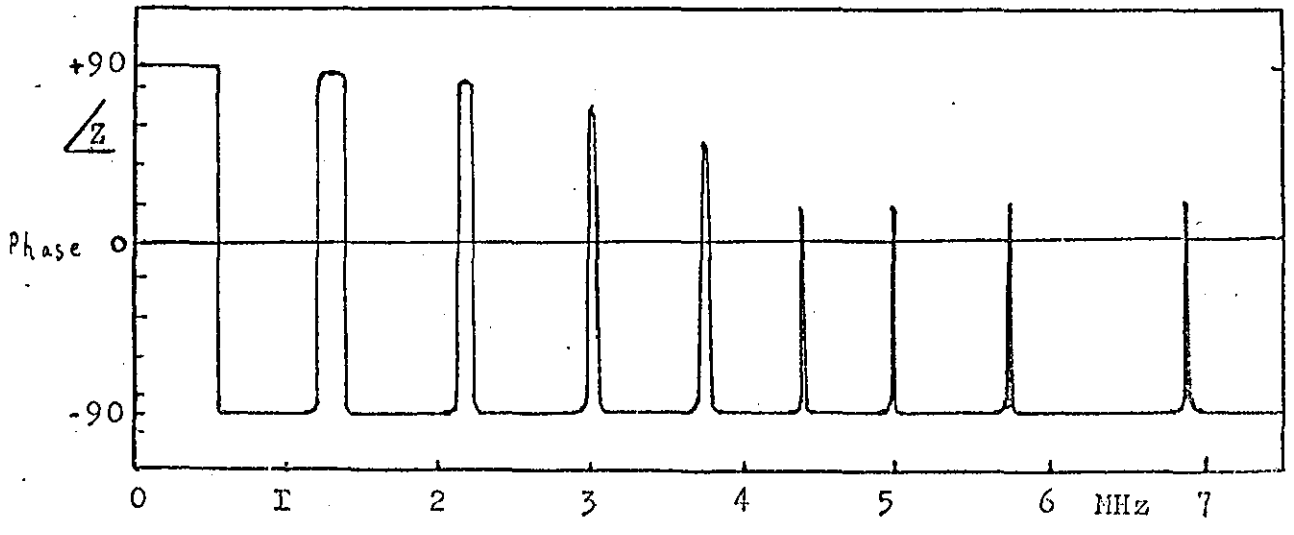

Figure 6-5

Comparison of theory with experiment for a 1000 turn coil, maximum impedance resonances only.				
Order of Resonance	Experiment Mhz	Error %	Theory Mhz	Diffrence %
1	0.514	±0.39	0.517	+0.53
2	1.344	±0.15	1.366	+1.65
3	2.232	±0.09	2.216	-0.72
4	3.218	±0.06	3.022	-6.1
5	4.101	±0.07	3.748	-8.6
6	5.005	±0.08	4.375	-12.6
7	6.008	±0.17	4.979	-17.2
8	6.888	±0.15	5.740	-16.7

Figure 6-6

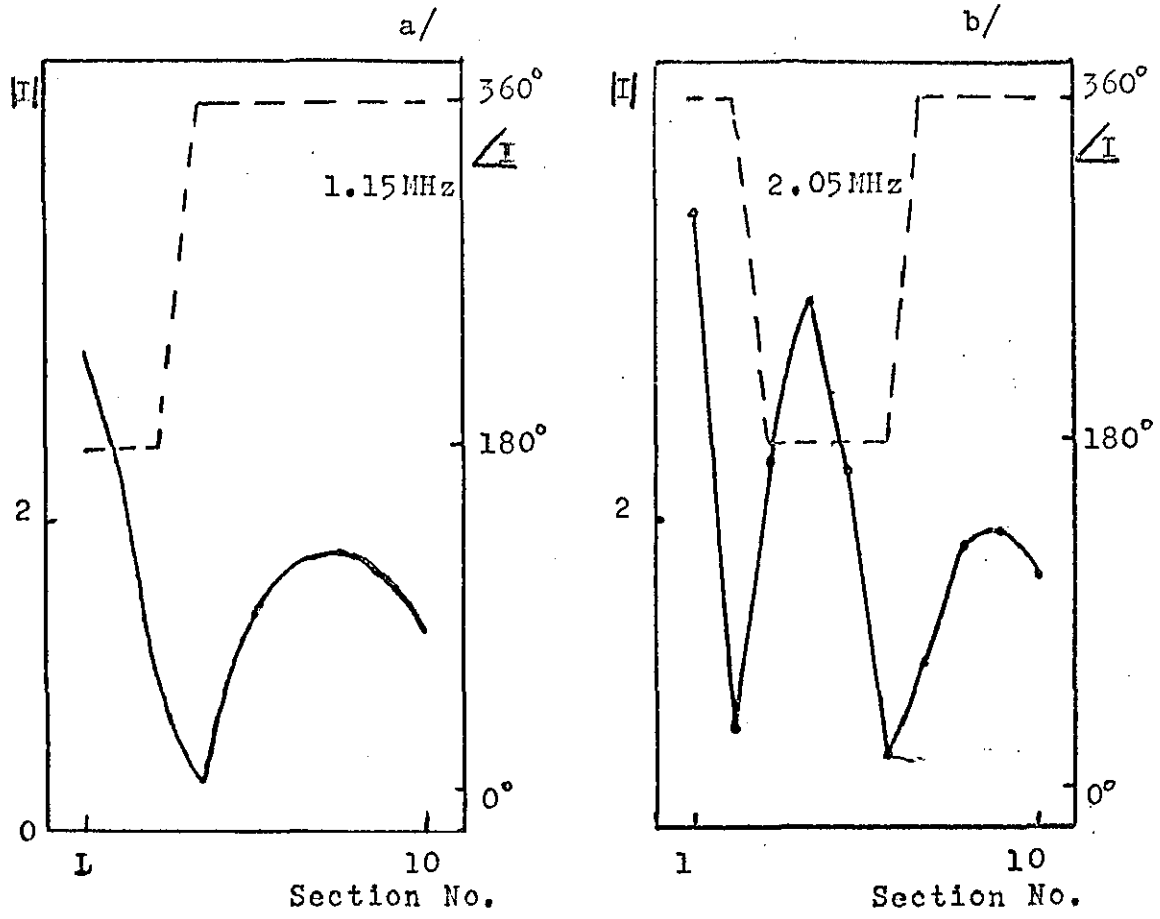

These graphs show the magnitude and phase of the current in each section, for the frequency shown.

——— Magnitude — — — — Phase

Figure 6-6

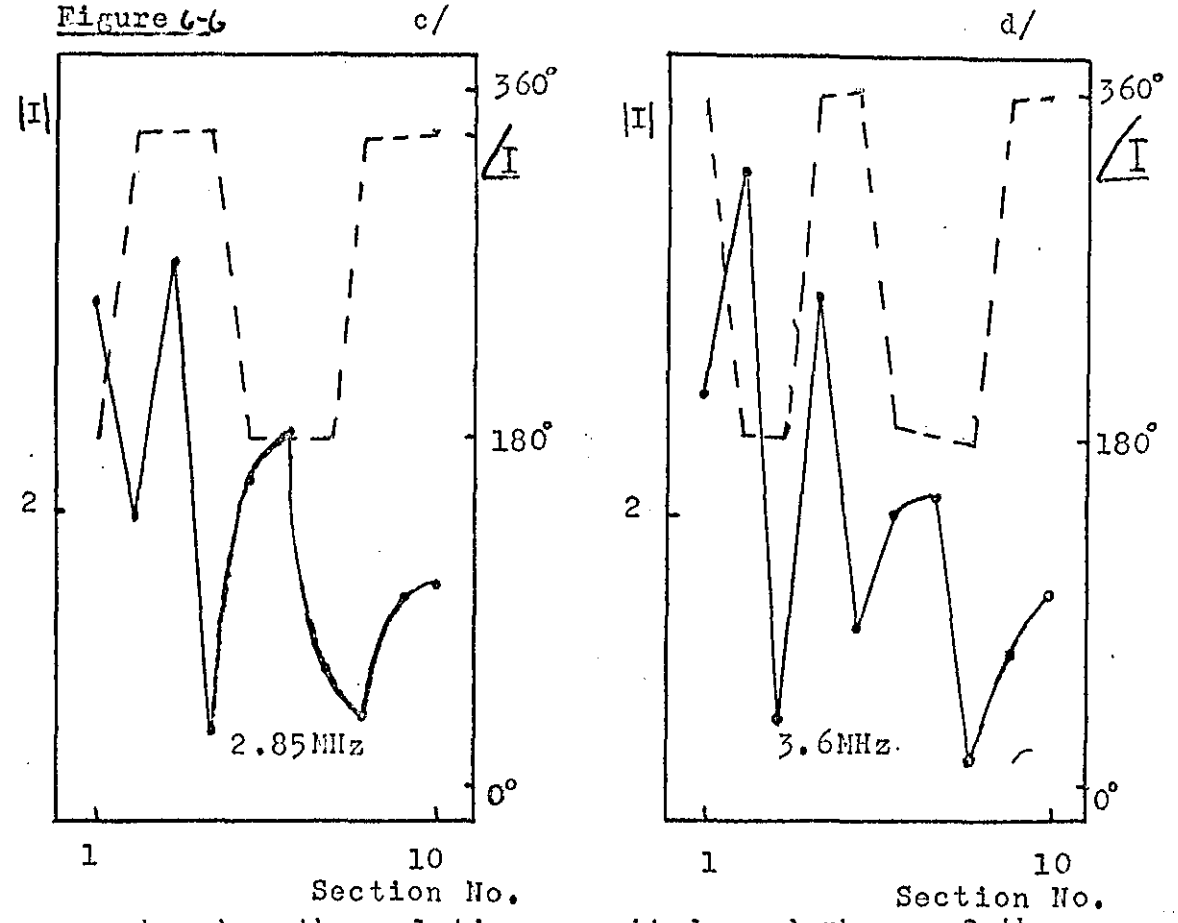

These graphs show the relative magnitude and phase of the current in each section, for the frequency shown.

——— Magnitude — — — Phase

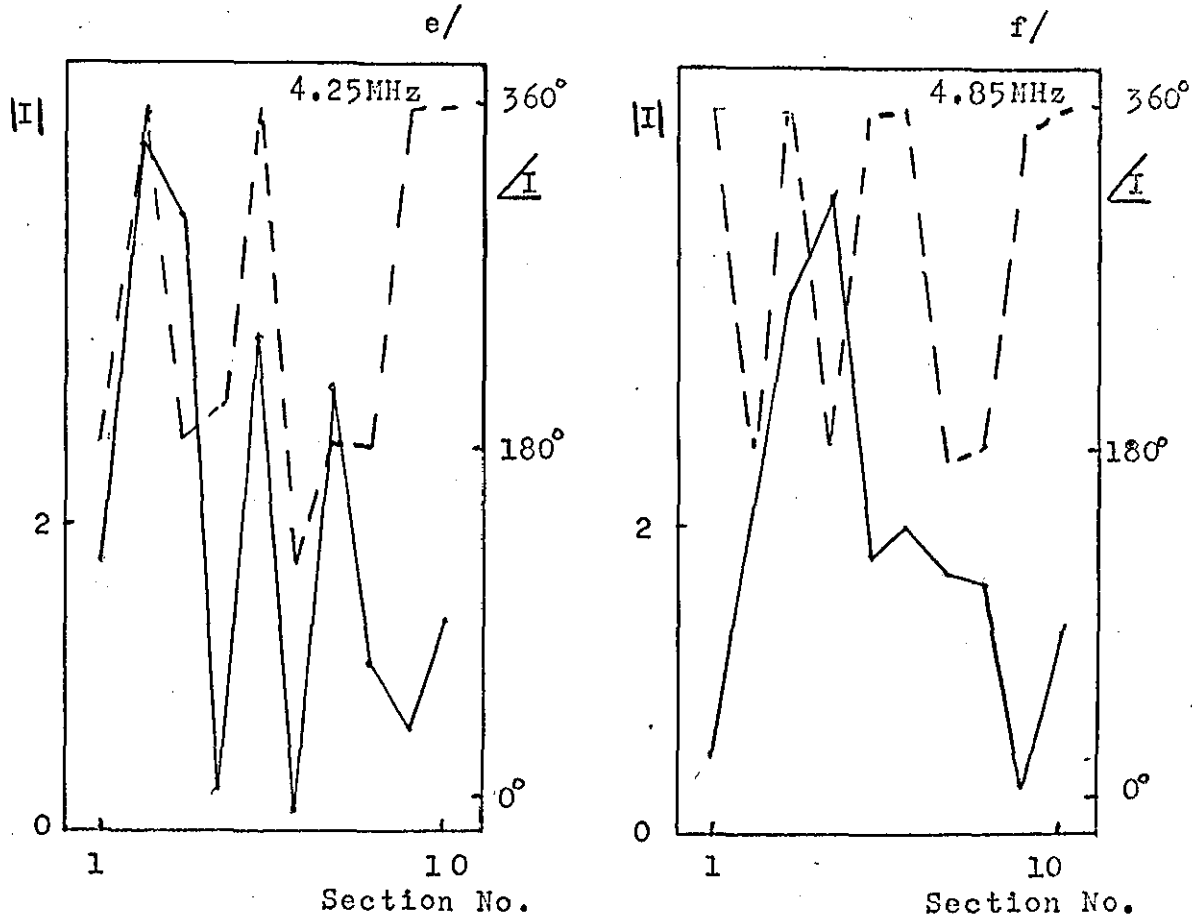

is better than 2%, but the accuracy of the 4th order has decreased to 6% and thereafter steadily decreases with increasing order until the 8th order where it improves slightly. As expected the order of resonance to which the model is accurate is limited to the first orders of resonance.

Now we examine the current distribution near the various resonances, Fig.6-6a to 6f. Fig.6-6a is just below the 2nd resonance, Fig.6-6b is just below the 3rd resonance, etc. We see that the number of phase changes is equal to the order of resonance minus one. But if we look at the magnitude of the current it is obvious that apart from the first few resonances the model cannot follow the changes in the current distribution accurately.

It would appear that to increase the accuracy for the higher orders of resonance, the number of sections into which the coil is split must be increased. However, this will incur the penalty of increased computation time, which increases as the cube of the number of sections.

4. To test the accuracy of the model against the size of the core, three 150 turn coils were constructed, the cores had radii of 0.2 cm, 0.5 cm. and 1.0 cm. The other dimensions are shown in Fig.6-7. These coils were heat treated.

The theory is compared with the experimental results, for the maximum impedance resonances below 20 MHz, in Fig.6-8. The theory for the coil with the largest core (coil 3) gives results which are low; for the coil with the smallest core (coil 1) the results are high, while the results for the intermediate coil (coil 2) are high for the fundamental resonance and low for the secondary resonance.

The indication is that the theory will predict increasingly low values for the resonant frequencies when the core radius is increased.

Figure 6-7

Number of Turns	150
Thickness of Metal Foil	5.0μm
Width " " "	3.9cm
Permittivity of Plastic Foil	2.2
Thickness " " "	12.5μm
Radius of Core; Coil 1	0.2cm
Coil 2	0.5cm
Coil 3	1.0cm

Figure 6-8

Order of Resonance	Experiment MHz	Theory	%Difference	
1	2.17 ±0.05	2.078	-4.25	Coil 3
2	9.88 ±0.01	9.154	-7.35	
3	18.3 ±0.03	17.35	-5.2	
1	4.72 ±0.03	4.738	+3.8	Coil 2
2	17.02 ±0.01	16.689	-1.95	
1	11.79 ±0.01	14.67	+26.5	Coil 1

5. The Q of a resonance is given by

$$Q = \frac{f_o}{\Delta f_o} \qquad 4\text{-}5\text{-}1$$

Where f_o is the frequency of the resonance and Δf is the half height width of the resonance in the power spectrum. On a dB power scale the half height point correspond to the points were the dB loss has fallen to 3 dB below the maximum loss or has risen to 3 dB above the minimum loss.

Employing the method of Section 2 the Q of the fundamental resonance of the 150 turn coil studied earlier in this section was measured at 172 ± 2.0.

The theoretical Q can be found from the impedance spectrum, the half height points correspond to the points where the impedance has fallen to $\frac{1}{\sqrt{2}}$ times the maximum value or has risen to $\sqrt{2}$ times the minimum value. The theoretical Q for the fundamental resonance of the 150 turn coil is 3,410.

The theoretical Q is too large by an order of magnitude, In an ordinary L, R, C resonant circuit (Section 1) the Q is given by

$$Q = \frac{1}{R}\left(\frac{L}{C}\right)^{\frac{1}{2}} \qquad 1\text{-}1\text{-}2$$

As L and C can be determined reasonably accurately, then the discrepancy between theory and experiment must be due to the value of R. As only the d.c. resistance is used, this suggests that the a.c. losses cannot be neglected.

Section 7. A.C. Resistance

1. The theoretical Q derived for the 150 turn coil studied in section 6 was a factor of 20 higher than the experimental value. This discrepancy could be due to the use of the d.c. resistance alone.

When an alternating current flows in a wire the magnetic field of the current induces eddy currents within the wire. These eddy currents redistribute the current, causing the density to be greater near the surface of the wire and hence the resistance rises. This is known as the skin effect. Magnetic fields from adjacent wires can also cause a redistribution which we formally distinguish by the term proximity effect, though in a given problem both may be present. In FWI the magnetic field of a turn and the field of adjacent turns are largely parallel to the axis of the coil. This enables the two effects, the skin and the proximity effects, to be combined and to treat the problem as one of a plate in a parallel a.c. magnetic field. An analysis of this situation is performed in several books, this one is from Stoll (11).

As the radius and the width of a turn are about 3 orders of magnitude greater than the thickness of the metal foil, the problem can be approximated to that of an infinite plate of thickness m. The place is infinite in the x and z directions. The magnetic field is in the z direction and is a spatial function of y alone. The magnetic field varies sinusoidally with time. The eddy currents are induced in the x direction. The situation is illustrated in Fig.4-I.

As the metal foil is aluminium, equation 4-1-1 can be used.

$$\nabla \times \underline{E} = -\frac{\partial \underline{B}}{\partial t} = -\mu\mu_0 \frac{\partial \underline{H}}{\partial t} \qquad 4\text{-}1\text{-}1$$

Also

$$\sigma \underline{E} = \underline{J} \qquad 4\text{-}1\text{-}2$$

where σ is the conductivity.

Figure 7-1 Diagram Showing the Parameters Used in Determining the a.c. Resistance of an Infinite Plate.

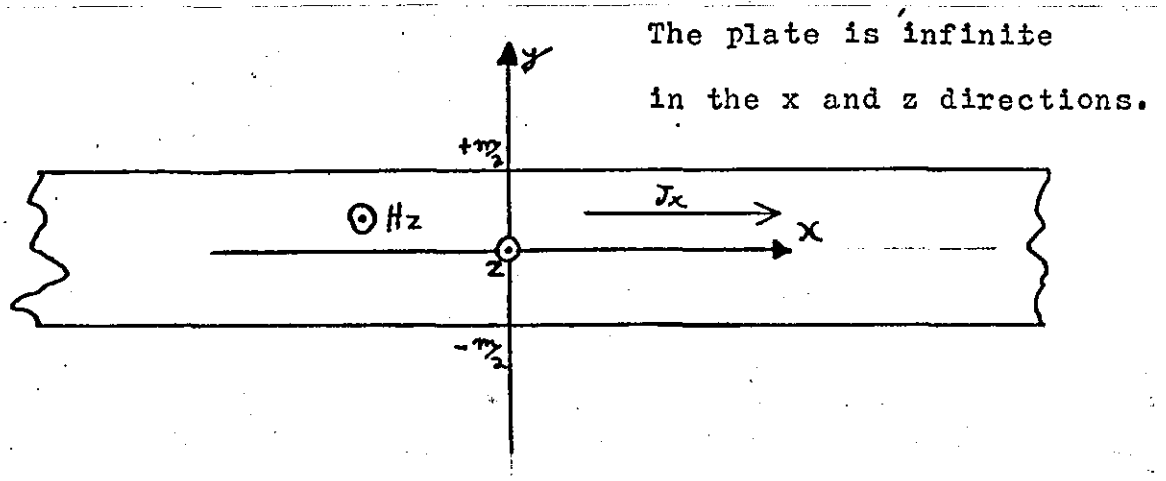

Figure 7-2 Theory for a 150 turn coil including the ac resistance

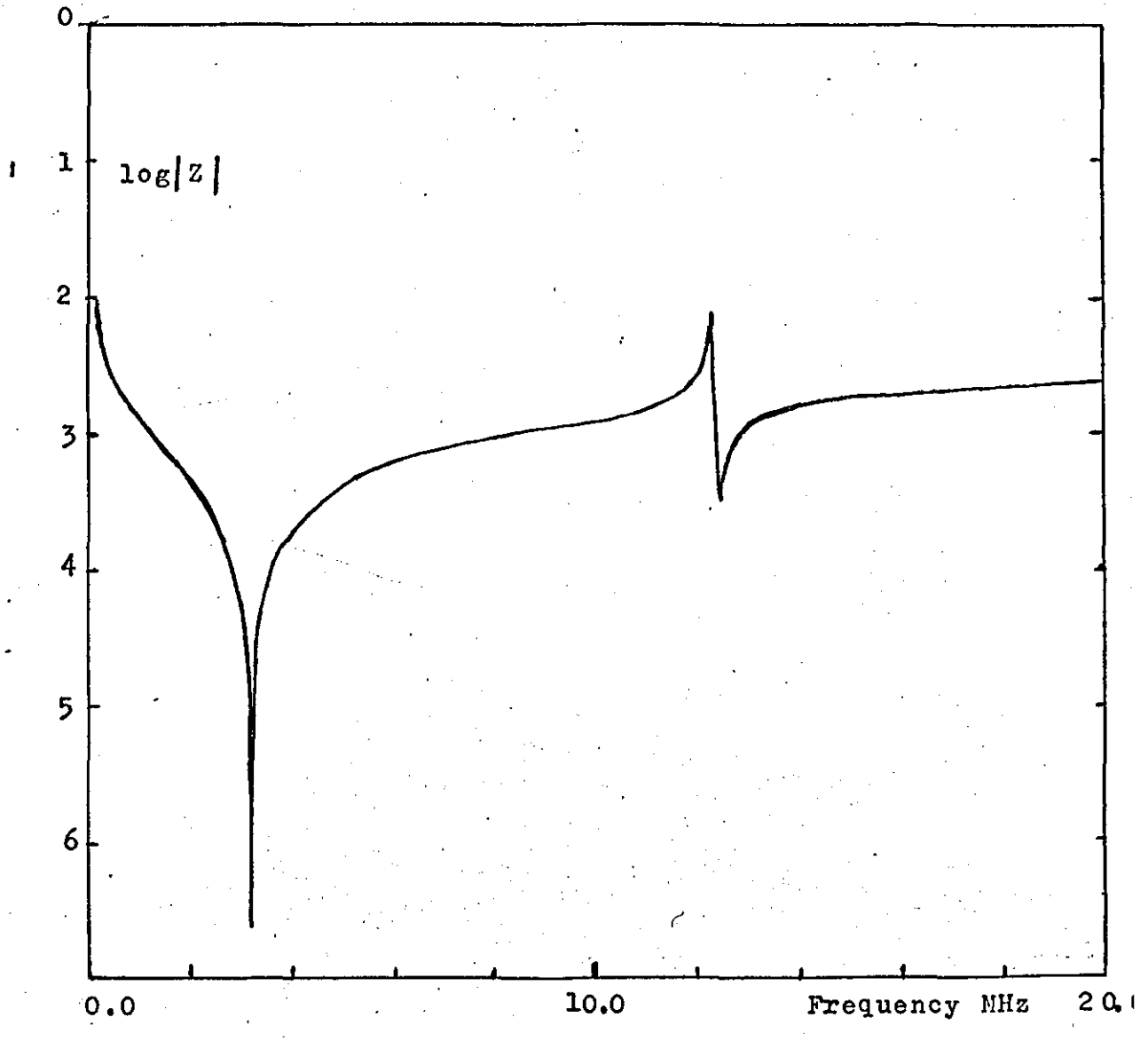

Combining equations 4-1-1 and 4-1-2

$$\nabla \times \underline{J} = -\sigma \mu \mu_0 \frac{\partial \underline{H}}{\partial t} \qquad 4\text{-}1\text{-}3$$

In this situation J_y and J_z are zero; therefore H_x and H_y are also zero. Equation 4-1-3 reduces to

$$\frac{\partial J_x}{\partial y} = \sigma \mu \mu_0 \frac{\partial \underline{H}_z}{\partial t} \qquad 4\text{-}1\text{-}4$$

From Maxwell's equations.

$$\nabla \times \underline{H} = \underline{J} \qquad 4\text{-}1\text{-}5$$

which in this case reduces to

$$\frac{\partial \underline{H}_z}{\partial y} = J_x \qquad 4\text{-}1\text{-}6$$

Partially differentiating w.r.t. y gives

$$\frac{\partial^2 \underline{H}_z}{\partial y^2} = \frac{\partial J_x}{\partial y} \qquad 4\text{-}1\text{-}7$$

Combining equations 4-1-7 and 4-1-4 gives

$$\frac{\partial^2 \underline{H}_z}{\partial y^2} = \sigma \mu \mu_0 \frac{\partial \underline{H}_z}{\partial t} \qquad 4\text{-}1\text{-}8$$

As H_z is a sine function of time

$$\frac{\partial^2 \underline{H}_z}{\partial y^2} = j\omega \sigma \mu \mu_0 H_z \qquad 4\text{-}1\text{-}9$$

The partial derivatives can be replaced with differentials, as $\underline{H}$ and $\underline{J}$ have specified directions. Equation 4-1-9 becomes

$$\frac{d^2 \underline{H}_z}{dy^2} = j\omega \sigma \mu \mu_0 H_z \qquad 4\text{-}1\text{-}10$$

Let

$$j\omega \sigma \mu \mu_0 = \alpha^2 \qquad 4\text{-}1\text{-}11$$

and

$$\alpha = (1 + j)/\delta \qquad 4\text{-}1\text{-}12$$

Therefore

$$\delta = \left(\frac{2}{\omega \sigma \mu \mu_0}\right)^{1/2} \qquad 4\text{-}1\text{-}13$$

The function δ is known as the skin depth.

Combining equations 4-1-10 and 4-1-11 gives

$$\frac{d^2 H}{dy^2} = \alpha^2 H \qquad 4\text{-}1\text{-}14$$

This equation has a solution of the form

$$H = K_1 e^{\alpha y} + K_2 e^{-\alpha y} \qquad 4\text{-}1\text{-}15$$

Before K_1 and K_2 can be found the values of H at $y = m/2$ and $y = -m/2$ are required. For this purpose it is assumed that a constant current flows through the coil and that this current has a constant magnitude and phase throughout the coil. In section 6 it was discovered that in the theoretical model the current could reverse its direction, and this means that the a.c. resistance would be dependent on the current distribution. To calculate this is for the whole coil would require an iterative procedure, so rather than attempt this the current is approximated to be constant in magnitude and direction.

The problem can be greatly simplified if the $\underline{H}$ field is regarded as being equal on both sides of the foil. This means that the solution, equation 4-1-15, is symmetrical. Therefore

$$K_1 = K_2 = \frac{H_{+m/2}}{e^{\alpha m/2} + e^{-\alpha m/2}} = \frac{H_{-m/2}}{e^{\alpha m/2} + e^{-\alpha m/2}} \qquad 4\text{-}1\text{-}16$$

Combining equations 4-1-16 and 4-1-15 gives

$$H = H_{+m/2}\,\frac{\cosh \alpha y}{\cosh \alpha m/2} = H_{-m/2}\,\frac{\cosh \alpha y}{\cosh \alpha m/2} \qquad 4\text{-}1\text{-}17$$

Remembering that J and H have fixed directions equation 4-1-6 is

$$J = \frac{dH}{dy} \qquad 4\text{-}1\text{-}18$$

The current follows from equation 4-1-17 by differentiation.

$$J = \alpha\, H_{\pm m/2}\,\frac{\sinh \alpha y}{\cosh \alpha m/2} \qquad 4\text{-}1\text{-}19$$

The mean power loss per unit surface area is given by

$$P = \frac{1}{2\sigma}\int_{-m/2}^{m/2} |J|^2\, dy \qquad 4\text{-}1\text{-}20$$

where J is the peak value of the current.

Equation 4-1-19 is an odd function of y, therefore the eddy current goes and returns inside the foil and the net. eddy-current is zero.

The peak value of J can be obtained from equation 4-1-19 by multiplying by the complex conjugate of the current and taking the square root.

$$(J\,J^*)^{1/2} = |J| = \frac{\sqrt{2}\,H_{\pm m/2}}{\delta}\,\frac{\cosh 2y/\delta - \cos 2y/\delta}{\cosh m/\delta + \cos m/\delta} \qquad 4\text{-}1\text{-}21$$

Combining equations 4-1-21 and 4-1-20 gives the total power loss per unit surface area as

$$P = \frac{H_{\pm m/2}^2}{\sigma\delta^2}\int_{-m/2}^{m/2}\left(\frac{\cosh 2y/\delta - \cos 2y/\delta}{\cosh m/\delta + \cos m/\delta}\right) dy \qquad 4\text{-}1\text{-}22$$

When the integral is evaluated

$$P = \frac{H_{\pm m/2}^2}{\sigma\delta} \frac{\sinh 2y/\delta - \sin 2y/\delta}{\cosh m/\delta - \cos m/\delta} \qquad 4\text{-}1\text{-}23$$

The skin depth for Aluminium (δ) of 5μm thickness is given by.

$$\delta = \frac{0.212}{\omega^{\frac{1}{2}}} \text{ metres} \qquad 4\text{-}1\text{-}24$$

As the fundamental resonance of the 150 turn coil in section 6, the skin depth will be 49.0μm, which is an order of magnitude greater than the thickness of the metal, 5.0μm. Therefore an approximate expression for P is valid:

$$P \simeq \frac{\omega^2 \sigma \mu^2 \mu_0^2 H_{\pm m/2} m^3}{24} \qquad 4\text{-}1\text{-}25$$

The simplest approximation to $H_{\pm m/2}$ can be derived from equation 4-2-17.

$$\bar{H}_z = \frac{I}{2\pi W^2} \int_0^{2\pi} \frac{r_1 (r_1 - r\cos\theta_1)\, d\theta_1}{(r_1^2 + r^2 - 2r_1 r\cos\theta_1)} \Big\{ \qquad 4\text{-}2\text{-}14$$

$$(r_1^2 + r^2 - 2r_1 r\cos\theta_1 + W^2)^{\frac{1}{2}} - (r_1^2 + r^2 - 2r_1 r\cos\theta_1)^{\frac{1}{2}} \Big\}$$

By assuming that the magnetic field is uniform across the area of the foil and is equal to the field at the centre of the foil we can derive the approximation

$$\bar{H}_z = \frac{I}{W^2}\left[(r_1^2 + W^2)^{\frac{1}{2}} - r_1\right] \qquad 4\text{-}1\text{-}26$$

Then by approximating $W >> r_1$

$$\bar{H}_z = \frac{I}{W} \qquad 4\text{-}1\text{-}27$$

If we assume that a turn, radially, has no external magnetic field, the u^{th} turn will only experience the magnetic field of the u-1 turns that are wound on top of it. To ensure the solution is symmetrical the field of the u^{th} turn itself is neglected. Given this assumption the magnetic field is given by

$$\bar{H}_z = (u-1)\, I/W = H_{\pm m/2} \qquad 4\text{-}1\text{-}28$$

Combining equations 4-1-28 and 4-1-25 gives the power loss per unit surface area for the u^{th} turn as

$$P = \omega^2 \sigma \mu^2 \mu_0^2 \frac{(u-1)^2 I^2}{24 W^2} m^3 \qquad 4\text{-}1\text{-}29$$

The total power loss in the u^{th} turn is given by

$$P_u = \pi r_u \omega^2 \sigma \mu^2 \mu_0^2 \frac{(u-1)^2 I^2}{12 W} m^3 \qquad 4\text{-}1\text{-}30$$

where r_u is the radius of the u^{th} turn.

Now, power dissipation in a resistor is given by

$$P = I^2 R \qquad 4\text{-}1\text{-}31$$

Therefore the equivalent A.C. resistance is

$$R^u_{ac} = \pi r_u \omega^2 \sigma \mu^2 \mu_0^2 \frac{(u-1)^2 m^3}{12 W} \qquad 4\text{-}1\text{-}32$$

The total resistance is given by

$$R_u = R^u_{DC} + R^u_{AC} \qquad 4\text{-}1\text{-}33$$

where R^u_{DC} is the d.c. resistance of the u^{th} turn. As the a.c. resistance is frequency dependent the resistance is better expressed as

$$R_u = R^u_{DC} + \omega^2 R'^u_{AC} \qquad 4\text{-}1\text{-}34$$

2. The a.c. resistance R'^{u}_{Ac} was calculated for each section of the coil from

$$T R'^{u}_{Ac} = T \sigma \pi \mu^2 \mu_0^2 \frac{r_u (u-1)^2 m^2}{12 W} \qquad 4\text{-}2\text{-}1$$

where r_u is now the mean turn of the section and T is the number of turns per section. For aluminium μ is close to 1. When the values are assigned to the matrix $[a]$ in the elimination program the total resistance per section is calculated from

$$R_{\text{per section}} = T R^{u}_{Dc} + \omega^2 T R'^{u}_{Ac} \qquad 4\text{-}2\text{-}2$$

The a.c. resistance was tested on the 150 turn coil of section 6-1. Without the a.c. resistance the Q of the fundamental resonance was found to be 3410. When the a.c. resistance was included the predicted Q was reduced to 1780. The experimental value of Q is 173 ± 5. Clearly the calculated values of the a.c. resistance are not adequate, either the approximations used are too crude or other factors have to be taken into account. The dielectric used is polypropylene, the loss factor of this does not increase greatly in the frequency range under investigation, therefore losses in the insulation and the core will be small. The major factor would seem to be that the approximations used are too crude.

The Q of the secondary maximum impedance resonance of the 150 turn coil is 162 ± 2, the theoretical Q is 160. The agreement is probably spurious, the result of two errors cancelling out. The approximations underestimate the magnetic field while the assumption that the currents in the coil all flow in the same direction overestimates the total magnetic field.

Section 8 Effect of the Current Standing Wave on the External Magnetic Field.

1. To show the existence of the current standing wave in an actual F.W.I. is not altogether an easy task. One method would be to investigate the voltage distribution within the coil. Fig.8-1 shows a plot of impedance, section by section, of the 1000 turn coil in Section 6-3 at a frequency just below the fourth resonance. The axis of the graph are real and imaginary ohms. Although each section does not have an independent impedance it does have a $^{V}/_{I}$. The impedance crosses the imaginary axis in two places, although the total impedance remains on the R.H.S. of the imaginary axis. The voltage will follow the impedance changes.

Measurement of the voltage distribution would require a probe to be attached to the coil and one could not be sure that the probe would not alter the current distribution within the coil, or that the effects observed were not due to impedance mismatching.

However there is a method that requires no mechanical connection to the coil and should cause a minimum of interference with the current distribution within the coil. Fig.8-2 shows the general method. The standing wave is a current phenomenon and should be visible as a variation of the external magnetic field. This variation should be detectable by the search coil.

The first task is to calculate the magnetic field of a given theoretical current distribution for the F.W.I. chosen for the experiment.

2. As the search coil will be near the end of the turn of foil, the magnetic field can be approximated as uniform and equal to the field on the axis of the foil. The field can also be approximated to be zero for radii greater than that of the foil; that is, the foil is treated as an infinitely long solenoid.

Figure 8-1

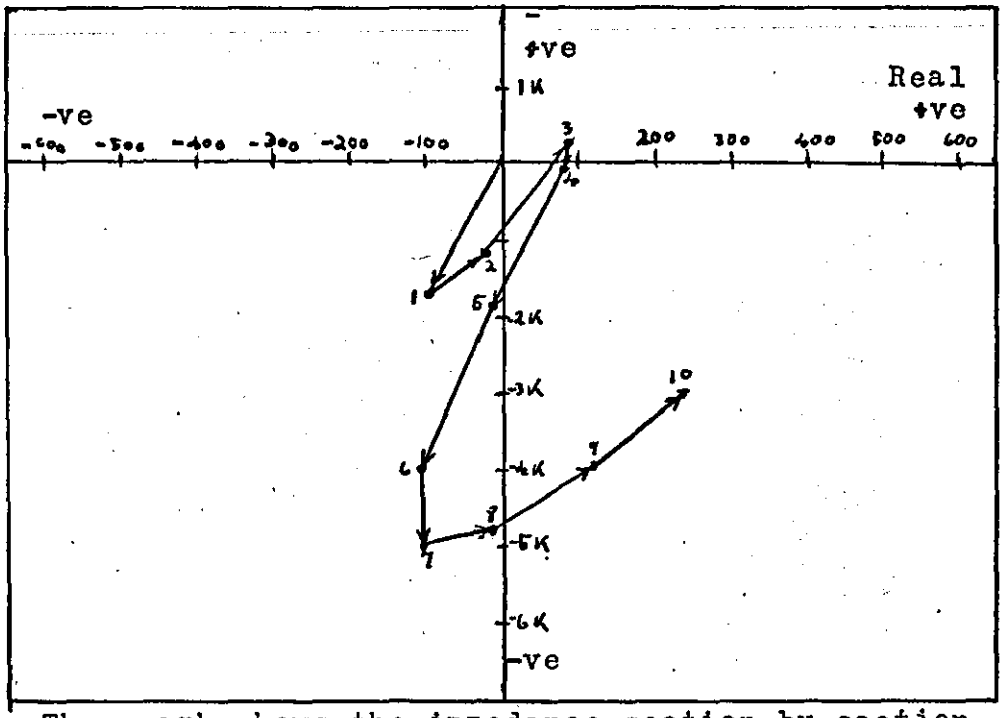

The graph shows the impedance, section by section, of the 1000 turn coil of section 6-3, at a frequency of 2.9MHz (just before the fourth resonance-).

Figure 8-2 Experiment Arrangement for Measuring the Magnetic Field.

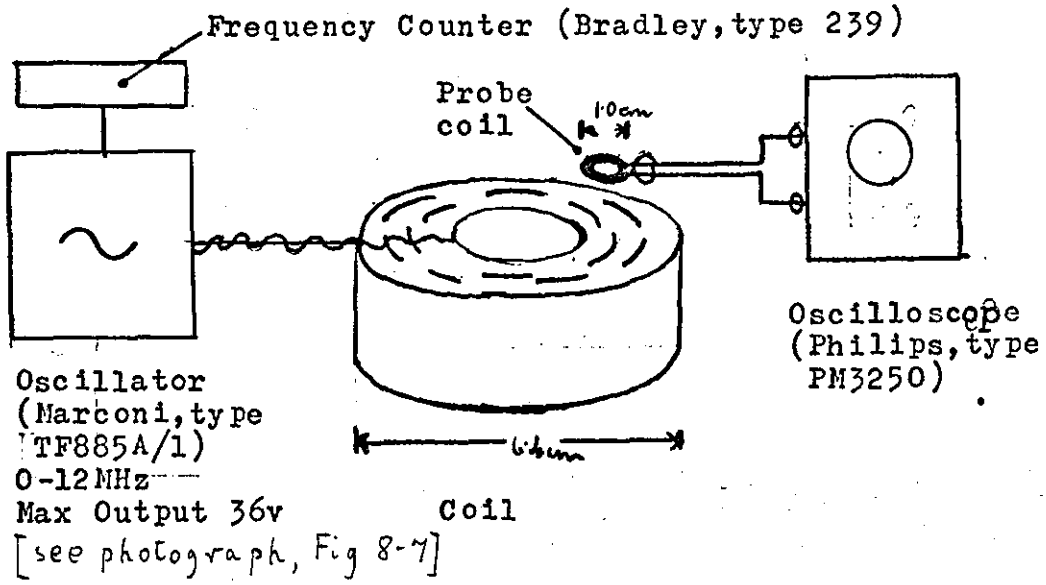

The magnetic field H_z is given by equation 4-2-14.

$$H_z = \frac{I}{4\pi W}\int_0^{2\pi} \frac{d\theta_1 (r_1 - r\cos\theta_1) r_1}{(r_1^2 + r^2 - 2r_1 r\cos\theta_1)} \left\{ \frac{(W/2 - z)}{\left[r_1^2 + r^2 - 2r_1 r\cos\theta_1 + (z - W/2)^2\right]^{1/2}} \right. \quad 4\text{-}2\text{-}14$$

$$\left. - \frac{(W/2 + z)}{\left[r_1^2 + r^2 - 2r_1 r\cos\theta_1 + (z + W/2)^2\right]^{1/2}} \right\}$$

When r is put equal to zero H_z becomes,

$$H_z = \frac{I}{4\pi W}\int_0^{2\pi} d\theta_1 \left\{ \frac{(W/2 - z)}{\left[r_1^2 + (z - W/2)^2\right]^{1/2}} - \frac{(W/2 + z)}{\left[r_1^2 + (z + W/2)^2\right]^{1/2}} \right\} \quad 8\text{-}2\text{-}1$$

The integration over θ_1 is trivial.

$$H_z = \frac{I}{2W} \left\{ \frac{(W/2 - z)}{\left[r_1^2 + (z - W/2)^2\right]^{1/2}} - \frac{(W/2 + z)}{\left[r_1^2 + (z + W/2)^2\right]^{1/2}} \right\} \quad 8\text{-}2\text{-}2$$

The current I is a sinusoidal function of time. The current varies in phase from section to section, however $\underline{H}$ fields superpose, therefore it is possible to add the magnetic fields of the relevant turns. The magnetic field between the U^{th} and the $U + 1^{th}$ turns will be given by

$$H_z^u = \sum_{\nu=1}^{u} \frac{I_\nu}{2W} \left\{ \frac{(W/2 - z)}{\left[r_\nu^2 + (z - W/2)^2\right]^{1/2}} - \frac{(W/2 + z)}{\left[r_\nu^2 + (z + W/2)^2\right]^{1/2}} \right\} \quad 8\text{-}2\text{-}3$$

where turn 1 lies on the circumference of the coil, and I_ν and r_ν are the current in the ν^{th} turn and the radius of the ν^{th} turn respectively.

The currents calculated by the elimination program are relative to the input current, and therefore any magnetic field calculated from these currents will be in terms of H per amp input. This is not a great disadvantage as it is not intended to find the absolute H_z experimentally but only the shape of the H_z distribution over the radius of the coil.

The subroutine to calculate the magnetic field from a given current

distribution is shown in Appendix 4. This subroutine was added to the basic elimination program. The output is in terms of the radius of the turn and the magnetic field at that turn for all the turns of the coil. The field within the core of the coil will be that of the last turn.

3. The coil chosen for the experiment was a 400 turn coil with a core diameter of 2.0 cm and an overall diameter of 6.0 cm, the other physical parameters are shown in Fig.8-3. The coil was heat treated. The calculated impedance spectrum, using only the d.c. resistances, is shown in Fig.8-4a The experimental impedance spectrum is shown in Fig.8-4b The frequencies of the first 3 resonances, theory and experiment, are shown in Fig.8-4c the calculated frequencies are in error by+33%. This may be due to the approximations used to calculate the inductances, Whatever is causing the discrepancy, it prevents a direct correspondence between the theoretical and experimental magnetic field distribution. However it is still possible to salvage something, ie, does the theoretical evolution of the magnetic field with increasing ffequency correspond with the experimental evolution.

4. The experimental apparatus is shown in Fig.8-2; the 400 turn FWI is fed from a high output (36V) signal generator and frequency counter. The search coil consists of 100 turns of wire, wound on a 0.7 cm diameter core, the total diameter being 1.0 cm. The search coil resonates at a frequency of 8.5 MH_z, the highest frequency at which the search coil is used is 6.0 MH_z, therefore the coil never becomes capacitive. The voltage across the FWI was kept at 15V.

The FWI and the search coil were both mounted on a metal table. The FWI was held on a perspex base which could be driven in both horizontal directions by screw drives with vernier scales. The search coil was mounted on a perspex arm, which in turn was mounted on a micro-manipulator, which had screw drives in all three directions, each drive having a vernier scale.

The voltage from the search coil is related to the magnetic field by

Figure 8-3

Thickness of Aluminium Foil	5.0μm
Width of " "	2.4cm
Permittivity of Plastic Foil	2.2
Width " " "	3.0cm
Thickness " " "	45.0μm

Figure 8-4

a/

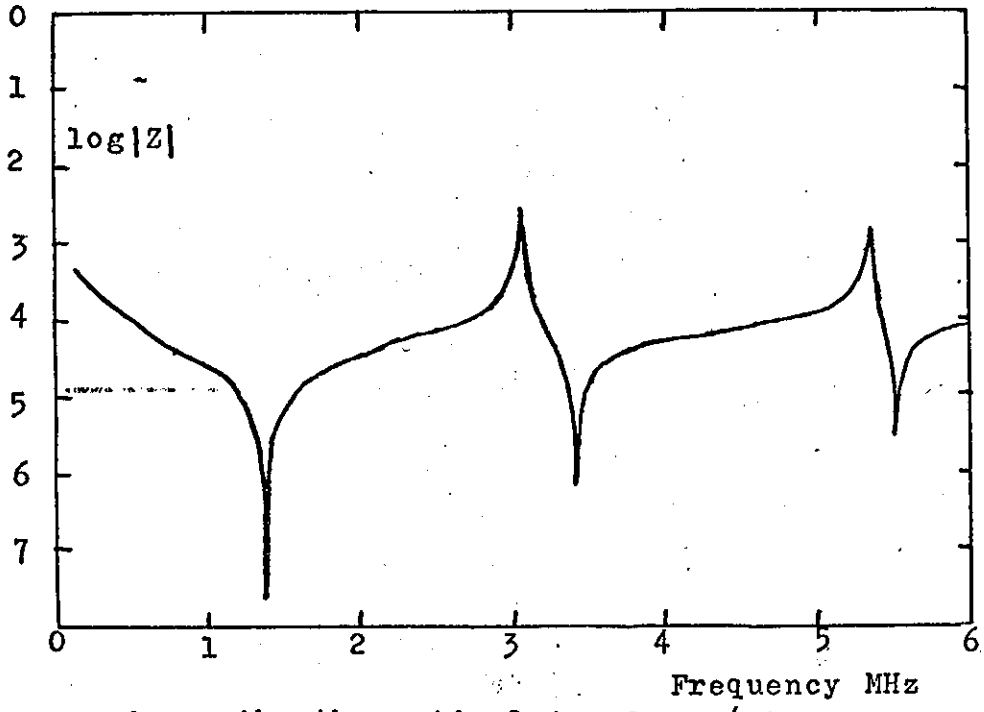

a shows the theoretical impedance/ frequency spectrum, and b the experimental impedance/ frequency spectrum, of the 400 turn coil.

b/

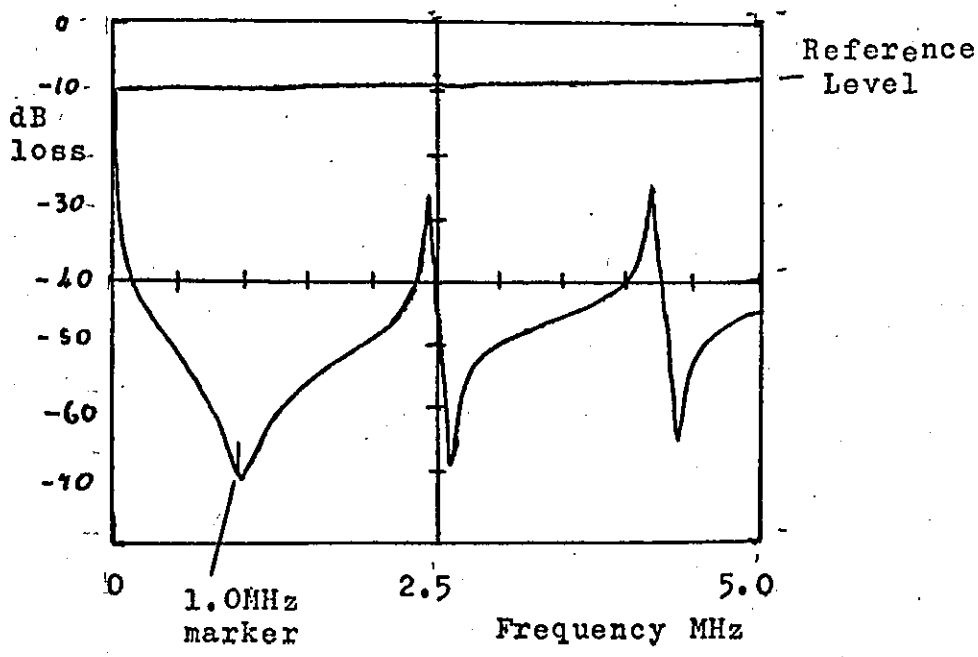

c/

Order of maximum Impedance resonance	Theory MHz	Experiment MHz	Error %
1	1.366	1.015±0.01	+34.6
2	3.41	2.55 ±0.01	+33.8
3	5.517	4.256 ± 0.005	+29.8

$$V = \sum \iint \mu_o \frac{\partial H_z}{\partial t} \qquad 8\text{-}4\text{-}1$$

Where the double integral goes over the area of a particular turn and the summation runs over all the turns of the coil. The finite area of the search coil means that the resolution of the probe is poor, it cannot resolve events which have a width less than that of the coil.

One serious problem encountered was the capacitive coupling between the search coil and the FWI, this could at some frequencies produce a larger signal than the magnetic coupling. This could be circumvented by floating the two outputs from the search coil and then subtracting the two signals. The capacitive signal should be the same on both outputs, and therefore should be eliminated by the subtraction. The oscilloscope used has the facility for subtracting the input to amplifier B from the input to amplifier A and displaying the result.

This procedure reduced the error to acceptable levels. The errors shown in Fig. 8-6a to 6j were estimated at each frequency by replacing the FWI by a metal plate at an appropriate distance from the search coil and measuring the resulting difference signal.

5. The evolution of the predicted peak magnetic field over the first three resonances is shown in Figs. 8-5a to 8-5h. The graphs show the peak magnitude of the magnetic field, in terms of H per amp input, against the distance from the centre of the coil. The magnetic field has cylindrical symmetry, therefore the field is shown over the radius and not the diameter.

Fig. 8-5a shows the field at a frequency of 1.0 MHz, just below the fundamental resonance, and at a frequency of 1.5 MHz. just above the fundamental resonance. The interesting part begins at Fig. 8-5b At 2.0 MHz the field begins to decrease and at 2.5 MHz has a minimum. At the second resonance - 3.0 MHz, Fig. 8-5c - the field has increased at the centre of the coil, at the same time the maximum has moved outwards from the centre of the coil.

Figure 8-5

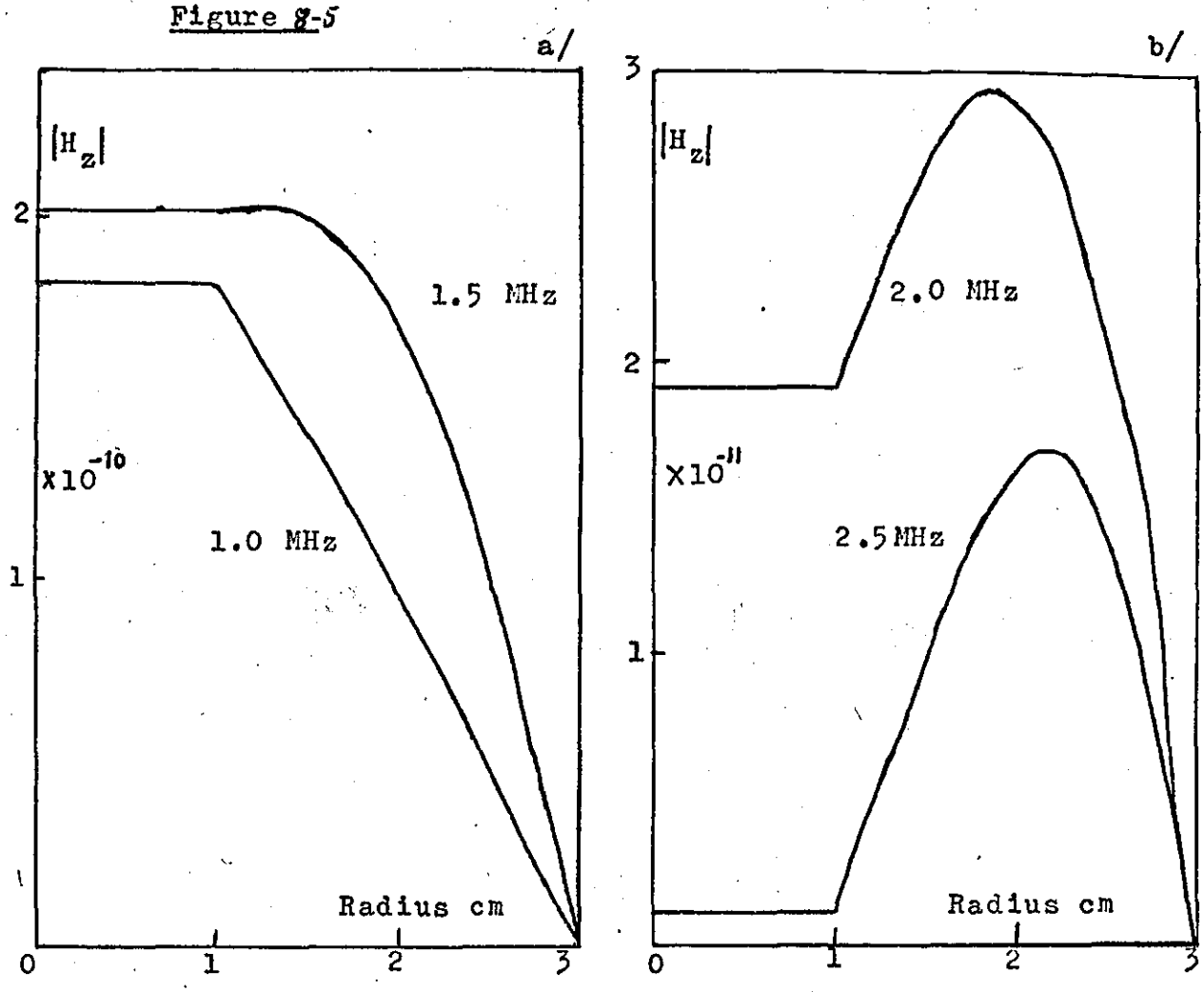

The graphs show the variation of the calculated peak value of $|H_z|$ over the radius of the coil, for the frequency shown.

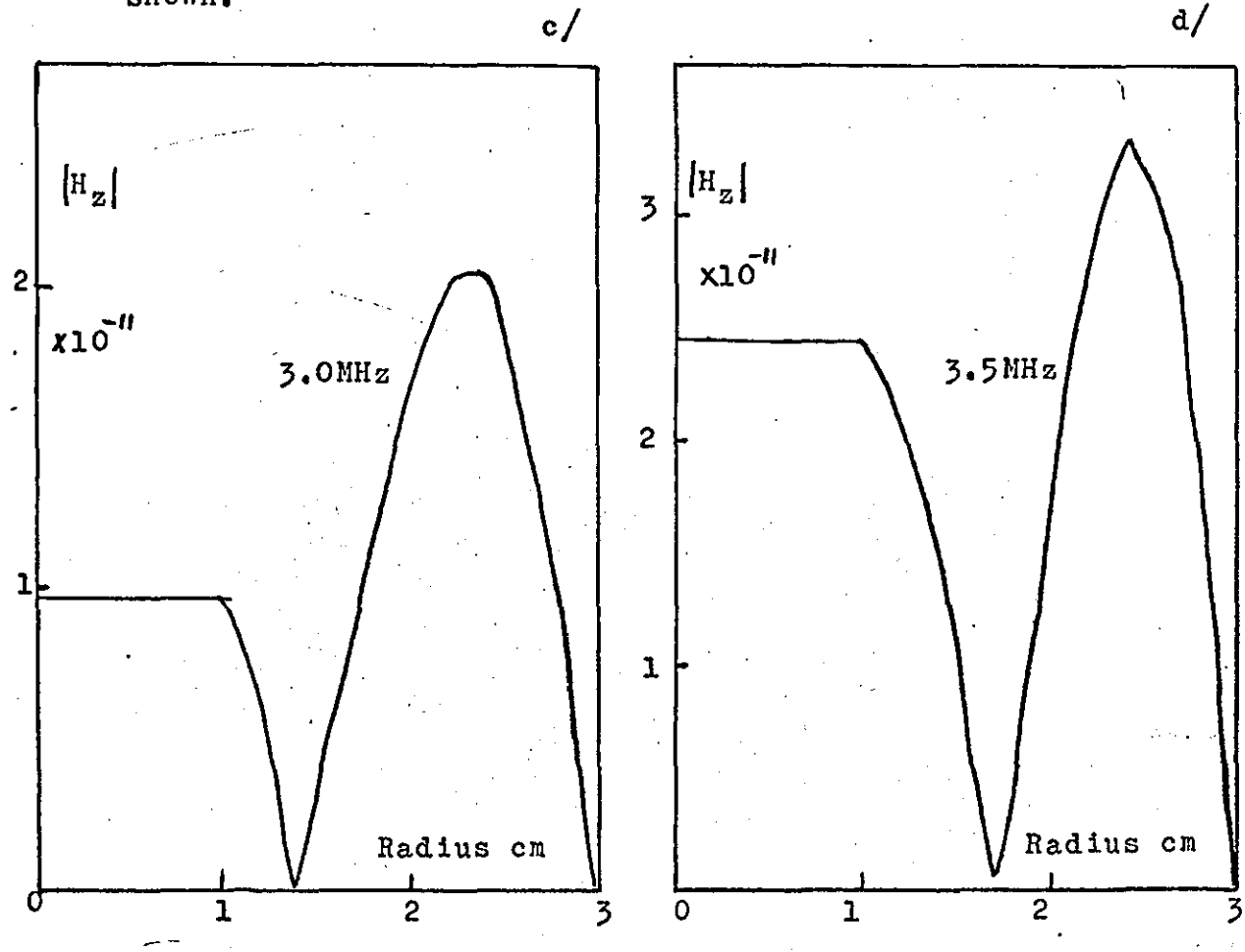

Figure 8-5

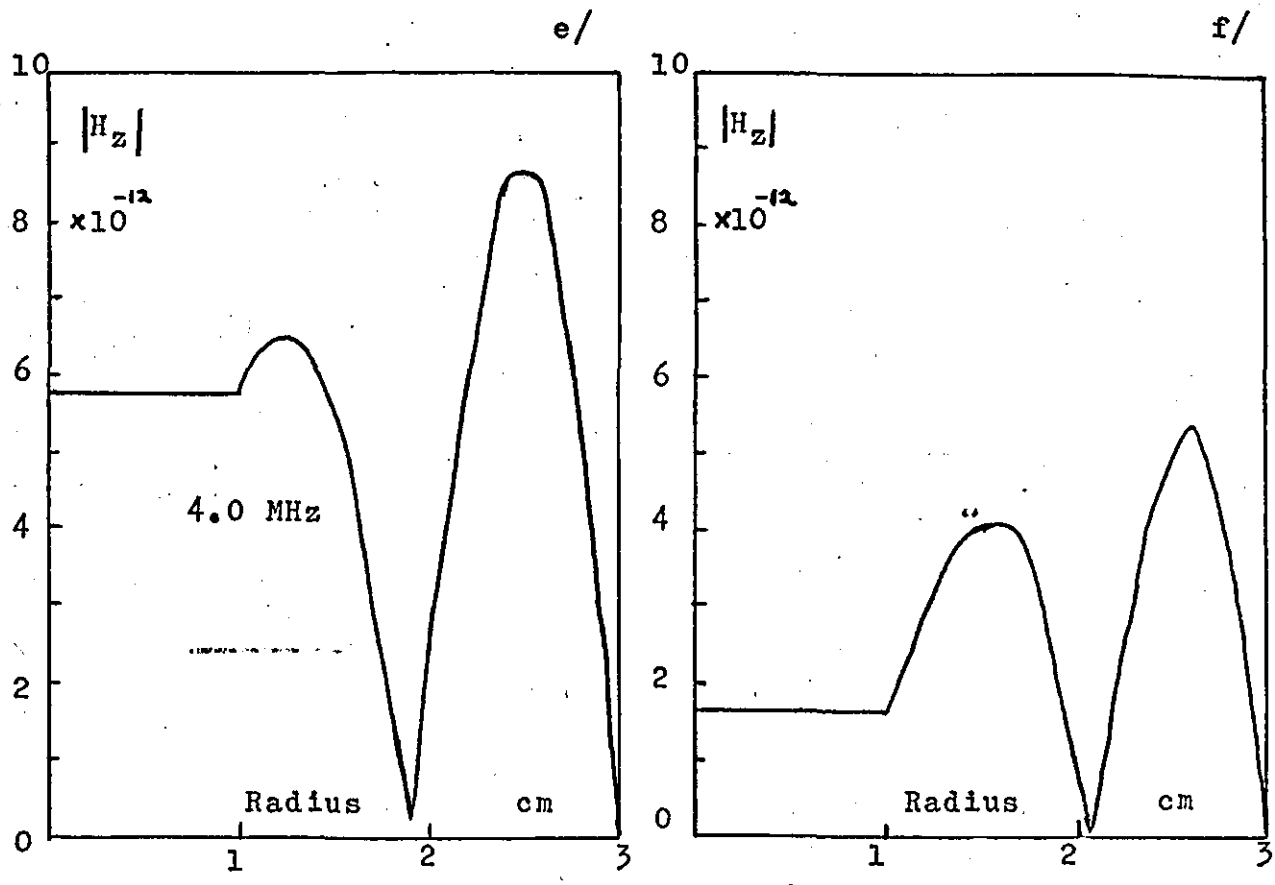

The graphs show the variation of the calculated peak value of $|H_z|$ over the radius of the coil, for the frequency shown.

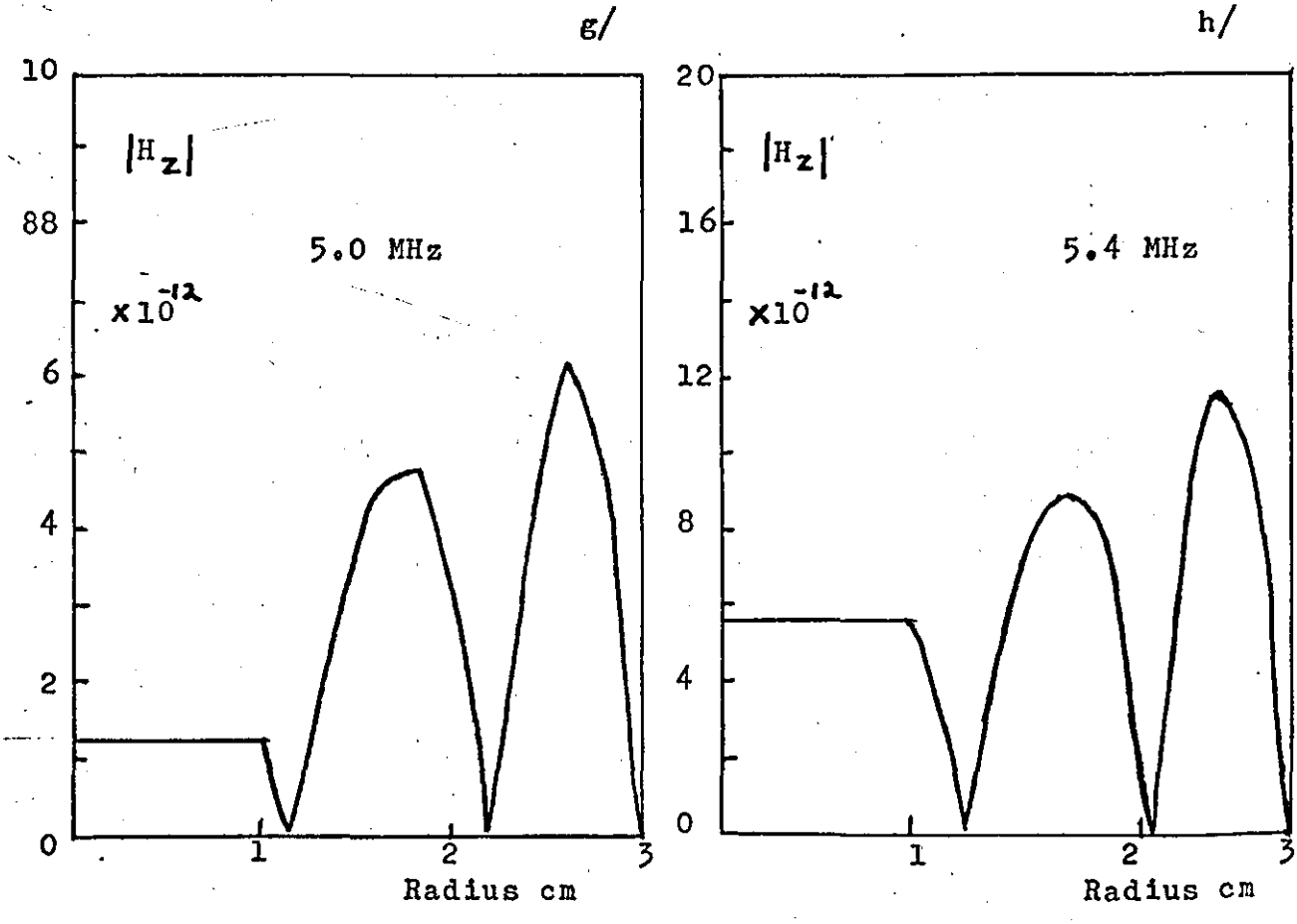

During the second resonance the field at the centre increases, Fig. 8-5d Between the second and third resonances - Figs. 8-5e and 8-5f- the field at the centre again decreases and a second maximum moves out from the centre of the coil. During the third resonance the field at the centre again increases creating a third maximum - Figs. 8-5g and 8-5f

The main characteristic of the evolution of the magnetic field with increasing frequency is that the field at the centre of the coil rises and decreases and that maxima and minima move outwards from the centre of the coil.

6. The experimental results are shown in Figs 8-6a to 8-6j The graphs in Figs 8-6a and 8-6b lie at frequencies below the first resonance, Fig 8-6c and 6d lie between the first and second resonances, Fig. 8-6e lies on the second resonance, Figs. 8-6f to 8-6i lie between the second and third resonances and [illegible] lies above the third resonance. The errors shown are the estimated errors due to the capacitive coupling. The relative size of the search coil is shown in Fig. 8-6a it covers one third of the radius of the FWI.

To correspond with the theoretical findings the magnetic field should have only one maxima below the first resonance, Figs 8-6a and 8-6b show that this is indeed the case. Between the first and second resonances the field at the centre of the coil should fall to zero and rise again, Figs. 8-6c and 8-6d show that the magnetic field does indeed fall and Fig. 8-6e shows that it does increase again to form a second maximum. Between the second and third resonances the theory indicates that the field should fall a second time to zero and rise again to form a third maximum at the third resonance, Figs. 8-6f to 8-6i show that in fact the magnetic field does this. Above the third resonance no more maxima could be found using the search coil, Fig. [illegible] at the fourth resonance shows only 1 large and 2 small maxima. This seems to be due to the size of the search coil making it impossible to resolve any more maxima.

Figure 8-6

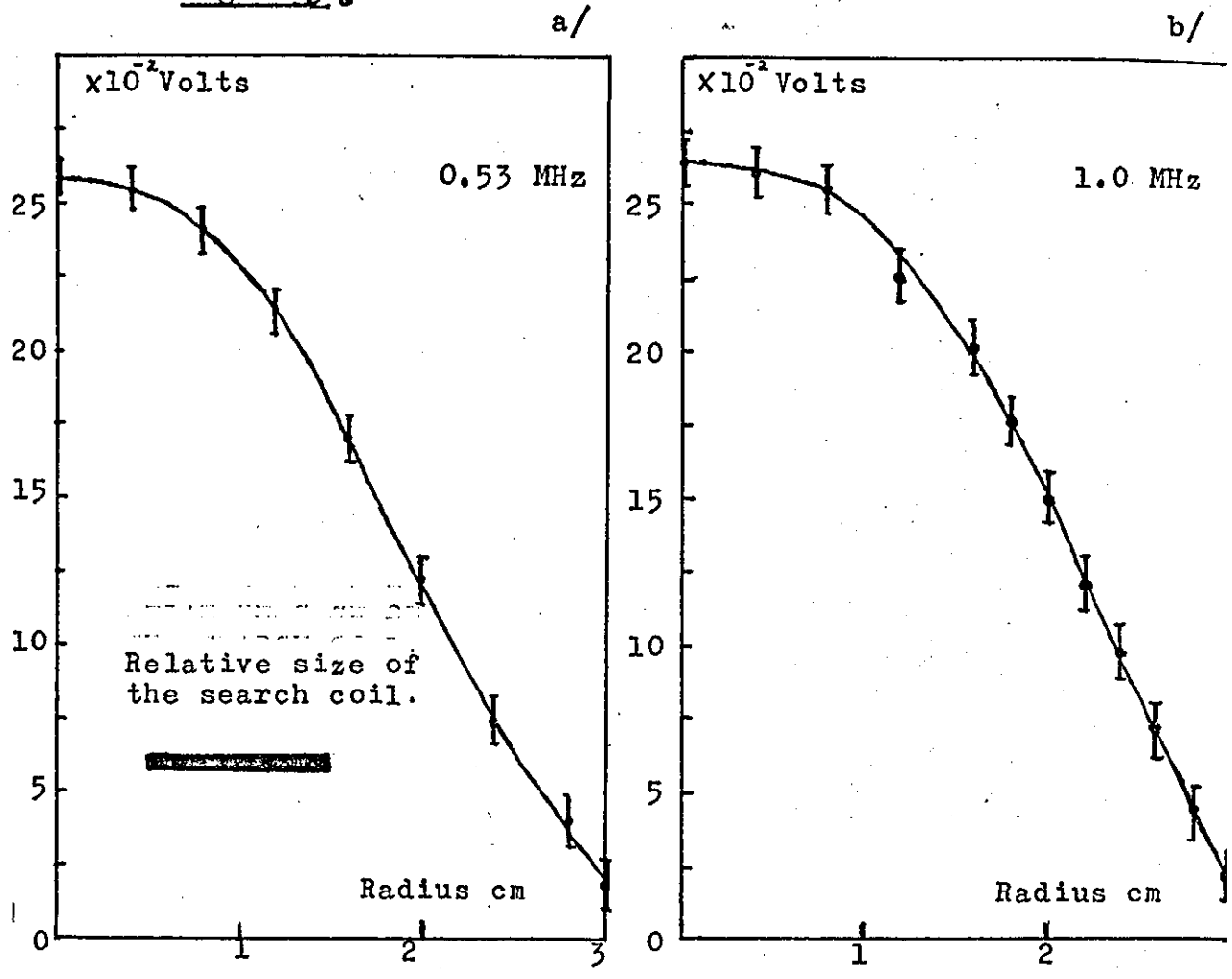

The graphs show the variation of the peak value of the voltage detected by the search coil over the radius of the coil, for the frequencies shown.

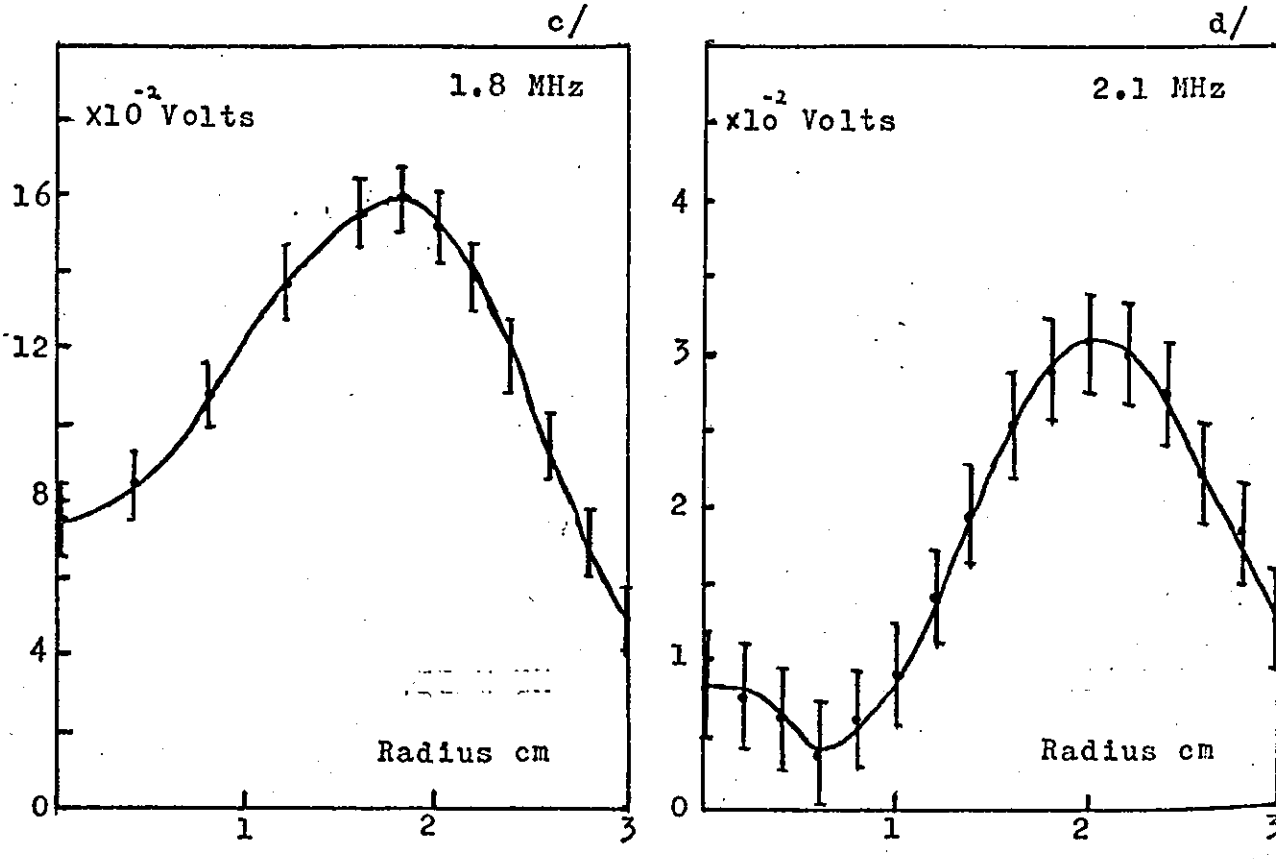

Figure 8-6

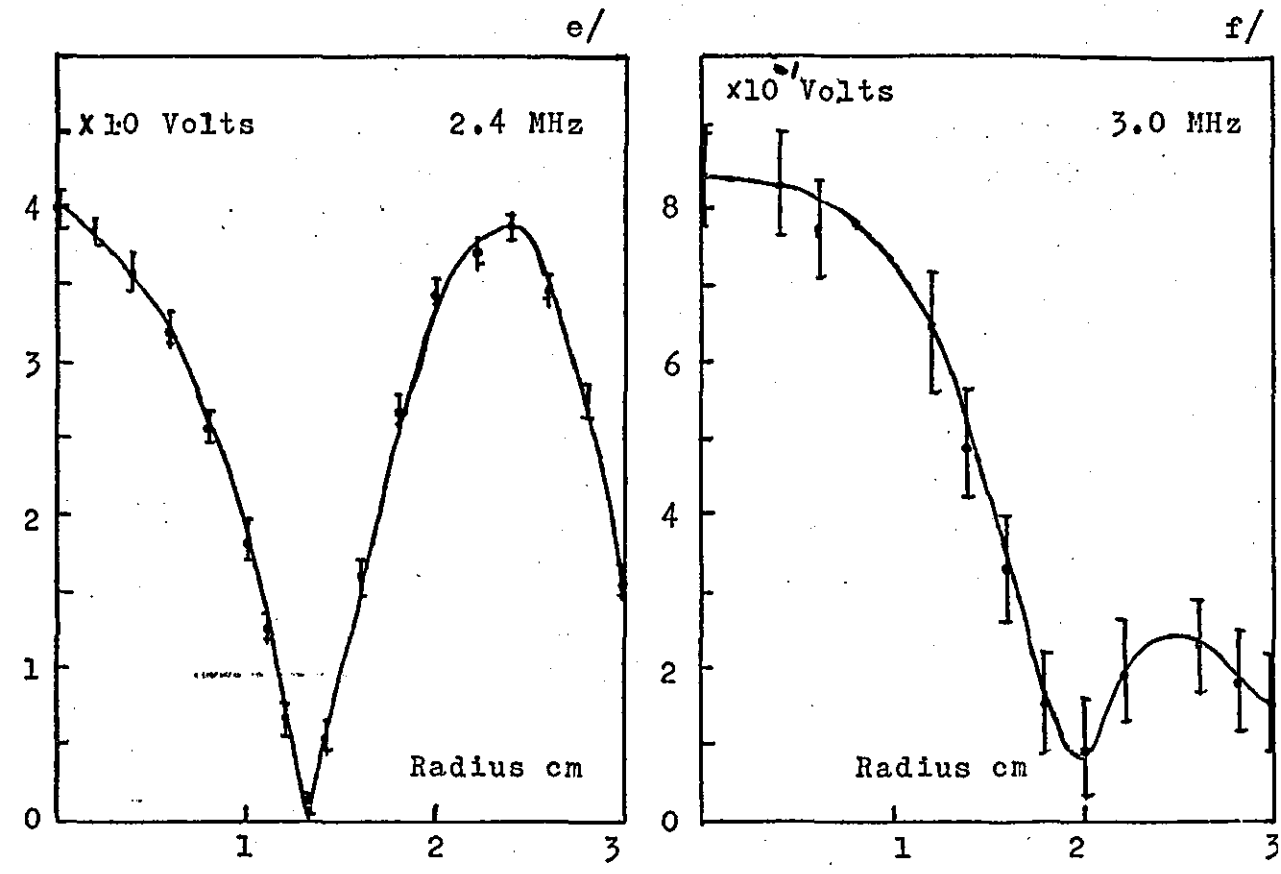

The graphs show the variation of the peak value of the voltage detected by the search coil over the radius of the coil, for the frequencies shown.

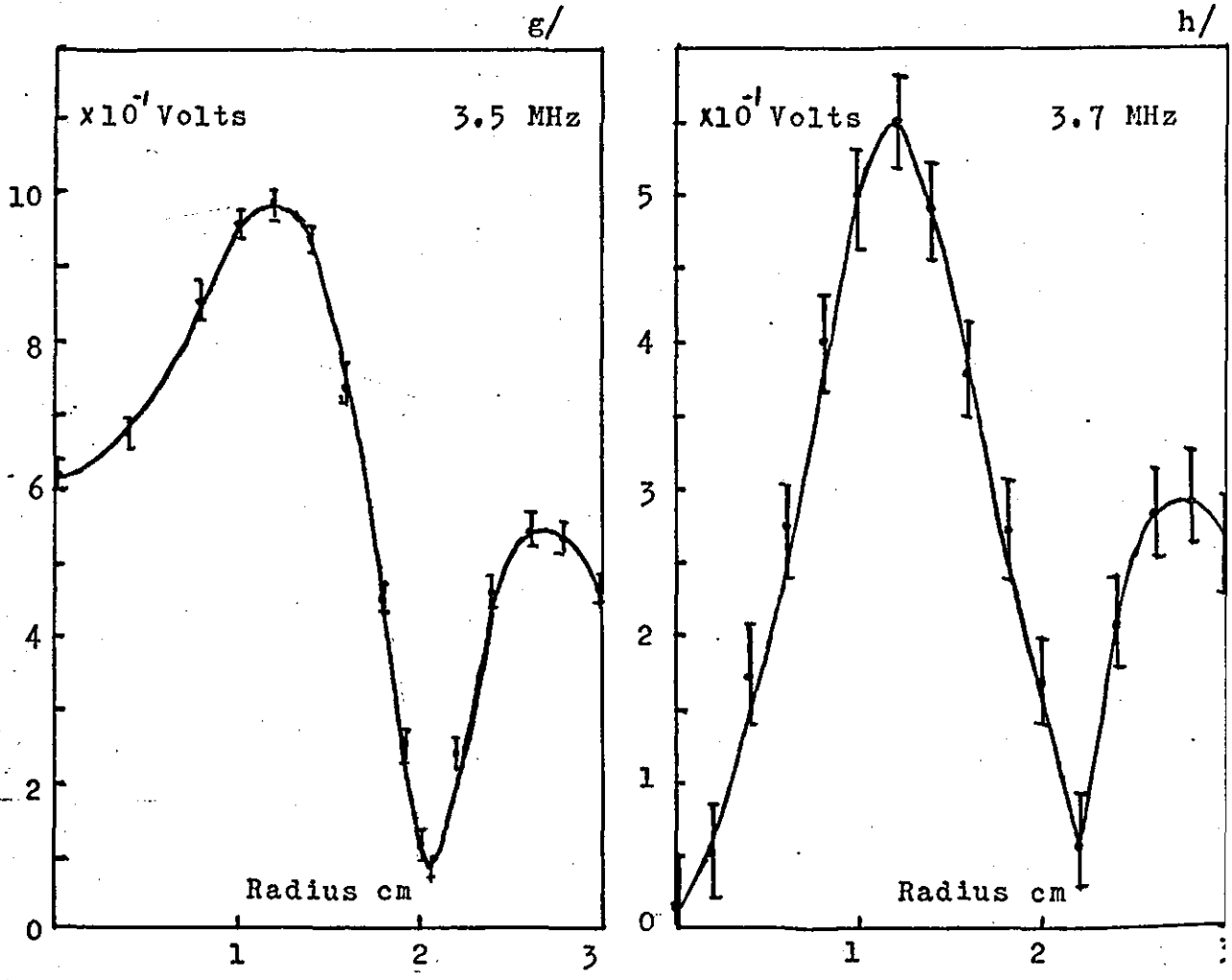

Figure 8-6

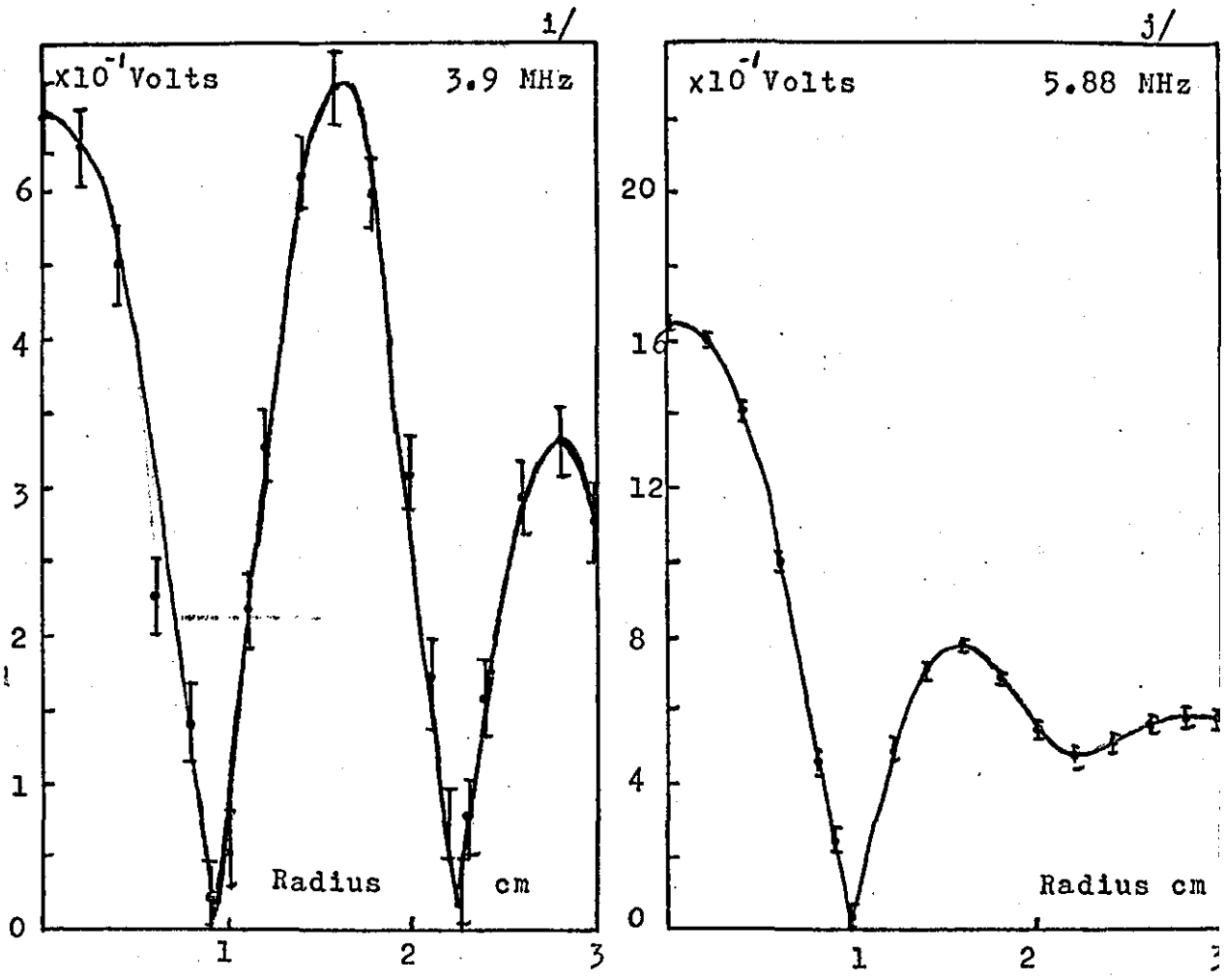

The graphs show the variation of the peak value of the voltage detected by the search coil over the radius of the coil, for the frequencies shown.

Figure 8-7 Photograph of the Experimental Arrangement for Measuring the Magnetic Field.

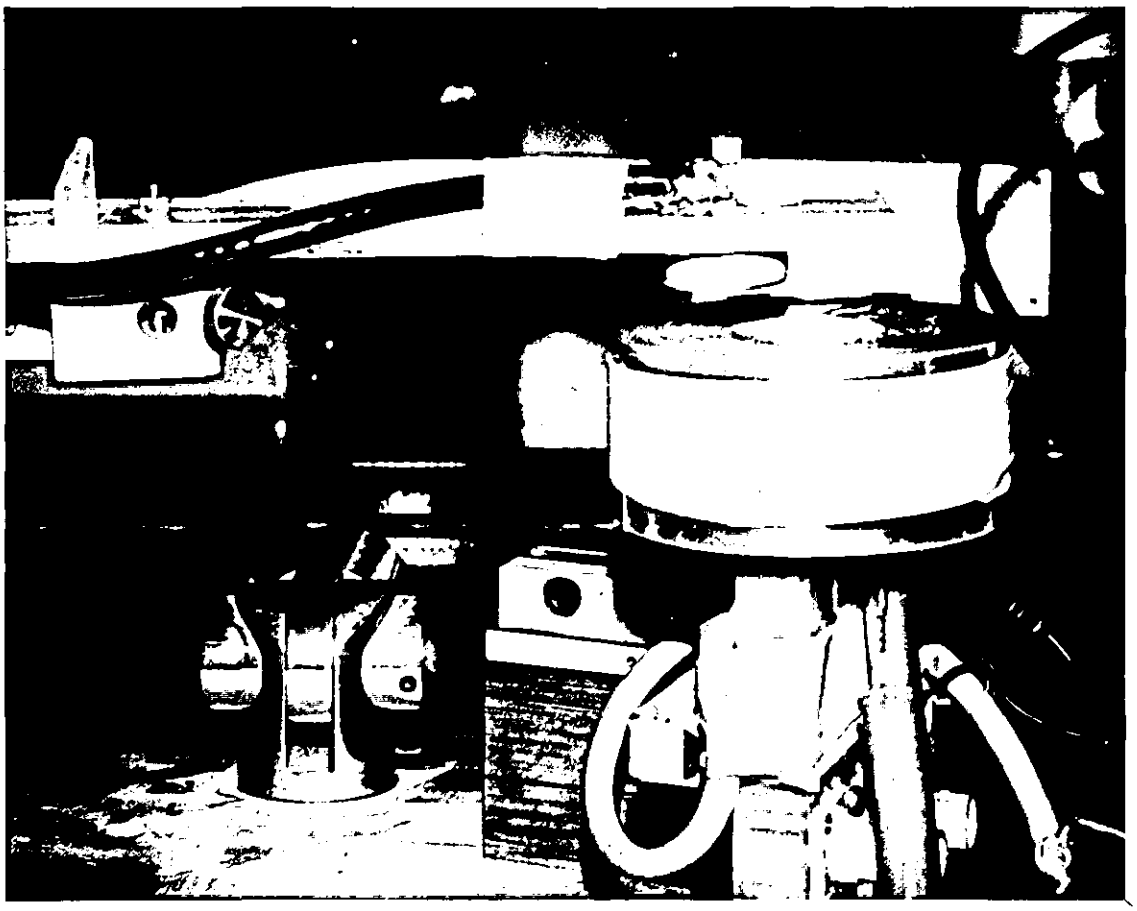

The photograph shows the search coil in place above the large (6.0cm) FWI to determine its magnetic field. The search coil is somewhat smaller than it appears to be on the photograph, the wire does not entirely fill the former. The distance the search coil moves can be read from a vernier scale. The signal is taken from the search coil by the two coaxial cables.

The value of Z, the height of the search coil above the centre of the coil, is 2 cm. This value was used in the calculation on page 66.

Section 9. Proposed Extension of the Model to Other Components.

1. One of the reasons for initiating a study of the inductance of FWI's is that if the inductance could be understood, then this could form the basis of an understanding of the inductance of wound foil capacitors.

Wound foil capacitors fall into two categories; inductively wound and extended foil. Inductivily wound capacitors have a construction similar to that of FWI's, extended foil capacitors have the construction shown in Fig.9-1. The foils are brought out from either side of the capacitors and soldered.

Inductively wound capacitors are more generally known as embedded lug capacitors.

Inductivily wound capacitors (IWC) are expected to exhibit multiple resonance; their construction is so similar to that of FWI's. To investigate the impedance spectrum of an IWC the experimental arrangements of Figs.9-2a and9-2b were used. The arrangement of Fig.9-2a will show where in the spectrum the impedance is large compared with 50Ω . The arrangement of Fig.9-2b will conversely show where the impedance is low compared with 50Ω . The 200 turn IWC used in this preliminary investigation had metal foil of width 3.9 cm and thickness 5.0μm ; polypropylene dielectric of thickness 12.5μm ; a core radius 1.0 cm.

The impedance spectrum using the arrangement of Fig.9-2a is shown in Fig.9-3a, correspondingly that using the arrangement of Fig.9-2b is shown in Fig.9-3b. The reference level in Fig.9-3a is with the capacitor shorted out, the reference level in Fig.9-3b is with the capacitor removed. In both cases the traces with the capacitors in place have been displaced downwards by 10 dB from the reference level. Fig.9-3a shows that the impedance spectrum has maxima at 1.8 MHz, 5.1 MHz, 8.8 MHz, 12.6 MHz and 16.4 MHz. Fig.9-3b shows that the impedance spectrum has minima at

Figure 9-1

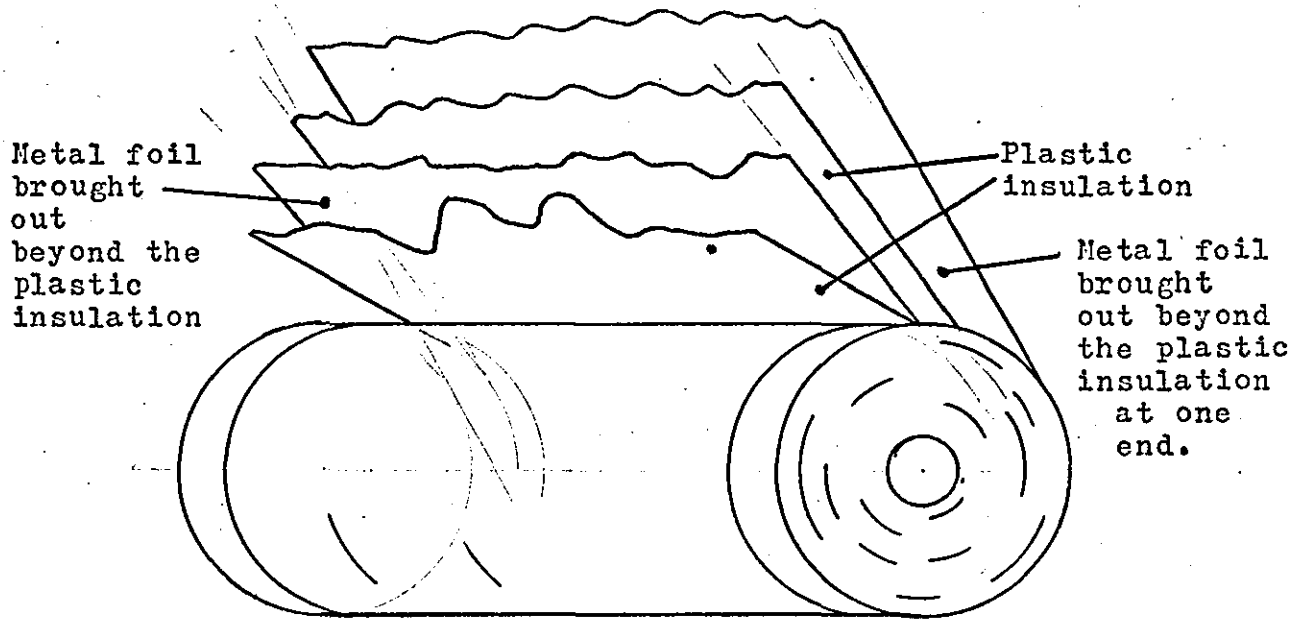

This diagram shows the construction of an extended foil capacitor. The metal foils are soldered together at the ends to reduce the self-inductance of the capacitor.

Figure 9-2

a/

This arrangement will show at what frequencies the impedance is large.

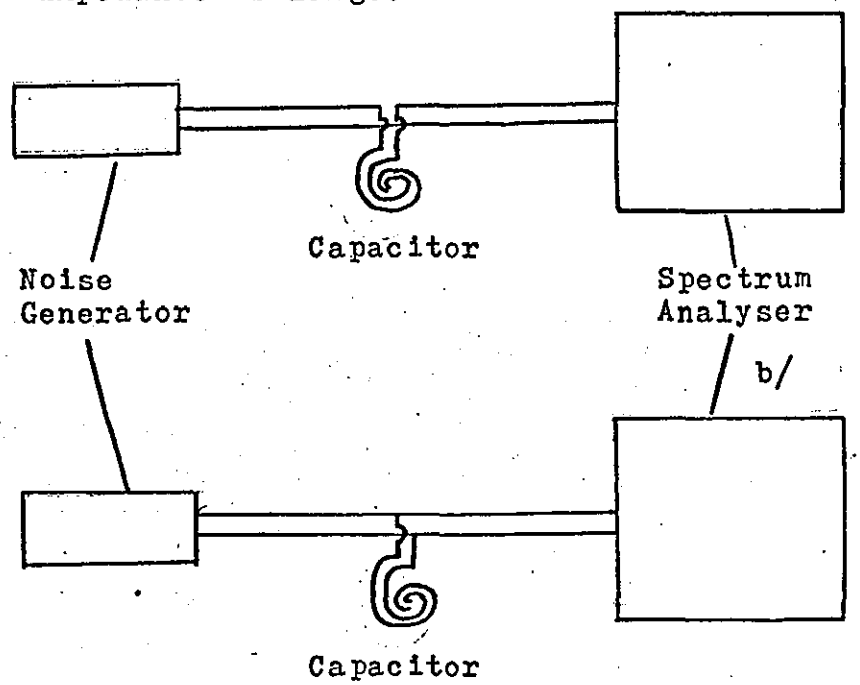

b/

This arrangement will show at what frequencies the impedance is small compared with 50ohms.

Figure 9-3

a/

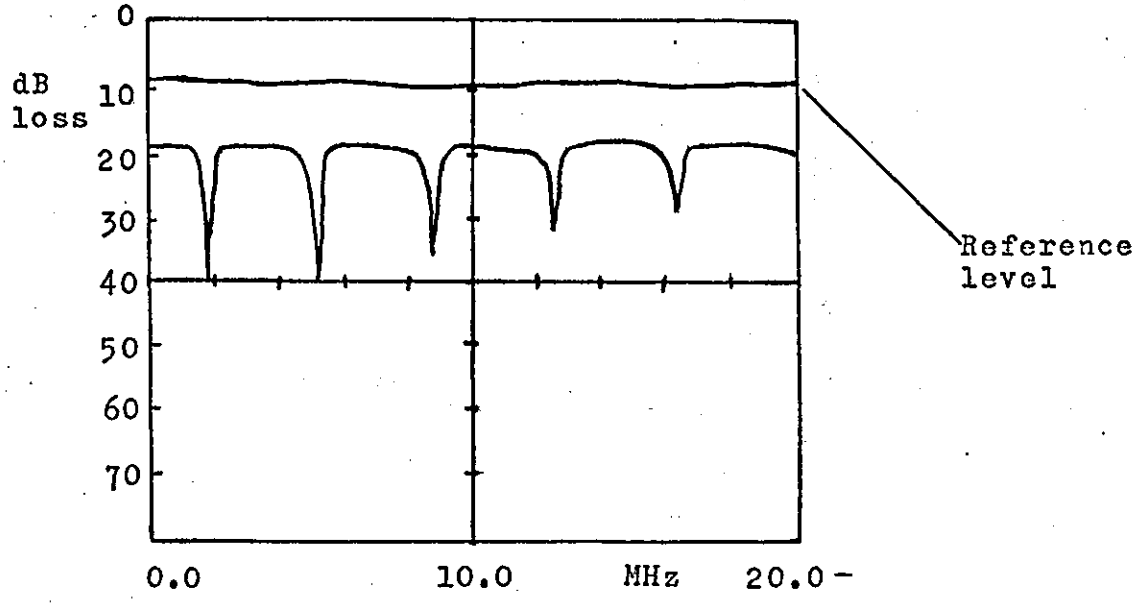

This graph shows the spectrum of the noise generator using the arrangement of Fig.2a.The trace with the capacitor in has been displaced downwards by 10dB.

b/

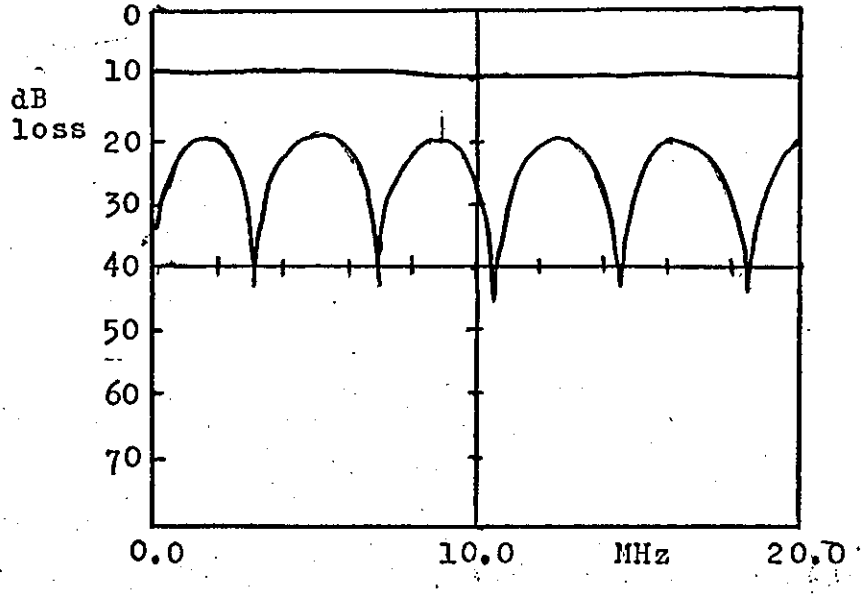

This graph shows the spectrum of the noise generator using the arrangement of Fig.2b.The trace with the capacitor in has been displaced downwards by 10dB.

<0.1 MHz, 3.0 MHz, 6.9 MHz, 10.6 MHz, 14.5 MHz and 18.5 MHz. In neither case are the dc values shown. Clearly this is a form of multiple resonant behaviour. The results of this experiment disagree with the present theory of multiple resonance in embedded lug capacitors.

2. To derive an equivalent circuit for an IWC we follow the same procedure used to derive the equivalent circuit of a FWI. Fig.9-4 shows the half-turn inductances $L/2$ and the turn-to-turn capacitors C. In the case of a capacitor the terminals can be connected anywhere. Intuitively the placing of the terminals will influence the impedance spectrum. There are two extreme cases; one where the terminals are both at the same ends of the foils, the other where the terminals are at opposite ends of the foils. To illustrate the difference the equivalent circuits for these two cases are laid out differently. The circuit in Fig.9-5a has the terminals at the same ends of the foils. The L's and the C's have been rearranged and the mutual inductances included. The circuit resembles the transmission line equivalent circuit. For this circuit there are $N+1$ mesh equations, N of the form

$$\sum_{v=1\neq u}^{N} -(-1)^{N} j\omega M_{u,v} I_v + j\omega L_u I_u + (I_u - I_{u+1})/j\omega C_{u+1}$$

$$+ (I_u - I_{u-1})/j\omega C_u = 0 \qquad 9\text{-}1\text{-}1$$

$$1 \leq u \leq N$$

The $N+1^{th}$ equation has the form

$$V_0 = (I_0 - I_1)/j\omega C_1 \qquad 9\text{-}1\text{-}2$$

When the frequency is low the inductances can be neglected and the equivalent circuit becomes purely capacitive, with a total capacitance of

$$C = \sum_{u=1}^{N} C_u \qquad 9\text{-}1\text{-}3$$

Figure 9-4

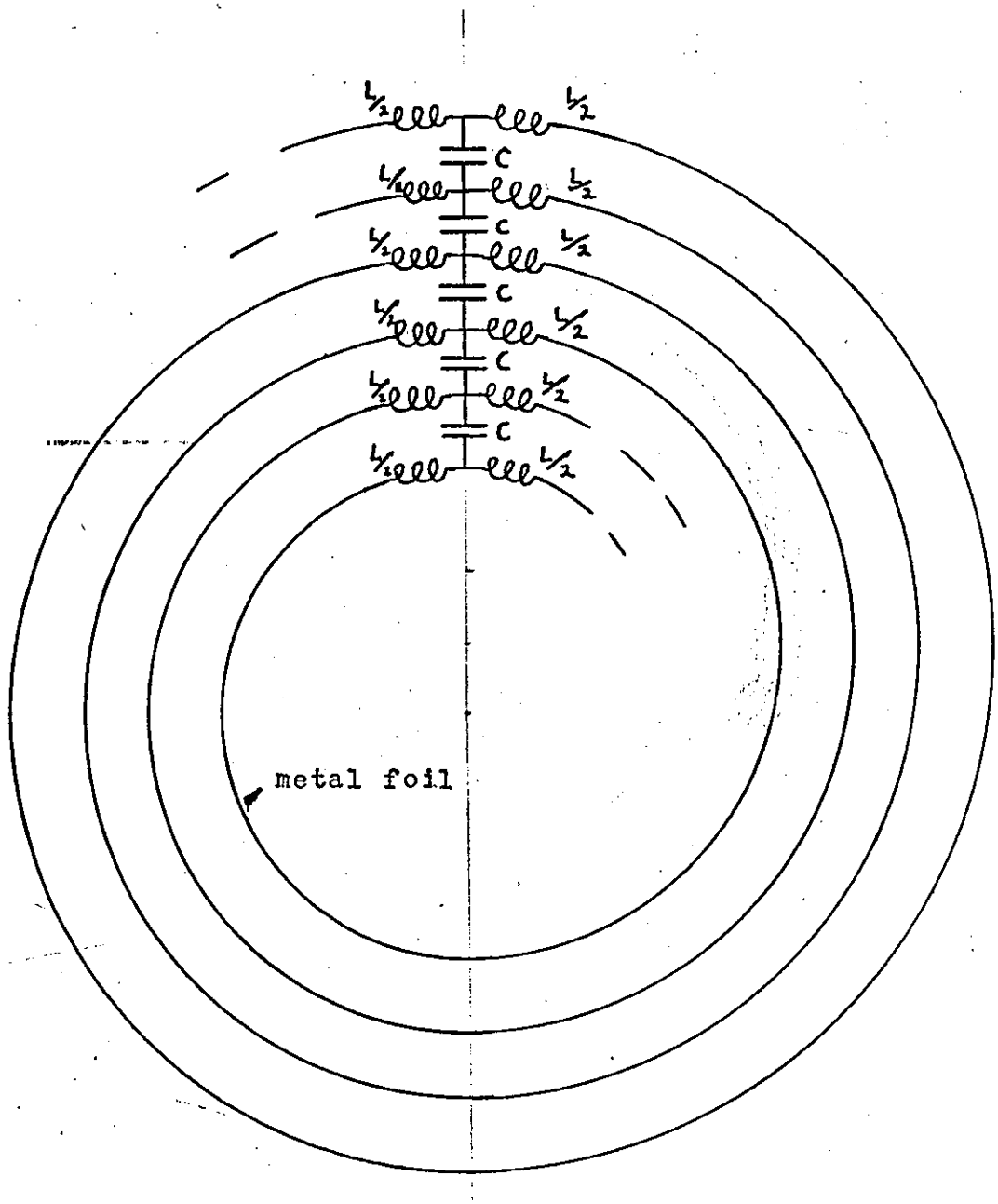

This diagram shows the method of deriving the lumped element equivalent circuit for an inductive wound foil capacitor.

Figure 9-5a

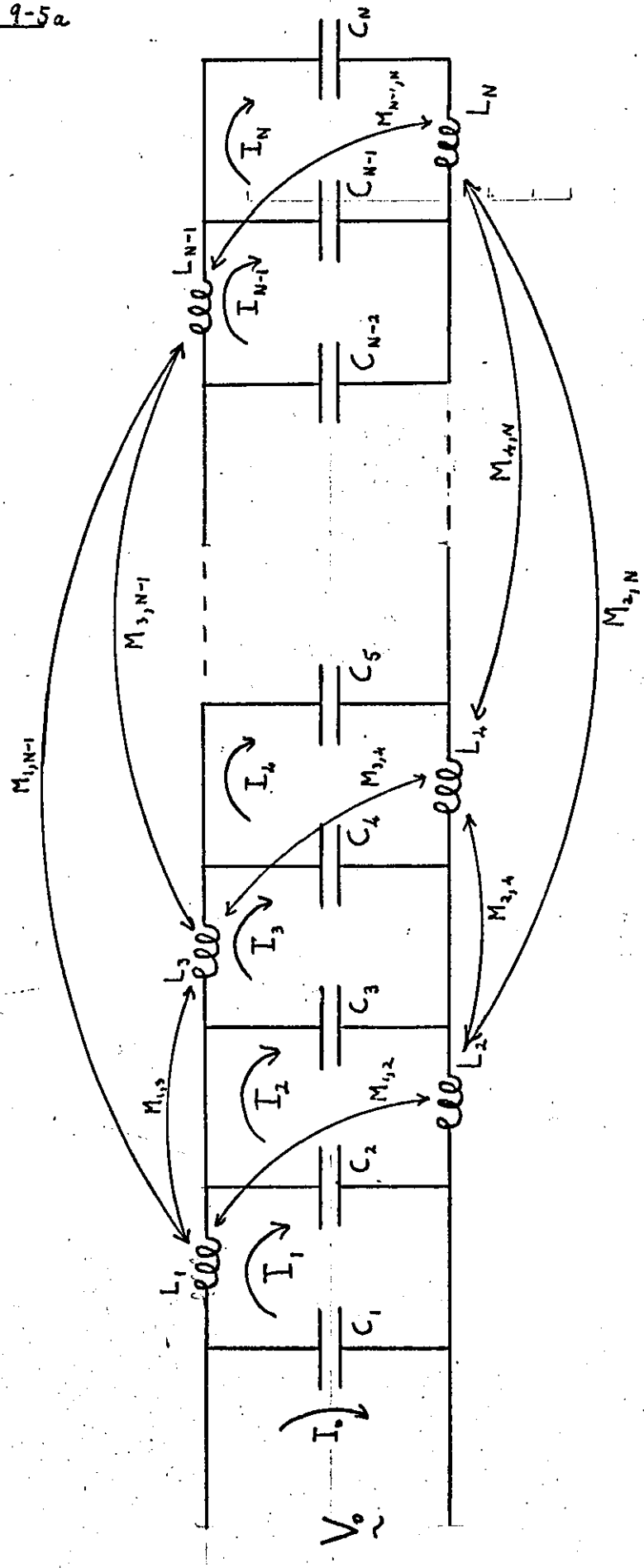

Proposed equivalent circuit for an inductive wound foil capacitor. The terminals are both at the same end of the winding.

The equivalent circuit of Fig.7-5b illustrates the situation when the terminals are at opposite ends of the foils. The L's and C's have again been rearranged and the mutual inductances included. The circuit resembles that of a FWI. There are $N+1$ mesh equations, N of the form

$$\sum_{v=1\neq u}^{N} j\omega M_{u,v} I_v + j\omega L_u I_u + (I_u + I_{u+1} - I_o)/j\omega C_{u+1} + (I_u + I_{u-1} - I_o)/j\omega C_u = 0 \qquad 9\text{-}1\text{-}4$$

$$1 \leq u \leq N$$

The $N+1^{st}$ mesh equation round the primary circuit is

$$V_o = (I_o - I_1)/j\omega C_1 + (I_o - I_1 - I_2)/j\omega C_2 + \cdots + (I_o - I_{N-1} - I_N)/j\omega C_{N-1} + (I_o - I_N)/j\omega C_N \qquad 9\text{-}1\text{-}5$$

At low frequency the inductances can be regarded as equal to zero, and the equivalent circuit becomes purely capacitive. The total capacitance is

$$C = \sum_{u=1}^{N} C_u \qquad 9\text{-}1\text{-}6$$

Provided that a method can be found for reducing the size of the equivalent circuit, without reducing its validity too much, it would be possible to adapt the numerical methods used for the FWI equivalent circuit and derive the impedance properties of inductively wound capacitors.

3. Foil Wound Transformers.

The extension of the model from foil wound inductors to foil wound transformers is a simple one. The equivalent circuit will be that of Fig.7-6. There are N turns on the primary and N' on the secondary, therefore there are $N+N'+2$ mesh equations, N of the form

Figure 9-5b

Proposed equivalent circuit for an inductive wound foil capacitor

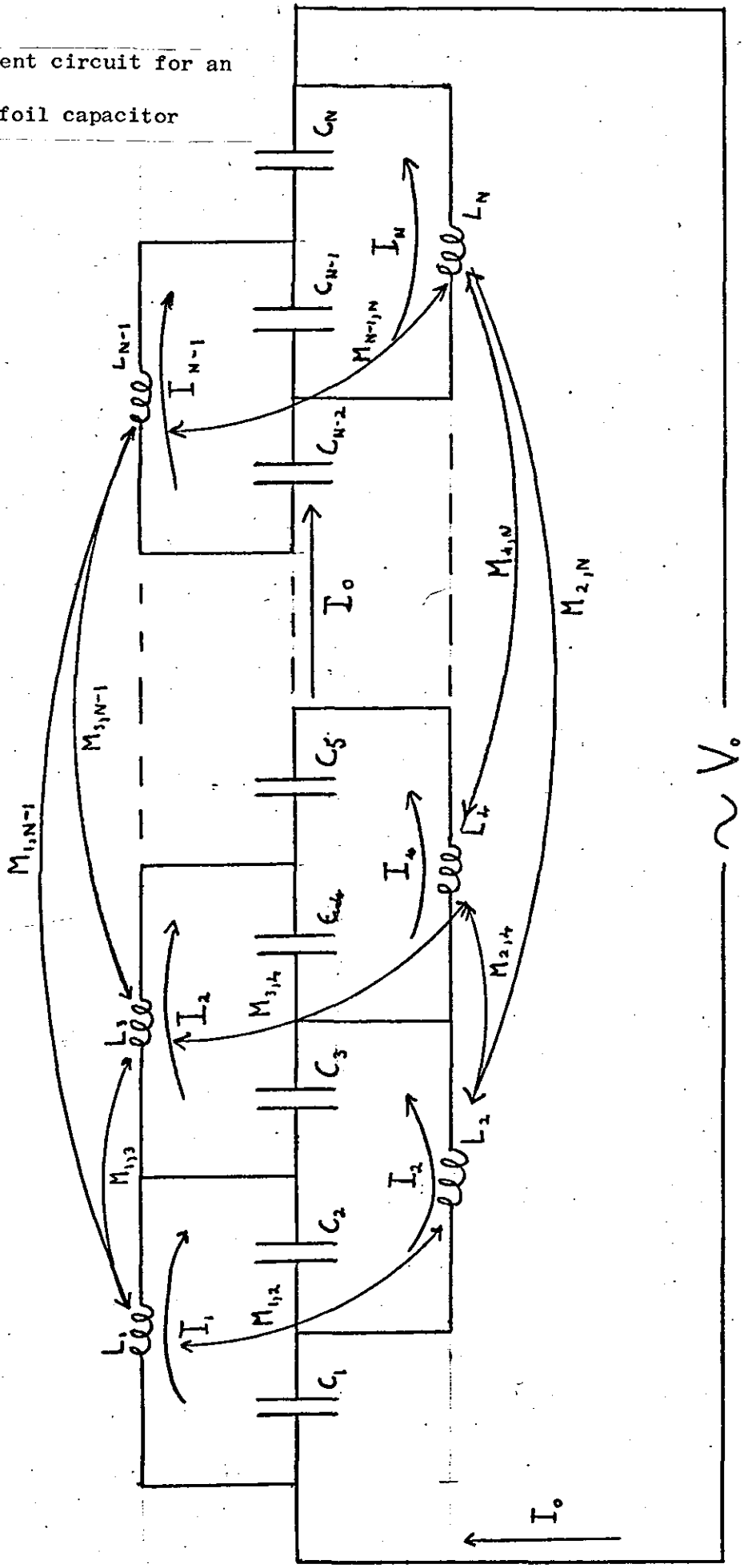

This equivalent circuit has the terminals at opposite ends.

Figure 9-6

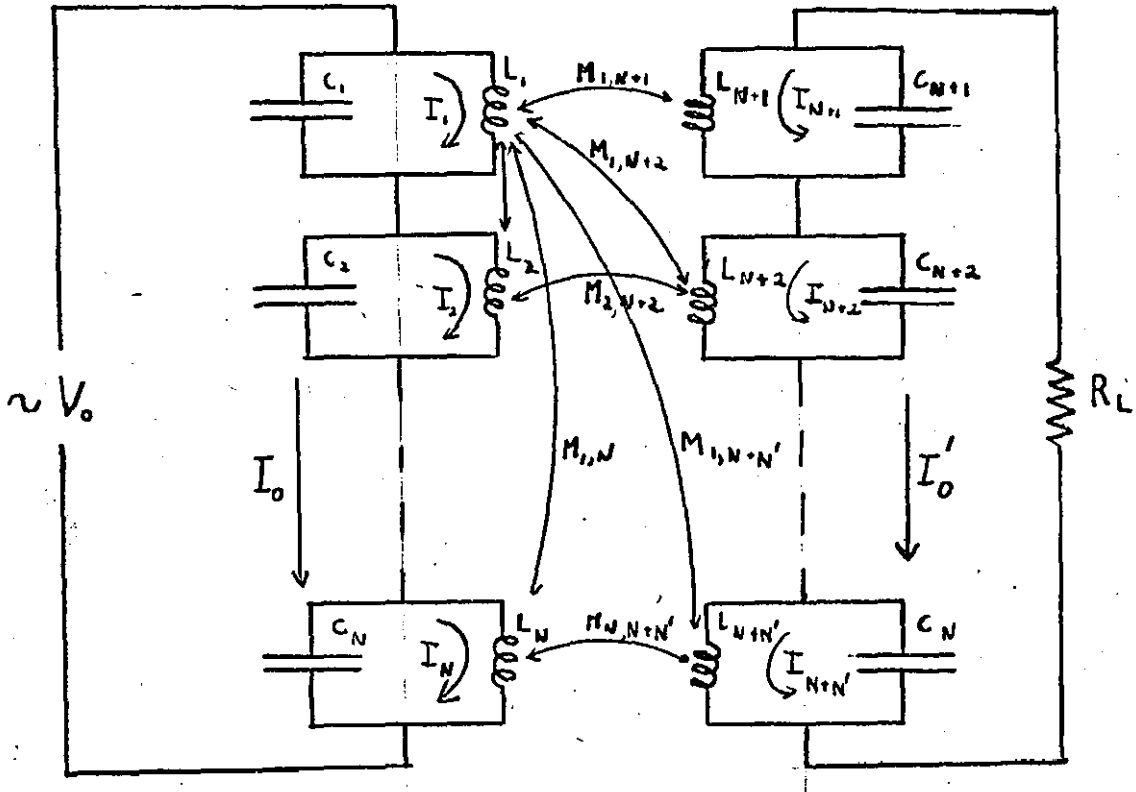

Proposed equivalent circuit of a foil wound transformer.

$$\sum_{v=1\neq u}^{N+N'} j\omega M_{u,v} I_v + (j\omega L_u + \tfrac{1}{j\omega C_u}) I_u = I_0 / j\omega C_u \qquad 9\text{-}3\text{-}1$$

$$1 \leq u \leq N$$

N' of the form

$$\sum_{v=1=u}^{N+N'} j\omega M_{u,v} I_v + (j\omega L_u + \tfrac{1}{j\omega C_u}) I_u = I'_0 / j\omega C_u \qquad 9\text{-}3\text{-}2$$

$$N \leq u \leq N'$$

The equation round the primary is

$$V_0 = \sum_{u=1}^{N} (I_0 - I_u) / j\omega C_u \qquad 9\text{-}3\text{-}3$$

The equation round the secondary is

$$I'_0 R_L = \sum_{u=N}^{N'} (I'_0 - I_u) / j\omega C_u \qquad 9\text{-}3\text{-}4$$

The method of reducing the equivalent circuit can be applied so no difficulties are anticipated in predicting the impedance spectrum.

Section 10

Conclusions

The theory of inductive and capacitive components can largely be separated into two different approaches, the lumped element and the transmission line approaches. These approaches are not entirely different methods but are only different aspects of one concept, that of the electromagnetic field. The model of FWI using turn inductances and turn to turn capacitances can be derived intuitively from the lumped element approach or by approximation from the field approach using the vector potential A. The model derived spans the two approaches.

Practical application of the model may be limited to foil components, wire components have an equivalent circuit that is much more complex. In its application to FWI the model has been broadly successful, although there are limitations. The model can predict the frequencies of a number of the lower orders of resonance to within two or three percent, the limiting factor being the number of sections used in the model. Increasing the number of sections would increase the range of the model, However, this increases the computation time, which rises as the cube of the number of sections. The accuracy is also limited by the radius of the core of the FWI. The reason in this case being the approximations used to calculate the inductances have a limited validity. The accuracy of the calculations could be improved by using a numerical integration technique in place of the approximations made to derive equation 4-2-21. The formula used to calculate the capacitances have a limited accuracy, the reason being that there are inherent difficulties associated with the winding technique. The difficulties lie with the stability of the winding tension, side slip of the metal foil and the slight air gap between the metal foil and the insulation. It is difficult to see how radical improvements could be made in this direction.

No direct comparison has been presented between the theoretical and experimental impedance spectra with regard to the actual magnitude of the impedance. Good agreement cannot be expected until reasonbly accurate calculations can be made of the a.c. resistance. The a.c. resistance largely determines the magnitude of the impedance at the resonances but not their frequency. The failure of the a.c. resistance model was probably due to the crudeness of the approximations used for the magnetic field. A more complex model may be successful.

A standing wave was found to exist in the current distribution at frequencies above the fundamental resonance. Theoretically it is understandable as a property of a set of coupled oscillators. Experimentally the current wave was shown to exist by analysing its effect on the external magnetic field.

Extensions of the theory to capacitors seems possible, enabling some light to be thrown on the inductance of large electrolytic capacitors. The model would also lead to some understanding of multiple resonance in inductively wound capacitors. The model can easily be extended to foil wound transformers.

These investigations have shown that there are applications in signal filtering but these have been superseded by digital techniques. However applications in interference suppression and filtering in power oscillators have not been discounted.

Appendix 1 Mutual Inductance Reciprocity Theorem

Consider two coupled circuits

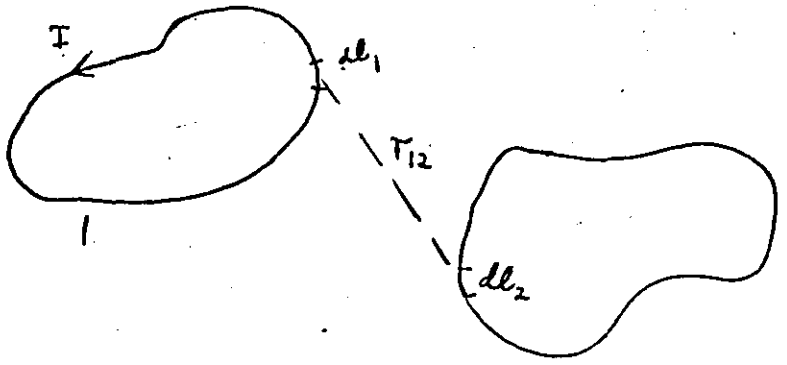

the total flux through 2 due to I in 1 is

$$\Phi_{21} = \oint_2 \underline{B}_1 \cdot d\underline{S}_2 = \oint_2 \nabla \times \underline{A}_2 \cdot d\underline{S}_2 = \oint_2 \underline{A}_2 \cdot d\underline{l}_2$$

Now $\underline{A}_1$ is calculable from the current flowing in 1

$$\underline{A}_1 = \oint_1 \frac{\mu_0 I \, d\underline{l}_1}{4\pi r_{12}}$$

Combining

$$\Phi_{21} = \oint_2 \oint_1 \frac{\mu_0 I \, d\underline{l}_1 \cdot d\underline{l}_2}{4\pi r_{12}}$$

Hence

$$M_{21} = \frac{\mu_0}{4\pi} \iint \frac{d\underline{l}_1 \cdot d\underline{l}_2}{r_{12}}$$

The integral can be performed in either order and is dependent only on the geometry, therefore

$$M_{12} = M_{21}$$

Appendix 2

The program is written in 1900 Fortran and calculates the values of L,R and C per section also calculated are the values of M from section to section.

```
      MASTER LRCANDM
      REAL RDC(20),RAC(20),MUT(20,20),C(20)
      INTEGER S
C
C   CONSTANTS OF THIS PROGRAM ARE
C
      U=1.257/(10.**6)
C   PERMEABILITY
      PY=2.0*ASIN(1.0)
C
      COND=3.53*10.**7
C
      RESIST=2.828/(10.**8)
C
C  CONDUCTIVITY OF AL
C
      E0=8.85525/(10.**12)
C
      READ(1,1)N
      READ(1,1)M
      S=N/M
C  N IS THE NO OF TURNS OF THE COIL
C  M IS THE NO OF TURNS  PER SECTION
C  S OS THE NO OF SECTIONS
      READ(1,2)RADI
C  RADI IS THE RADIUS OF THE CORE OF THE COIL
      READ(1,2)W
C  W IS THE WIDTH OF THE METAL FOIL
      READ(1,2)TD
C  TD IS THE THICKNESS OF THE PLASTIC FOIL
      READ(1,2)TM
C  TM IS THE THICKNESS OF THE METAL FOIL
      READ(1,2)E
C  E IS THE DIALECTRIC CONSTANT OF TH EPLASTIC FOIL
    1 FORMAT(I0)
    2 FORMAT(E0.0)
C
      WRITE(2,3)N
    3 FORMAT(1H ,'NO OF TURNS ON THE COIL          =',I4)
      WRITE(2,4)M
    4 FORMAT(1H ,'NO OF TURNS PER SECTION          =',I4)
C
      WRITE(2,5)S
    5 FORMAT(1H ,'NO OF SECTIONS                   =',I4)
```

```
      WRITE(2,6)RADI
    6 FORMAT(1H ,'RADIUS OF THE CORE OF THE COIL (CM)    =',E10.4)
C
      WRITE(2,7)W
    7 FORMAT(1H ,'WIDTH OF THE METAL FOIL        (M)     =',E10.4)
C
      WRITE(2,9)TM
    9 FORMAT(1H ,'THICKNESS OF THE METAL FOIL  (M)       =',E10.4)
C
      WRITE(2,8)TD
    8 FORMAT(1H ,'THICKNESS OF THE PLASTIC FOIL  (M)     =',E10.4)
C
      WRITE(2,25)E
   25 FORMAT(1H ,'DIALECTRIC CONATANT OFT HE PLASTIC     =',E10.4)
C
C THIS CALS THE INDUCTANCE CAPACITANCE AND RESISTANCE
C
      DO 10 IBA=1,S
C
      R=RADI+(N-(IBA-0.5)*M)*(TD+TM)
C
      C(IBA)=E*E0*W*2.0*PY*R/TD/M
C
      RDC(IBA)=RESIST*2.0*PY*R*M/W/TM
C
      IXA=IBA*M
      IXB=(IBA-1)*M
      RA=R
C
      RAC(IBA)=COND*U*U/W/3.0*TM**3*2.0*PY*RA/6.0*((IXA-1.0)*IXA*(2.0*
     1A-1.0)-((IXB-1.0)*IXB*(2.0*IXB-1.0)))
      RAC(IBA)=RAC(IBA)/8.0
C
C
      DO 12 IBD=IBA,S
      RB=RADI+(N-(IBA-0.5)*M)*(TM+TD)
      RC=RADI+(N-(IBD-0.5)*M)*(TD+TM)
      MUT(IBA,IBD)=PY*RC*RC/W/W*U*(SQRT(W*W+RB*RB)-RB)*M*M
   12 CONTINUE
C
   10 CONTINUE
C
      WRITE(2,20)
      WRITE(2,17)
      WRITE(2,24)
      DO 15 IBF=1,S
C
      WRITE(2,16)IBF,MUT(IBF,IBF),C(IBF),RDC(IBF),RAC(IBF)
```

THIS IS THE MEAN RADIUS OF THE SECTION

CAPACITANCE PER SECTION

DC. RESISTANCE PER SECTION

AC. RESISTANCE PER SECTION

INDUCTANCE PER SECTION

AND MUTUAL INDUCTANCE FROM SECTION TO SECTION.

```
   16 FORMAT(1H ,I3,5X,E10.4,14X,E10.4,14X,E10.4,18X,E10.4)
   17 FORMAT(1H ,'INDUCTANCE (HENRIES)    CAPACITANCE (FARADS)    CD R
     1ISTANCE (OHMS)    AC RESISTANCE (OHMS/W/W)  ')
   15 CONTINUE
C
      WRITE(2,20)
   20 FORMAT(///)
C
      WRITE(2,21)
   21 FORMAT(1H ,'MUTUAL INDUCTANCE MATRIX STARTS AT 1,1 AND GOES TO
     1 10,10 ')
C
      DO 22 IBH=1,S
      WRITE(2,23)(MUT(IBH,IBI),IBI=IBH,S)
      WRITE(2,24)
   22 CONTINUE
   23 FORMAT(1H ,10(E10.4,1X))
   24 FORMAT(/)
C
      STOP
      END
```

Appendix 3

The program is written in 1900 Fortran and is basically an implementation of the flow diagrams in Section 5.

```
      MASTER ELIMIN
      REAL A(40,40),B(20),X(20),LIN(20),C(20),RDC(20),RAC(20),MUT(20,2(
      REAL WA(10,3)
      COMPLEX XCOM(20)
      COMPLEX Z,ZT
C
C THIS PROGRAM CONTAINS THE AC RESISTANCE SECTION
C
      DATA NCA/10/
      M=NCA
      N=2*NCA
      PY=2.0*ASIN(1.0)
C
C THIS READS IN THE START AND FINISH FRQUENCIES
C
      DO 60 IPA=1,10
      READ(1,61)WA(IPA,1),WA(IPA,2),WA(IPA,3)
      IPB=IPA
      IF(WA(IPA,1).EQ.0.0) GO TO 62
      WRITE(2,112)
      WRITE(2,63)WA(IPA,1),WA(IPA,2),WA(IPA,3)
   61 FORMAT(3(E0.0))
   63 FORMAT(1H ,'ATART FREQ=',E10.4,'    FINISH FREQ=',E10.4,'    STEP
     1FREQ=',E10.4)
      WA(IPA,1)=WA(IPA,1)*2.0*PY
      WA(IPA,2)=WA(IPA,2)*2.0*PY
      WA(IPA,3)=WA(IPA,3)*2.0*PY
   60 CONTINUE
   62 CONTINUE
C
C  READ IN INDUCTANCE THEN CAPACITANCE THEN RESISTANCE
C
      DO 115 IR=1,M
      READ(1,116)LIN(IR),C(IR),RDC(IR),RAC(IR)
      WRITE(2,112)
      WRITE(2,117)IR,LIN(IR),IR,C(IR),IR,RDC(IR),IR,RAC(IR)
  115 CONTINUE
      WRITE(2,114)
  116 FORMAT(4(E0.0))
  117 FORMAT(1H ,'L(',I2,')=',E14.4,3X,'C(',I2,')=',E14.4,3X,'  RDC(',I
     1,')=',E10.4,'   RAC(',I2,')=',E10.4)
C
C  THIS READS IN THE MUTUAL COUPLING MATRIX
C
      DO 118 IRE=1,M
      READ(1,119)(MUT(IRE,IRF),IRF=IRE,M)
  118 CONTINUE
  119 FORMAT(30(E0.0))
C
```

THIS READS IN THE FREQUENCY RANGES OVER WHICH THE SPECTRUM IS REQUIRE

THIS READS IN THE L's, C's AND THE R's WHEN NOT NEEDED THE AC RESISTANCE IS SET EQUAL TO ZERO OR THE INPUT DATA

THIS READS IN THE MUTUAL INDUCTANCE MATRIX

```
C THIS SECTION WRITES OUT THE COUPLING MATRIX
C
      WRITE(2,114)
      WRITE(2,122)
  122 FORMAT(1H ,'MUTUAL COUPLING MATRIX IS'/)
      DO 123 IRM=1,M
      DO 123 IRD=1,M
      MUT(IRD,IRM)=MUT(IRM,IRD)
      WRITE(2,124)IRM,IRD,MUT(IRM,IRD)
  123 CONTINUE
  124 FORMAT(1H ,I3,2X,I3,2X,E14.4)
C
      DO 1000 IPC=1,IPB
      W=WA(IPC,1)
  999 W=WA(IPC,3)+W
C
C THIS SECTION ASSIGNS VALUES TO THE MATRIX A
C
      DO 128 NVA=1,N
      DO 128 NVB=1,N
      A(NVA,NVB)=0.0
  128 CONTINUE
      I=1
  105 J=1
  102 A(I+M,J)=W*MUT(I,J)
      A(I,J+M)=-A(I+M,J)
      IF(J-M)100,101,101
  100 J=J+1
      GO TO 102
  101 A(I+M,I)=W*LIN(I)-1.0/(W*C(I))
      A(I,I+M)=-A(I+M,I)
      A(I,I)=RDC(I)+RAC(I)*W*W
      A(I+M,I+M)=A(I,I)
      B(I)=0.0
      B(I+M)=-1.0/(W*C(I))
      IF(I-M)103,104,104
  103 I=I+1
      GO TO 105
  104 CONTINUE
```

THERE ARE A NUMBER OF FREQUENCY RANGES OVER WHICH THE PROGRAM HAS TO CYCLE. THE DO LOOP CYCLES OVER THE RANGES WHILE THE GO TO LOOP CYCLES OVER THE INDIVIDUAL RANGE

THIS PART ASSIGNS VALUES TO THE MATRICES [A] AND [B]

```
C
C       THIS SECTION IS THE ELIMINATION
C
      1 K=1
      2 I=K+1
C
C       THIS SECTION DOES THE PARTIAL PIVOTING
C
     79 L=K
     80  IF (ABS(A(I,K))-ABS(A(L,K)))  82,81,81
     81 L=I
        GO TO 82
     82 IF (I-N) 83,84,84
     83 I=I+1
        GO TO 80
     84 IF(L-K)85,90,85
     85 J=K
     89 U=A(K,J)
        A(K,J)=A(L,J)
        A(L,J)=U
     86 IF (J-N) 87,88,88
     87 J=J+1
        GO TO 89
     88 U=B(K)
        B(K)=B(L)
        B(L)=U
     90 I=K+1
     91 CONTINUE
      4 AM=A(I,K)/A(K,K)
      5 A(I,K)=0
      6 J=K+1
      7 A(I,J)=A(I,J)-AM*A(K,J)
        IF (J-N) 9,10,10
      9 J=J+1
        GO TO 7
     10 B(I)=B(I)-AM*B(K)
        IF (I-N) 11,12,12
     11 I=I+1
        GO TO 4
     12 IF(K-N+1) 13,14,14
     13 K=K+1
        GO TO 2
     14 CONTINUE
```

THE COLUMN TO BE ELIMINATED IS SEARCHED THROUGH TO FIND THE LARGEST ELEMENT, THEN THE ROWS ARE EXCHANGED

AM IS THE MULTIPLIER m, THIS IS USED TO ELIMINATE THE ELEMENTS IN THE PARTICULAR COLUMN K

```
C
C     THIS SECTION BACK SUBSTITUTES
C
   30 X(N)=B(N)/A(N,N)
   31 I=N-1
   32 J=I+1
   33 S=0
   34 S=S+A(I,J)*X(J)
   35 IF (J-N) 36,37,37
   36 J=J+1
      GO TO 34
   37 X(I)=(B(I)-S)/A(I,I)
   38 IF (1-I) 39,40,40
   39 I=I-1
      GO TO 32
   40 CONTINUE
C
C  THIS SECTION OUTPUTS THE CURRENT AND IMPEDANCE PER SECTION
C
      WRITE(2,202)
  202 FORMAT(1H ,'CURRENT REAL CMPLX MAG ANGLE     IMPEDANCE REAL CMPLX
     1AG ANGLE')
      ZT=CMPLX(0.0,0.0)
      AMZT=CABS(ZT)
      AAZT=ATAN(AIMAG(ZT)/REAL(ZT))*57.2958
C
C    CZT IS THE LOG OF THE IMPEDANCE
C
C    DZT IS THE LOG OF THE VOLTAGE OUT FROM 50 OHM INTO 50 OHM
C
      CZT=ALOG10(AMZT)
      DZT=20.*ALOG10(AMZT+100.)-20.*ALOG10(100.)
C
      WRITE(2,205)ZT,AMZT,AAZT,CZT,DZT
      WRITE(2,113)
      WXKV=W/2.0/PY
      WRITE(2,206)WXKV
  206 FORMAT(1H ,'FREQUENCY (MHZ)=',F11.2)
      WRITE(2,112)
      DO 200 IJ=1,M
      XCOM(IJ)=CMPLX(X(IJ),X(IJ+M))
      AMI=CABS(XCOM(IJ))
      AAI=ATAN(AIMAG(XCOM(IJ))/REAL(XCOM(IJ)))*57.2958
      Z=(1.0-XCOM(IJ))*CMPLX(0.0,-1.0/(W*C(IJ)))
      AAZ=ATAN(AIMAG(Z)/REAL(Z))*57.2958
      AMZ=CABS(Z)
      ZT=ZT+Z
      GO TO 200
      WRITE(2,201)XCOM(IJ),AMI,AAI,Z,AMZ,AAZ
  201 FORMAT(1H ,3(F14.8,3X),F6.2,3X,3(F14.8,3X),F6.2)
  200 CONTINUE
      WRITE(2,112)
      WRITE(2,204)
  204 FORMAT(1H ,'TOTAL IMPEDANCE REAL CMPLX MAGNITUDE AND ANGLE')
```

THIS SECTION DOES THE BACK SUBSTITUTION

THIS PUTS THE CURRENT IN COMPLEX FORM

THIS CALCULATES THE IMPEDANCE PER SECTION

```
  205 FORMAT(1H ,3(F14.8,3X),F6.2,2X,E14.8,2X,E14.8)
      IF(W.LT.WA(IPC,2)) GO TO 999
 1000 CONTINUE
  301 FORMAT(3(I8))
  302 FORMAT(F6.2,F8.4)
  303 FORMAT(F6.4,F6.4,F6.4)
  114 FORMAT(///)
  113 FORMAT(//)
  112 FORMAT(/)
      STOP
      END
```

Appendix 4

The subroutine is written in 1900 Fortran and from a given current current distribution calculates the external magnetic field of the coil in terms of H per amp input to the coil.

```
      MASTER ELIMIN
      REAL A(40,40),B(20),X(20),LIN(20),C(20),R(20),MUT(20,20)
      REAL WA(100)
      COMPLEX XCOM(20)
      COMPLEX Z,ZT
      COMMON ZP,RADI,W,TD,TM
C     PUT DATA AS TO NCA THE SIZE OF THE MATRIX IN HERE
      DATA NCA/10/
      M=NCA
      N=2*NCA
      PY=2.0*ASIN(1.0)
       READ(1,17)ZP
      READ(1,16)NUMBT
      READ(1,17)RADI
      READ(1,17)W
      READ(1,17)TD
      READ(1,17)TM
C
C    NCA IS THE NUMBER OF SECTIONS INTO WHICH THE COIL IS DIVIDED
C
C    ZP IS THE HEIGHT OF THE SEARCH COIL  ABOVE THE COIL
C
C    N IS THE NUMBER OF TURNS ON THE COIL
C
C    W IS THE WIDTH OF THE METAL FOIL
C
C    TD IS THE THICKNESS OF THE PLASTIC FOIL
C
C    TM IS THE THICKNESS OF THE METAL FOIL
C
   16 FORMAT(I0)
   17 FORMAT(E0.0)
```

```
      CALL MAGBF(NCA,XCOM,NUMBT)
```

This statement inserted in the elimination program at the end calls the subroutine.

```
      SUBROUTINE MAGBF(NCA,XCOM,NUMBT)
      COMPLEX BT,B(1000)
       COMPLEX XCOM(NCA)
      COMMON ZP,RADI,W,TD,TM
      N=NUMBT
      NUMT=NUMBT
      UZ=0.000001257
      BT=CMPLX(0.0,0.0)
      IA=1
      LC=N/NCA
    7 IM=1
    4 IN=(IA-1)*LC+IM
      RADA=(N-IN)*(TD+TM)+RADI
      B(IN)=UZ*XCOM(IA)/2./W*((ZP-W/2.0)/SQRT(RADA*RADA+(ZP-W/2.0)**2)-
     1ZP+W/2.0)/SQRT(RADA*RADA+(ZP+W/2.0)**2))
      IF(IN.EQ.1) GO TO 20
      IXT=IN-1
      B(IN)=B(IXT)+B(IN)
   20 CONTINUE
      IF(IM-LC)2,3,3
    2 IM=IM+1
      GO TO 4
    3 IF(IA-NCA)5,6,6
    5 IA=IA+1
      GO TO 7
    6 CONTINUE
      BTMAX=0.0
      DO 8 LB=1,NUMT
      XAU=CABS(B(LB))
      IF(XAU.LT.BTMAX) GO TO 12
      BTMAX=XAU
   12 CONTINUE
    8 CONTINUE
C
      WRITE(2,13)
   13 FORMAT(//)
      WRITE(2,14)
   14 FORMAT(1H ,'TURN NO      RADIUS    MAG FIELD MAGNITUDE        REAL
     1 COMPLEX     RELATIVE')
C
      DO 15 LD=1,NUMT,5
C
      RADB=(NUMT-LD)*(TM+TD)+RADI
C
      BTR=CABS(B(LD))
      BTRA=BTR/BTMAX
C
      WRITE(2,16)LD,RADB,BTR,B(LD),BTRA
   16 FORMAT(1H ,3X,I4,1X,E10.4,12X,E10.4,1X,E10.4,1X,E10.4,2X,E10.4)
C
   15 CONTINUE
      RETURN
      END
```

THIS CALCULATES THE MAGNETIC FIELD OF A TURN. THE VALUES CALCULATED ARE THEN INSERTED IN THE MATRIX B

THE PRINT OUT CONTAINS THE RADIUS AND THE MAGNITUDE OF THE MAGNETIC FIELD AT THE TURN

REFERENCES

1. Kemp,R.J.:"Foil Wound Inductors",Final Year Report, University of Technology,Loughborough,1974
2. Welsby,V.G.:"The Theory and Design of Inductance", Coils",Macdonald,London,1960
3. Bleaney,B.I.,Bleaney,B.:"Electricity and Magnetism", Oxford,1965
4. Murgatroyd,P.N.:"Notes on Foil Wound Inductors 1", University of Technology, Loughborough, Leics., 1973
5. French,A.P.:"Vibrations and Waves",Nelson,1971
6. Reeves,R.:Private Communication
7. Petit-Bois,G.:"Tables of Indefinite Integrals",Dover
8. Murgatroyd,P.N.:"Notes on Foil Wound Inductors 3", University of Technology, Loughborough, Leics., 1973
9. Froberg,C.:"Introduction to Numerical Analysis", Addison Wesley,London,1965
10. McCraken,P.D.and Dorn,W.S.:"Numerical Methods and Fortran Programming with Applications in Engineering and Science",Wiley,New York, 1964
11. Stoll,R.L.:"The Analysis of Eddy Currents", Clarendon Press,Oxford,1974